Negative microfilm 65–5930
received from university

MATEER, Carlton Livingstone, 1926–
A STUDY OF THE INFORMATION CONTENT
OF UMKEHR OBSERVATIONS.

The University of Michigan, Ph.D., 1964
Physics, meteorology

University Microfilms, Inc., Ann Arbor, Michigan

A STUDY OF THE INFORMATION CONTENT OF UMKEHR OBSERVATIONS

by

Carlton Livingstone Mateer

A dissertation submitted in partial fulfillment
of the requirements for the degree of
Doctor of Philosophy in The
University of Michigan
1964

Doctoral Committee:

Associate Professor Edward S. Epstein, Co-Chairman
Professor Aksel C. Wiin-Nielsen, Co-Chairman
Doctor Hans U. Dütsch, National Center for Atmospheric Research
Professor E. Wendell Hewson
Assistant Professor Donald A. Jones

ACKNOWLEDGMENTS

The author wishes to express his gratitude to all who assisted him during the course of this study. He is particularly appreciative of the advice and assistance rendered by Professors Edward S. Epstein and Aksel C. Wiin-Nielsen, Co-Chairmen of his Doctoral Committee. The author also wishes to thank Professors E. Wendell Hewson and Donald A. Jones for serving as members of the committee and for the help they have given.

An expression of deepest gratitude is due Dr. Hans U. Dütsch, National Center for Atmospheric Research, for serving as a member of the committee, for his guidance and encouragement and his interest in the work, and for his generous provision of tables, data, and other information connected with his method of evaluating Umkehr observations. The tabular and graphical material related to Dr. Dütsch's method are reproduced here with his kind permission.

The author also wishes to express his appreciation for many helpful discussions with, and the constant interest and encouragement of his associates, particularly Messrs. Allan H. Murphy, Chien-Hsiung Yang, and Charles Young. Mr. S. Roland Drayson pointed out the approximate equivalence of the evaluation method developed by the author and that proposed by Twomey. Dr. Paul R. Julian suggested the interpretation of the generating function curves in terms of the resolving power of the Umkehr observations.

Acknowledgment is due to Professor Alan W. Brewer, University of Toronto, and Mr. Wayne S. Hering, Geophysics Research Directorate, for provision of unpublished ozone sonde data, and to the Meteorological Service of Canada and Mr. Walter D. Komkyr, United States Weather Bureau, for provision of Umkehr data.

While engaged in this work, the author has been supported by the Meteorological Service of Canada, and the National Science Foundation. The support of the National Center for Atmospheric Research, where the author was a summer visitor in 1963, is also appreciated. The author also wishes to acknowledge the support of The University of Michigan through the use of the IBM 7090 at the Computing Center, Professor R.C.F. Bartels, Director.

TABLE OF CONTENTS

	Page
LIST OF TABLES	v
LIST OF FIGURES	x
1. INTRODUCTION	1
1.1 A Brief Survey of the History of Ozone-Meteorological Research	1
1.2 A Description and Qualitative Explanation of the Umkehr Effect	4
1.3 The Problem and the Approach	8
2. REVIEW OF UMKEHR EVALUATION TECHNIQUES	11
2.1 Preliminary Remarks	11
2.2 Method A	14
2.3 Method B	19
2.4 Method of Dütsch	22
2.5 Sources of Error	25
2.5.1 Multiple scattering and reflected light	25
2.5.2 Empirical cloud corrections and large particle scattering	31
3. THE CHARACTERISTIC PATTERNS OF UMKEHR CURVES	35
3.1 Preliminary Remarks	35
3.2 The Statistical Procedure	37
3.3 The Application of the Statistical Procedure	40
3.4 Physical Explanation	57
4. DISCUSSION OF THE LINEARIZED EVALUATION METHOD	68
4.1 Preliminary Remarks	68
4.2 The "Complete" Solution of the Linear Equations	70
4.3 The Problem of Information Versus Noise	76
4.3.1 The use of the characteristic patterns of the Umkehr curve	76
4.3.2 Stepwise solutions using the eigenvectors of $\Delta^*\Delta$	78

TABLE OF CONTENTS (Concluded)

		Page
4.4	Objective Methods of Smoothing the Solution	82
4.4.1	Truncation of the eigenvector expansion	82
4.4.2	Twomey's method	83
4.5	Solution Contributions Associated with the Characteristic Patterns of Umkehr Curves	89
5.	FURTHER REMARKS ON EVALUATION METHODS AND PRESENTATION OF RESULTS	92
5.1	The Scaling Problem	92
5.2	The Effect of Adding Random Noise to the Observations	109
5.3	The Need for More than One Standard Distribution	109
5.3.1	Convergence of the iterative procedure using the second derivatives	109
5.3.2	Average solutions	111
5.4	The Need for Second Derivative Corrections	115
5.5	Comparison with Dütsch's Solutions	118
5.6	Another Orthogonal Vector Expansion for Solutions	121
5.7	Vertical Distributions Using Other Wavelength Pairs	129
6.	CONCLUSIONS AND SUGGESTIONS FOR FUTURE WORK	140
APPENDIX		
A.	TERMINOLOGY AND UNITS USED IN OZONE-METEOROLOGICAL RESEARCH	143
B.	FURTHER DETAILS OF DÜTSCH'S EVALUATION METHOD	148
C.	THE COMPUTATION OF THE GENERATING FUNCTION CURVES FOR PRIMARY SCATTERING	160
D.	THE PROCEDURE USED WITH OZONE SONDE DATA	163
E.	TABULATIONS OF INDIVIDUAL SOLUTIONS	168
BIBLIOGRAPHY		193

LIST OF TABLES

Table		Page
1.	Higher Order Scattering Corrections to be Subtracted From Observed N-Values at Various Zenith Angles	27
2.	The First Eight Eigenvalues of the Correlation Matrix of the Points on the Umkehr Curve, Including (in parentheses) Correlation Between the Eigenvector Coefficient and Total Ozone	43
3.	The First Eight Eigenvalues for the Correlation Matrix of the Points on the Umkehr Curve When the Instrument Constant is Eliminated and Total Ozone is Used	46
4.	The First Eight Eigenvalues for the Covariance Matrix of the Points on the Umkehr Curve When the Instrument Constant is Eliminated and Total Ozone is Used	50
5.	Characteristic Patterns for the Covariance Matrix of the Points on the Umkehr Curve When the Instrument Constant is Eliminated and Total Ozone is Used for the North American C Wavelength Data Sample	54
6.	Frequency Distributions of Truncation Levels for Expansions of Umkehr Curves in Terms of Their Characteristic Patterns	56
7.	Eigenvalues and Vectors for one Configuration of Dütsch's First Derivative Matrix for his Standard Distribution I	74
8.	Averages of Smoothed and Error Dot Products and Fractional Variance Explained by Each and by the Combined Dot Products	77
9.	Frequency Distribution of the Number of Eigenvectors Used in the Stepwise Solution Procedure and Average Fractional Umkehr Curve Variance Explained by Each Vector	79
10.	Stepwise Solutions for March 21, 1962, Showing Individual Solution Contributions by Each Eigenvector	81

LIST OF TABLES (Continued)

Table		Page
11.	Stepwise Solutions for March 21, 1962, Showing the Individual Solution Contributions by Each Eigenvector Using Twomey's Method With $\gamma = 0.5$	87
12.	Average Solution for Arosa Data Sample by Twomey's Method With Column Scaling of 10, $W_\Omega = 0.1$, and $\gamma = 0.5$	94
13.	Average Solution for Arosa Data Sample by Twomey's Method With Column Scaling Equivalent to Standard Distribution Layer Partial Pressures, $W_\Omega = 0.1$ (1.0), and $\gamma = 0.5$	96
14.	Solution Statistics for Arosa Data Sample for Solutions by Truncated Eigenvector Expansion Method With Column and Equation Scaling Vectors Determined From Derivative Matrix	97
15.	Solution Statistics for Arosa Data Sample for Solutions by TEVE and Twomey Methods With Column Scaling Vector Determined From Derivative Matrix, $W_\Omega = 0.1$, and $\gamma = 0.1$	99
16.	Averages and Standard Deviations of Layer-Mean Partial Pressures for Balloon Soundings and Umkehr Data	101
17.	Column Weighting Vectors Used With Derivative Matrices in Solutions	102
18.	Statistics for Arosa Data Sample Solutions Carried out by TEVE and Twomey Methods Using Column Weighting Vector CI, $W_\Omega = 0.1$, and SI	103
19.	Statistics for Arosa Data Sample Solutions to Illustrate the Effect of Variations in the Weight on the Ozone Conservation Equation, with $\gamma = 0.5$	104
20.	Statistics for Arosa Data Sample Solutions Using CII and CIII with Twomey's Method and Using CI With the "Combined" TEVE-Twomey Method	105
21.	Statistics for Arosa Data Sample Solutions With Respect to Standard Distribution II when Total Ozone is Less than 300 m atm-cm, With $W_\Omega = 0.5$	107

LIST OF TABLES (Continued)

Table		Page
22.	Statistics for Arosa Data Sample Solutions With Respect to Standard Distribution III When Total Ozone Exceeds 375 m atm-cm	108
23.	Statistics for Arosa Data Sample Solutions When Random Noise Has Been Added to the Umkehr Curves	110
24.	Frequency Distributions of the Number of Iterations Required for Convergence When the Second Order Partial Derivatives are Used	112
25.	Average Solutions for Arosa Data Sample With Second Derivative Corrections Included when Total Ozone is Less Than 300 m atm-cm	114
26.	Average Solutions for Arosa Data Sample With Second Derivative Corrections Included When Total Ozone Exceeds 375 m atm-cm	116
27.	Average Solutions for Arosa Data Sample to Illustrate Differences Between Linear (L) and Nonlinear (NL) Solutions	117
28.	Individual Solutions Chosen to Illustrate the Differences Between Linear (L) and Nonlinear (NL) Solutions	118
29.	Solution Statistics for Arosa Data Sample to Compare the Dütsch, TEVE, and Twomey Methods of Solution With Second Derivative Corrections Applied	120
30.	Correction Factors for AD Total Ozone Measurements Used in Umkehr Evaluations	131
31.	First Four Eigenvalues of $\Delta^*\Delta$ With Mean and RMS Residuals for the Various Wavelength Combinations	138
B-1.	Standard Vertical Distributions of Ozone Used by Dütsch	152
B-2.	Umkehr Curve Points for the Various Standard Distributions and Wavelength Pairs, With Secondary Scattering Effects Included	153

LIST OF TABLES (Continued)

Table		Page
B-3.	First Order Partial Derivatives for Standard Distribution I, A Wavelength Pair, With Secondary Scattering Effects Included	154
B-4.	First Order Partial Derivatives for Standard Distribution I, C Wavelength Pair, With Secondary Scattering Effects Included	155
B-5.	First Order Partial Derivatives for Standard Distribution I, D Wavelength Pair, With Secondary Scattering Effects Included	156
B-6.	First Order Partial Derivatives for Standard Distribution II, C Wavelength Pair, With Secondary Scattering Effects Included	157
B-7.	First Order Partial Derivatives for Standard Distribution III, C Wavelength Pair, With Secondary Scattering Effects Included	158
B-8.	The Overlapping-Layer Zenith-Angle System Used by Dütsch to Obtain Smooth Solutions	159
D-1.	Statistical Parameters Used in Estimating Layer-Mean Partial Pressures From Total Ozone	166
E-1.	Individual Solutions for Arosa Data Sample, by Twomey's Method, With Respect to SI, and With Second Derivative Corrections Applied	169
E-2.	Individual Solutions for 42 Low-Ozone Arosa Umkehrs, by Twomey's Method, With Respect to SII, and With Second Derivative Corrections Applied	173
E-3.	Individual Solutions for 29 High-Ozone Arosa Umkehrs, by Twomey's Method, With Respect to SIII, and With Second Derivative Corrections Applied	175
E-4.	Individual Solutions for Arosa Data Sample, by TEVE Method, With Respect to SI, and With Second Derivative Corrections Applied	177

Table		Page
E-5.	Individual Solutions for 42 Low-Ozone Arosa Umkehrs, by TEVE Method, With Respect to SII, and With Second Derivative Corrections Applied	181
E-6.	Individual Solutions for 29 High-Ozone Arosa Umkehrs, by TEVE Method, With Respect to SIII, and With Second Derivative Corrections Applied	183
E-7.	Individual Solutions for 93 Arosa Umkehrs by Dütsch's Technique	185
E-8.	Individual Solutions for 98 North American Umkehrs on C Wavelengths, by Twomey's Method, With Respect to SI, and With Second Derivative Corrections Applied	189

LIST OF FIGURES

Figure		Page
1.	Umkehr curve for observations at Edmonton on the afternoon of May 22, 1961.	5
2.	Average vertical distribution of ozone from ozone sonde and Umkehr data (Table 16).	7
3.	Schematic diagram showing the path of the direct solar beam to the scattering point and that of the scattered beam from there to the instrument on the ground.	12
4.	Schematic diagram showing the atmospheric layer division used in Method A (after Walton).	15
5.	Curves of $\eta(\Theta_k,\Omega,x_1,x_2) = N(\Theta_k,\Omega,x_1,x_2)$ for $\Theta_1 = 80°$ and $\Theta_2 = 86.5°$, on x_1, x_2 diagram.	18
6.	Corrections (to be subtracted from observed N-values) for ground reflection in the case of 80% albedo. (After Dave and Furukawa.)	31
7.	Cloud corrections (N-units to be subtracted from observed values) as a function of luxmeter ratio and solar zenith angle.	32
8.	Sample Umkher curve for Arosa, March 30, 1962, showing observed values and corrected values. Total ozone is 394 m atm-cm.	33
9.	"Standard" Umkehr curves for Arosa and North America for the C wavelength pair.	45
10.	First Characteristic Pattern of the correlation matrix, with the instrument constant eliminated.	48
11.	Second Characteristic Pattern of the correlation matrix, with the instrument constant eliminated.	49
12.	Third Characteristic Pattern of the correlation matrix, with the instrument constant eliminated.	49

LIST OF FIGURES (Continued)

Figure		Page
13.	First Characteristic Pattern of the covariance matrix, with the instrument constant eliminated. Compare with Fig. 10 but note difference in scale.	51
14.	Second Characteristic Pattern of the covariance matrix, with the instrument constant eliminated.	52
15.	Third Characteristic Pattern of the covariance matrix, with the instrument constant eliminated.	53
16.	Scatter diagram of first pattern vector coefficient plotted against total ozone deviation from mean for C wavelength pair, North America sample.	58
17.	Scatter diagram of first pattern vector coefficient plotted against total ozone deviation from mean for C wavelength pair, Arosa sample.	59
18.	Vertical distribution of ozone used in the computation of source function $\chi(\Theta,z)$.	61
19.	Source functions $\chi(\Theta,z)$ plotted against height for various zenith angles for the A wavelengths.	62
20.	Source function $\chi(\Theta,z)$ plotted against height for various zenith angles for the C wavelengths.	63
21.	Source functions $\chi(\Theta,z)$ plotted against height for various zenith angles for the D wavelengths.	64
22.	Relative intensities and intensity ratios for wavelengths A, C and D plotted on a logarithmic scale against solar zenith angle.	65
23.	Solution contribution in the various layers for each of the first four Characteristic Patterns.	91
24.	Illustrating the smooth curve obtained from the original block distribution.	124

Figure		Page
25.	Average solutions for 42 low-ozone cases at Arosa using the Characteristic Pattern method, with TEVE solutions for comparison.	125
26.	Average solutions for 29 high-ozone cases at Arosa using the Characteristic Pattern method, with TEVE solutions for comparison.	127
27.	Average solutions for 100 Arosa Umkehr curves using the Characteristic Pattern method, with TEVE solutions for comparison.	128
28.	Average solutions for 98 North American Umkehr curves for the individual wavelength pairs.	132
29.	Average solutions for 98 North American Umkehr curves for the double wavelength pairs.	133
30.	Average solutions for 98 North American Umkehr curves for combined wavelength pairs and double pairs.	134
31.	Average solutions for 98 North American Umkehr curves for the C wavelength pair by different methods.	135

1. INTRODUCTION

1.1 A BRIEF SURVEY OF THE HISTORY OF OZONE-METEOROLOGICAL RESEARCH

Ever since the first systematic measurements, by Dobson and his collaborators (1926, 1927, 1929, 1930), of the total amount of ozone in a vertical column of the atmosphere, meteorologists have been fascinated by the strong relationship between ozone amount and day-to-day weather variations. Equally interesting are the pronounced seasonal and latitudinal variations in ozone amount with a spring maximum and autumn minimum at all latitudes. In all seasons, the ozone amount increases from the equator toward the poles.

The above discoveries were followed immediately by a series of papers by Chapman (1930), Mecke (1931), Wulf (1932, 1934), and Wulf and Deming (1936a, 1936b), in which the photochemical theory of ozone formation in the upper atmosphere was advanced, and the vertical distribution of ozone calculated on the basis of an equilibrium between the reactions producing and destroying ozone under the influence of solar ultraviolet radiation. The photochemical equilibrium theory suggested a vertical distribution in qualitative agreement with that deduced from the observations of E. Regener and V. H. Regener (1934), who employed a small ultraviolet quartz spectrograph sent aloft on a balloon to measure the vertical distribution of ozone up to 32 km. At the same time, Götz, Meetham, and Dobson (1934) were able to infer the main features of the vertical dis-

tribution from measurements of the Götz (1931) Umkehr or inversion effect. These studies showed a maximum ozone density between 20 and 30 km, the latter study indicating a rapid decrease with height above 30 km, with most of the ozone in the atmosphere being below 30 km.

In 1937, Wulf and Deming calculated an approximate "rate of maintenance" of the photochemical equilibrium. They found that the rate increased with height and suggested that ozone below 30 km was "protected" from the influence of the photochemical reactions and that air motions would be important in determining the vertical distribution in these layers. Taking advantage of later information available, Schröer (although not published until 1949, his work was completed in 1944), Dütsch (1946), and Craig (1948), independently, considered the effects of variation of solar elevation (and hence latitude) on the photochemical distribution, as well as the reaction times. They found a summer solstice maximum and a winter solstice minimum of total ozone, with a latitudinal gradient such that ozone increased from the poles to the equator. These predictions are in distinct contradiction of the observations. However, the studies also showed that the time required to approach equilibrium decreased very rapidly as height increased, being of the order of a year or more at 20 km, of days at 30 km, and hours at 40 km (Craig's results). Thus ozone is neither created nor destroyed at an appreciable rate below about 25 to 30 km. These results led to the conclusion that ozone mixing ratio was a conservative property of the atmosphere below these levels and, hence, that the explanation for the observed seasonal and latitudinal

distribution of ozone must be sought in the general circulation of the atmosphere. Conversely, any acceptable theory of the general circulation of the atmosphere must also be consistent with the observed distribution of ozone. Thus ozone plays a unique role in general circulation research for not only does it influence, through its radiative properties, the distribution of heat sources and sinks in the stratosphere and mesosphere, but it is also important as a tracer in studies of atmospheric motions.

The period following the second world war has seen many advances in ozone-meteorological research. The global network of stations measuring total atmospheric ozone has greatly increased. The balloon observation technique of E. and V. H. Regener was continued (Paetzold, 1954). The vertical distribution of ozone has been measured from rocket-borne equipment (Johnson et al., 1952). Instruments for use with balloons have been developed by Kulcke and Paetzold (1957), Vassy (1958), Brewer and Milford (1960), and Regener (1960). With regard to indirect methods, the Umkehr technique has been improved by Dütsch (1957, 1959a, 1959b) and infrared techniques have been developed by Epstein, Osterberg and Adel (1956), Goody and Roach (1956), and Vigroux (1959). Other methods proposed and used include lunar eclipse measurements (Paetzold, 1952), twilight balloon or satellite photometry (Pittock, 1961, 1963; and Venkateswaran, Moore and Kreuger, 1961), and measurements from a satellite (Singer and Wentworth, 1957, Twomey, 1961, and Rawcliffe et al., 1963). During this period, further impetus was given to ozone-meteorological research by the discovery, reported by Teweles and Finger (1958), of the large in-

creases in ozone amount which were associated with the explosive stratospheric warmings (Scherhag, 1952).

Most of these developments, and many others, have been recorded in greater detail in the reviews of Craig (1950), Götz (1951) and Taba (1961).

1.2 A DESCRIPTION AND QUALITATIVE EXPLANATION OF THE UMKEHR EFFECT

The Umkehr effect is observed when measurements are made with an ultraviolet spectrophotometer,[1] of the ratio of the zenith sky light intensities of two wavelengths in the solar ultraviolet when the sun is near the horizon. The shorter of the two wavelengths (intensity I) is strongly absorbed by ozone, the other (intensity I') is weakly absorbed. If the value of log I/I' is plotted against the sun's zenith angle, it is observed that this log-intensity ratio decreases as the zenith angle increases until a minimum is reached for a zenith angle of about 85° (when the wavelengths are 3114 and 3324 Å). As the zenith angle increases further, the log-intensity ratio increases again. This effect, first noticed by Götz (1931), is illustrated in Fig. 1, where the quantity (-100.0 log I/I' + constant, called the N-value) is plotted against the fourth power of the zenith angle. It is customary to use a high power of the zenith angle as abscissa so that the values obtained when the sun is close to the horizon are spread out on the graph.

[1] A brief description of the instrument, the terms, and the units used in ozone-meteorological research, insofar as used in this report, is given in Appendix A.

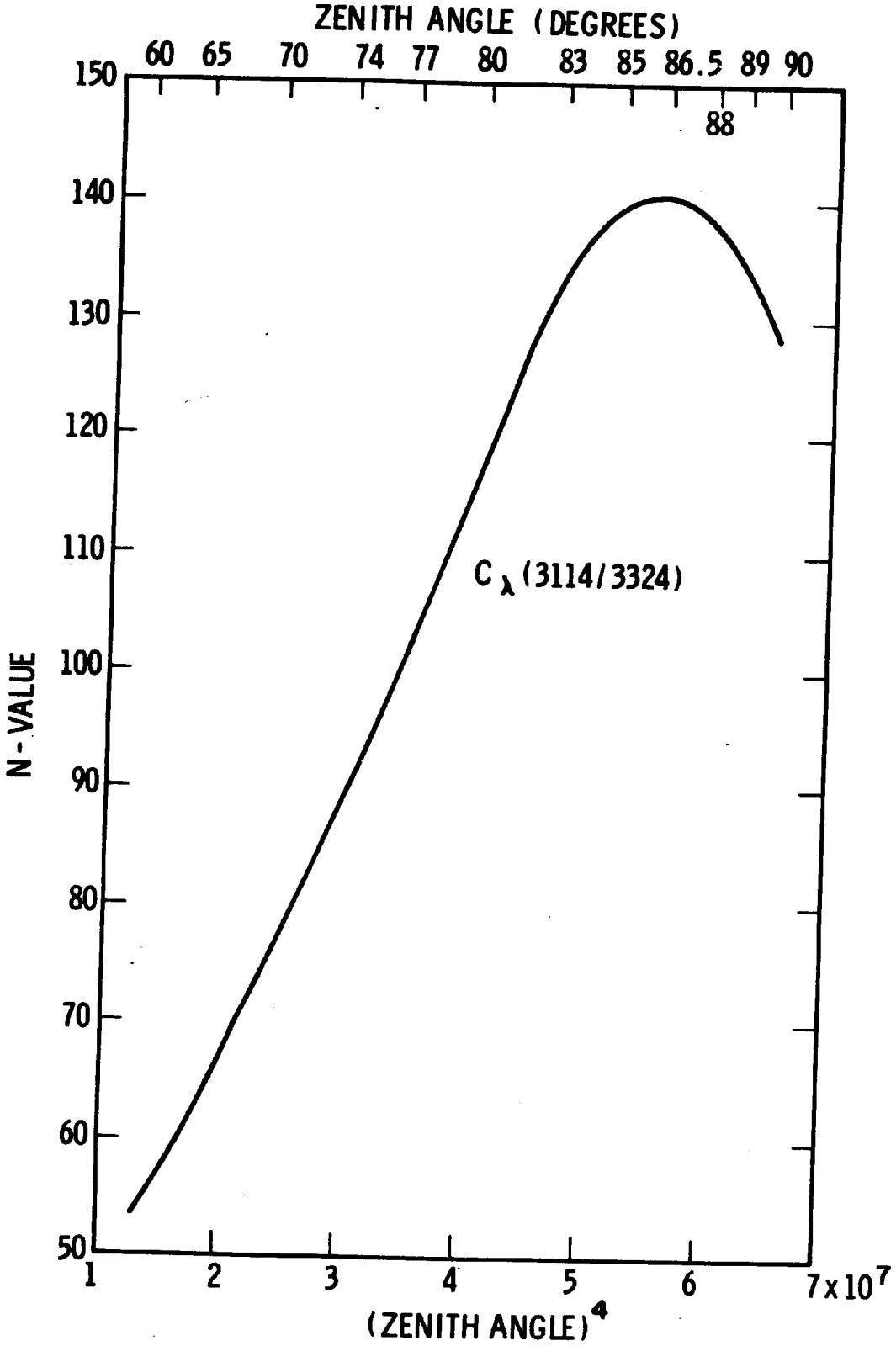


Fig. 1. Umkehr curve for observations at Edmonton on the afternoon of May 22, 1961.

The reason for the occurrence of this effect and for its sensitivity to the gross features of the vertical distribution of ozone were explained by Götz, Meetham, and Dobson (1934) as follows. We first note the main features of the vertical distribution of ozone as shown in Fig. 2, with a maximum of ozone partial pressure just above 20 km and lower values above and below this level. Considering light which is scattered only once in the atmosphere, the light received by the instrument is contributed by light scattered downwards from all levels in the atmosphere. The amount of light contributed by scattering at any particular level depends on (a) the number of air molecules available at that level to scatter the light, and (b) the absorption by ozone and the scattering by air molecules both before and after the scattering. For any given zenith angle of the sun, the effect of (a) is to decrease the contribution as height increases, while the effect of (b) is to increase the contribution, since more and more of the longer slant path of the direct ray before the scattering event is replaced by the shorter vertical path after the scattering event. It turns out (see Figs. 19-21) that, for a given zenith angle, the light contributing to the intensity comes from a fairly well-defined layer of the atmosphere and that it is possible to consider an effective scattering height. This effective scattering height depends on the ozone absorption coefficient and on the solar zenith angle, increasing, in fact, with each of these. Hence, the effective scattering height will always be higher for the short wavelength which is more strongly absorbed. Thus, as the sun approaches the hori-

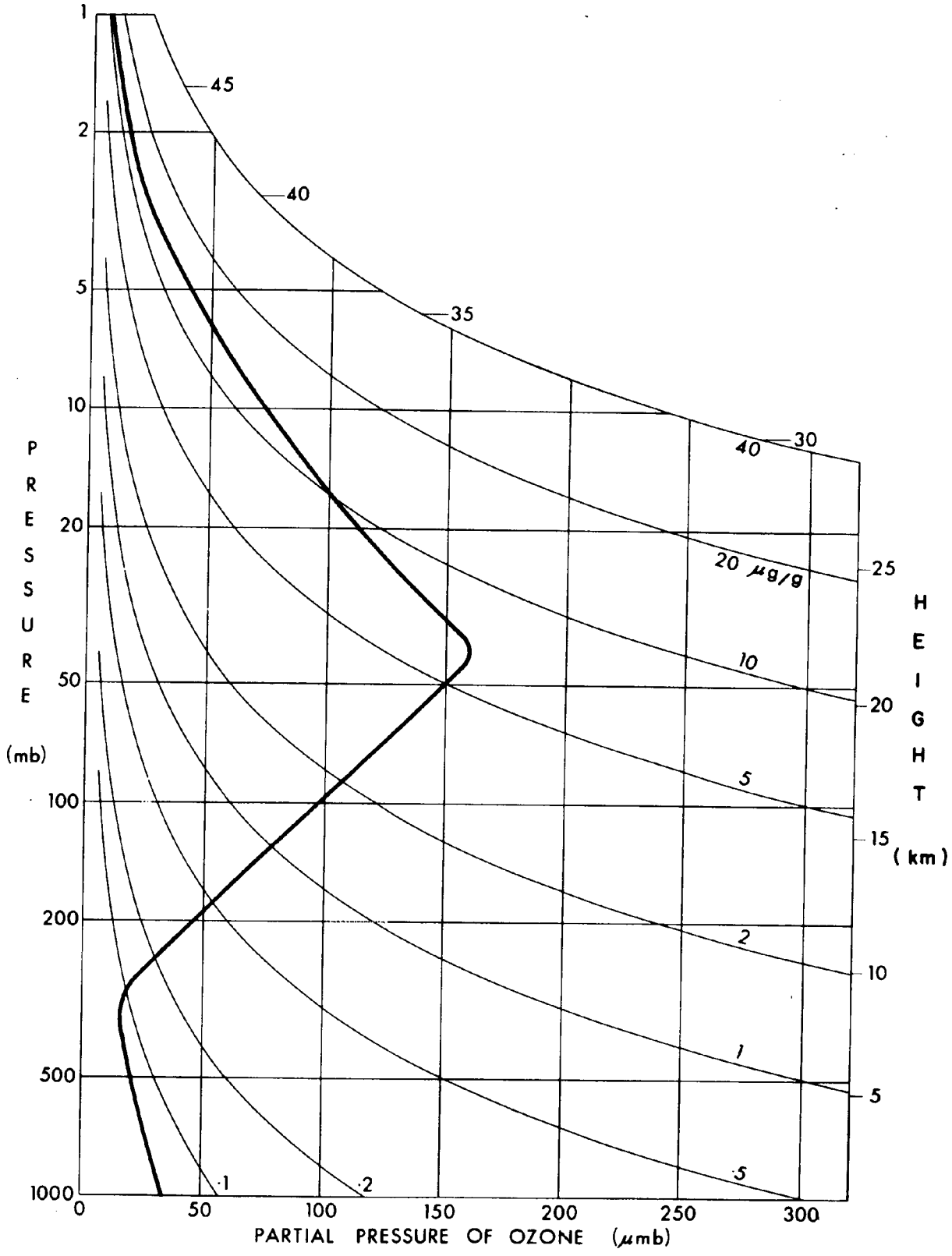


Fig. 2. Average vertical distribution of ozone from ozone sonde and Umkehr data (Table 16).

zon, the two intensities decrease, but I more rapidly than I', so that I/I' decreases. However, when the effective scattering height for the short wavelength is above the ozone maximum, I decreases more slowly than I', because the ozone absorption occurs mostly in the shorter vertical path after the scattering event, and the ratio I/I' increases until the effective scattering height for I' is also above the ozone maximum. Then the ratio I/I' again decreases. For all pairs of wavelengths used with the ozone spectrophotometer, this second reversal occurs when the sun is below the horizon.

It is clear that the existence of the reversal or inversion in the Umkehr curve implies the existence of a maximum of ozone concentration at some level in the atmosphere. Moreover, one would expect the position of the reversal to be related to the total amount of ozone and to the position of this concentration maximum in the atmosphere. Thus, it is reasonable to expect to be able to infer some information about the vertical distribution of ozone from measurements of the Umkehr effect.

1.3 THE PROBLEM AND THE APPROACH

In recent years, ozone workers have sought to extract more and more information about the vertical distribution of ozone from Umkehr observations. In particular, there has been considerable interest in the possibility that the main features of the lower stratospheric structure, viz., the existence or nonexistence of the so-called secondary maximum, might be inferred from such observations. The aim of the present study

was to determine precisely how much information about the vertical distribution of ozone could be obtained from the Umkehr observations, with particular reference to the lower stratospheric structure. As a by-product of this study, an extension of the Dütsch evaluation technique has led to the development of another method for estimating the vertical distribution. This method, which was developed independently of a very similar one proposed by Twomey (1963), takes into account the actual information content of the observations and, in addition, permits the incorporation of known facts about the vertical distribution and its variability as mathematical constraints on the solution.

Following a brief review of the literature pertaining to research on Umkehr evaluation techniques in the second chapter, the problem of determining the information content of the observations is approached from two quite separate points of view. First, in the third chapter, the problem of statistically deriving a linear transformation between the points on the Umkehr curve and the vertical distribution is considered by examining the curve to determine how many linearly independent pieces of information may be derived from it. In this process, the characteristic patterns of the Umkehr curve, and their relative importance, are determined. Second, in the fourth chapter, the linear physical-mathematical transformation of Dütsch is examined by eigenvalue analysis to determine the number of pieces of information that may be deduced from the system. From this analysis, another method of solving for the vertical distribution is developed and its approximate equivalence to the

method proposed by Twomey is indicated. Finally, in the fifth chapter, the imposition of constraints consistent with our independent knowledge of the vertical distribution is considered and results are presented showing the effects of these constraints on the derived vertical distribution. The results are compared with those obtained by Dütsch. In addition, other possible solution methods are discussed and some results presented.

2. REVIEW OF UMKEHR EVALUATION TECHNIQUES

2.1 PRELIMINARY REMARKS

Certain basic principles are common to all evaluation techniques and it will be convenient to discuss these first. The evaluation of the Umkehr effect involves the computation, by numerical quadrature, of the quantity log I'/I plus an unknown instrumental constant. This constant is usually eliminated by taking a further ratio. Thus, if θ is the solar zenith angle, we use $(\log I'/I)_{\theta} - (\log I'/I)_{\theta_o}$, where θ_o is a zenith angle such that the quantity $(\log I'/I)_{\theta_o}$ depends mostly on the total amount of ozone and very little on the vertical distribution.

Referring to Fig. 3, if I_o is the intensity in a narrow spectral region outside the earth's atmosphere, then the intensity, I_s, at the scattering point will be,

$$I_s = I_o \exp\left\{-\int_z^{\infty} (\alpha r_3 + \beta)(\sec \zeta)\rho dh\right\} \qquad (1)$$

where depletion by ozone absorption and molecular scattering only are considered, and where

α = ozone absorption coefficient (gm^{-1})

r_3 = ozone mixing ratio (mass of ozone/mass of air containing the ozone) at height h

β = Rayleigh scattering coefficient (gm^{-1})

ζ = angle of incidence of direct beam at height h, and

ρ = air density at height h.

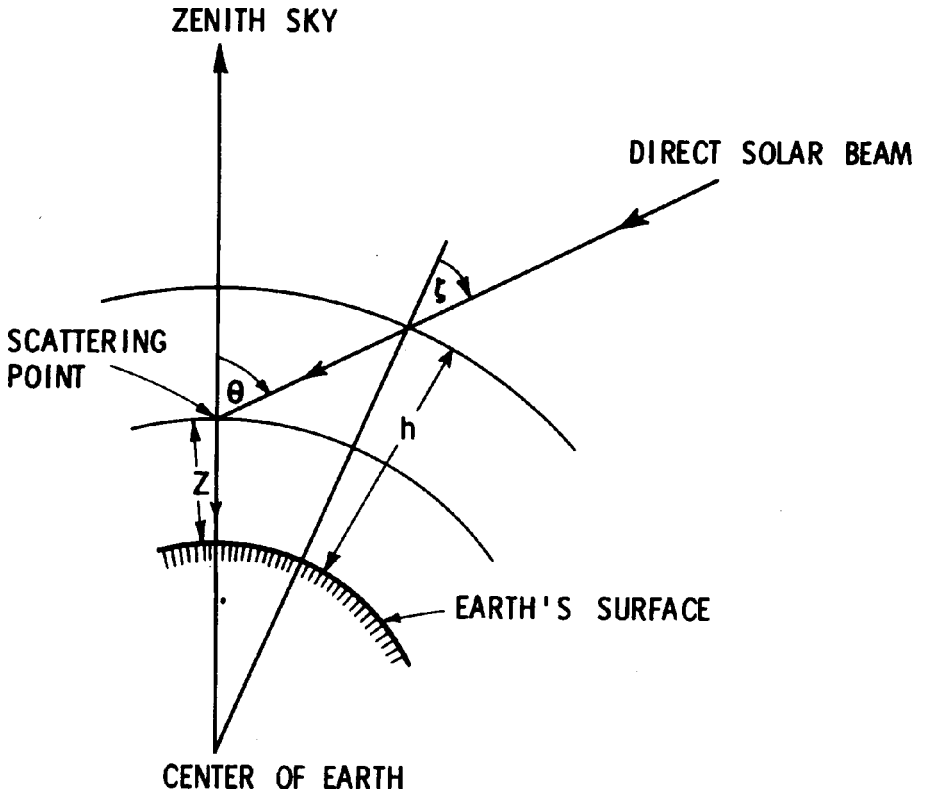


Fig. 3. Schematic diagram showing the path of the direct solar beam to the scattering point and that of the scattered beam from there to the instrument on the ground.

The amount of energy scattered downwards in the direction of the instrument from the air molecules in a layer of thickness dz is just

$$dI_S = K\beta(1+\cos^2\theta)I_S\rho dz \qquad (2)$$

where K is a constant. This energy will undergo further depletion in its vertical path from the scattering point to the instrument. The amount of this energy finally received at the instrument is

$$dI = dI_S \exp\left\{-\int_0^z (\alpha r_3+\beta)\rho dh\right\} \quad . \qquad (3)$$

The total intensity received at the instrument, for light scattered down-

wards at all heights in the atmosphere, is obtained by integrating (3) over the entire vertical column. Combining (1), (2), and (3), the total intensity I is then given by

$$I = I_o K\beta(1+\cos^2\theta)\int_o^\infty \exp\left\{-\int_o^z(\alpha r_3+\beta)\rho dh-\int_z^\infty(\alpha r_3+\beta)(\sec\zeta)\rho dh\right\}\rho dz \quad . \tag{4}$$

A similar expression is valid for I', the intensity of the longer wavelength. The evaluation of (4) involves a double quadrature, since ρ, r_3, and ζ are all functions of height. First, we have to evaluate the exponent in the exponential term by a quadrature. We may compute a source function

$$\chi(z) = \rho(z)\cdot\exp\left\{-\int_o^z(\alpha r_3+\beta)\rho dh - \int_z^\infty(\alpha r_3+\beta)(\sec\zeta)\rho dh\right\} \tag{5}$$

and then perform a second quadrature to evaluate the integral of $\chi(z)$ over all heights. The above expression may be simplified slightly by noting that multiplying factors common to both I and I' will cancel out when the ratio is taken. Moreover, multiplying factors common to all zenith angles will cancel out when the instrumental constant is eliminated. Thus we may omit from further consideration the quantity

$$K\beta(1+\cos^2\theta)\exp\left\{-\int_o^\infty(\alpha r_3+\beta)\rho dh\right\} \quad .$$

The quantity remaining may be written as

$$Q(\theta) = \int_o^\infty \exp\left\{-\int_z^\infty(\alpha r_3+\beta)[(\sec\zeta)-1]\rho dh\right\}\rho dz \tag{6}$$

and the source function of (5) redefined as

$$\chi(\theta,z) = \rho(z)\exp\left\{-\int_z^\infty (\alpha r_3+\beta)[(\sec\zeta)-1]\rho dh\right\} \quad . \qquad (7)$$

The quantity required for comparison with the instrumental observations is

$$100\left\{\log\left(\frac{Q'(\theta)}{Q(\theta)}\right) - \log\left(\frac{Q'(\theta_o)}{Q(\theta_o)}\right)\right\} \quad .$$

2.2 METHOD A

The classical method A was developed by Götz, Meetham, and Dobson (1934) and yields an approximate picture of the vertical distribution of ozone. The method has also been used by Tønsberg and Langlo (1944). More recently, Walton (1957) compiled instructions for use during the International Geophysical Year (IGY). The method described here is that of Walton, which differs only slightly from the earlier methods. The atmosphere is divided up into five layers as shown in Fig. 4, which also indicates the symbol used for the amount of ozone in each layer. The symbol Ω is used for the total amount of ozone and k is a constant derived from aircraft measurements, which have shown that ozone concentration in the troposphere is nearly proportional to the total amount (Kay et al., 1954). The uppermost ozone-bearing layer, in which ozone decreases rapidly with height, is split up into three sublayers for improved accuracy. The ozone concentration is assumed to be uniform in each of the layers or sublayers. For all rays scattered downwards within each layer, a mean ozone absorption path through each layer is computed by taking

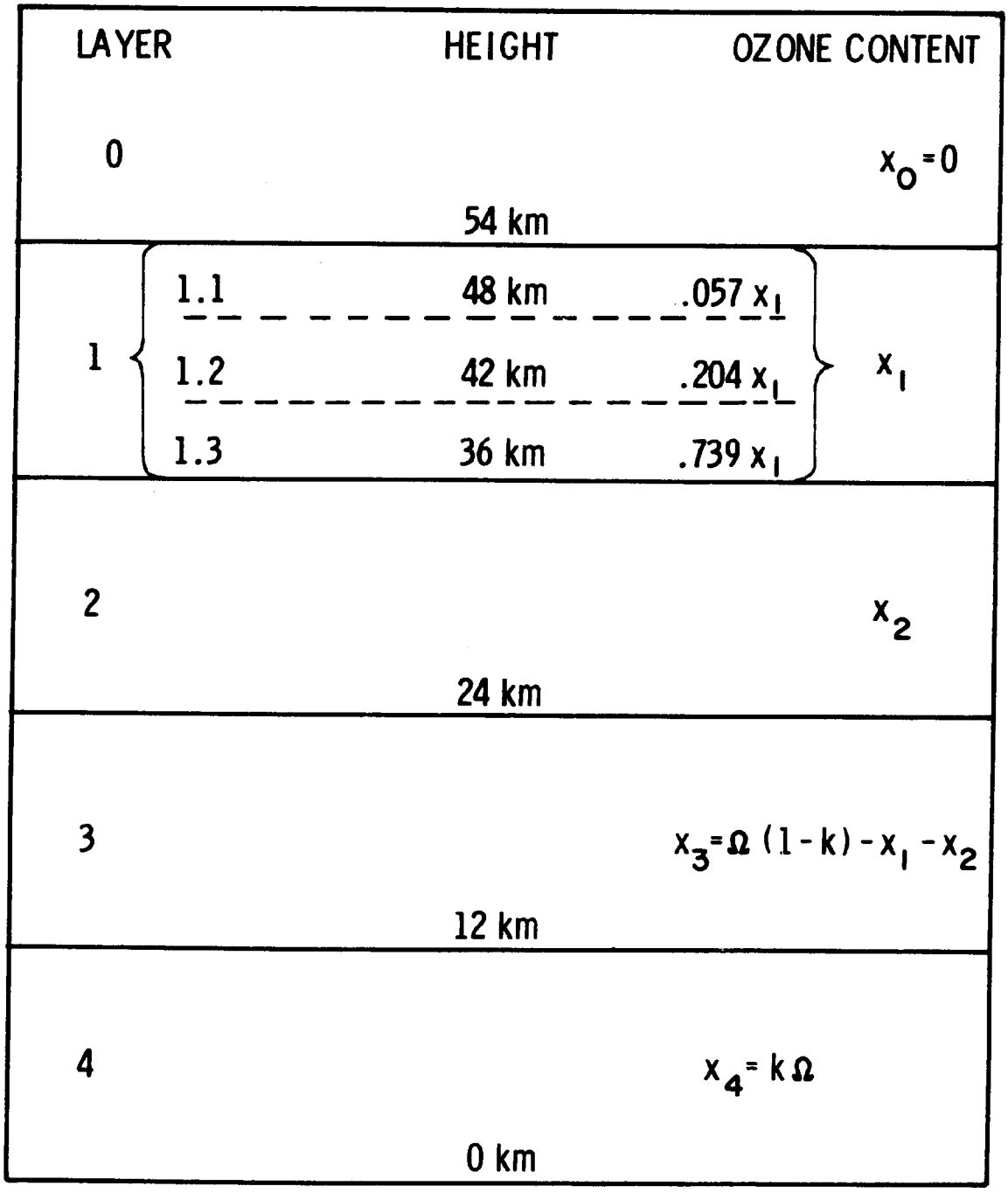


Fig. 4. Schematic diagram showing the atmospheric layer division used in Method A (after Walton).

the average of the geometric paths for rays separated by 1-km intervals in the vertical. Thus, if i refers to the layer in which the scattering event takes place, and j to a layer in which absorption occurs, we may define an ozone absorbing mass, ℓ_i, as follows:

$$\ell_i = \sum_{j=0}^{i} \overline{[(\sec\zeta)-1]}_{ij} x_j \tag{8}$$

where the bar refers to an average for rays, through the jth layer, which are scattered downward in the ith layer. More generally, an ozone absorbing mass, ℓ, and a Rayleigh scattering mass, L, may be defined as follows:

$$\begin{aligned} \ell &= \int_z^\infty [(\sec\zeta)-1] r_3 \rho dh \\ L &= \int_z^\infty [(\sec\zeta)-1] \rho dh \end{aligned} \tag{9}$$

Substituting these in (6), we get

$$\begin{aligned} Q(\theta) &= \int_0^\infty e^{-\alpha\ell-\beta L} \rho dz \\ &= \sum_{i=0}^{4} e^{-\alpha\ell_i} \int_{z_i}^{z_{i-1}} e^{-\beta L} \rho dz \end{aligned}$$

or

$$Q(\theta) = \sum_{i=0}^{4} A_i e^{-\alpha\ell_i} \quad , \tag{10}$$

where α is now in $(\text{m atm-cm})^{-1}$, because ℓ_i is expressed in m atm-cm. Since $\rho e^{-\beta L}$ is always positive, the approximation of (10) is a legit-

imate one, provided the correct value of l_i is used. However, l_i as defined by (8) is not, in general, the correct value. Indeed, since the averaging is carried out over rather deep layers of the atmosphere, one would expect a not inappreciable error to be introduced.

It is customary to use tabulations of Bemporad's function, or Chapman's grazing incidence integral (Wilkes, 1954), to get L. Finally, we may compute the quantity

$$\eta(\theta_k,\Omega,x_1,x_2) = 100\left\{\log\frac{Q'(\theta_k)}{Q(\theta_k)} - \log\frac{Q'(\theta_o)}{Q(\theta_o)}\right\} \qquad (11)$$

which we wish to have agree with the observed quantity

$$N(\theta_k,\Omega,x_1,x_2) = 100\left\{\left(\log\frac{I'}{I}\right)_{\theta_k} - \left(\log\frac{I'}{I}\right)_{\theta_o}\right\} . \qquad (12)$$

Walton provides tables for calculating η for $\theta_o = 60°$, $\theta_1 = 80°$, and $\theta_2 = 86.5°$. In their original paper, Götz et al., recommended the use of an additional angle as a check. In practice, a series of values of x_1 is chosen, then calculations are performed to find, by successive approximations, the value of x_2, such that

$$\eta(\theta_k,\Omega,x_1,x_2) = N(\theta_k,\Omega,x_1,x_2), \qquad k=1,2 \quad .$$

The results are plotted in a graph as in Fig 5. The intersection of the two curves gives the desired solution.

The calculations are somewhat tedious and Walton (1959) has essentially pre-computed all possible solutions and plotted the results on a series of graphs so that the points required to plot the curves in

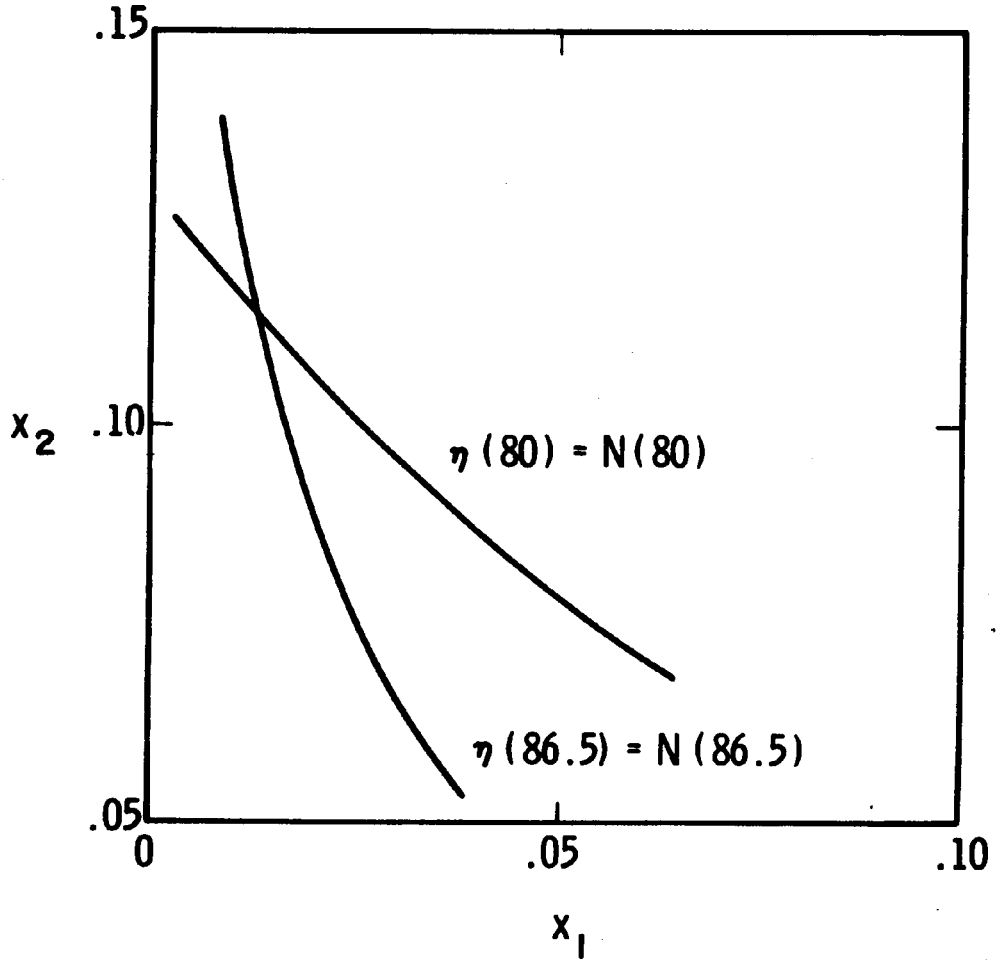


Fig. 5. Curves of $\eta(\Theta_k,\Omega,x_1,x_2) = N(\Theta_k,\Omega,x_1,x_2)$ for $\Theta_1 = 80°$ and $\Theta_2 = 86.5°$, on x_1, x_2 diagram.

Fig. 5 may be read directly without computation. The resulting solution for the vertical distribution is usually plotted as a block diagram, and a smooth curve, which leaves the same amount of ozone in each layer, is drawn through the block distribution.

Method A serves to give a rather crude picture of the vertical distribution. However, although the physical-mathematical model of the atmosphere is a little crude and the final solution depends on the layer division chosen, the method certainly has the advantage of objectivity in

that a "unique" solution is obtained.

2.3 METHOD B

The classical method B was also developed by Götz et al., in an attempt to use more information from the Umkehr curve to obtain greater detail in the vertical distribution. The method has also been used by Karandikar and Ramanathan (1949). Instructions for use during the IGY were prepared by Ramanathan and Dave (1957) and the summary given below follows these.

The ozone-bearing atmosphere is divided into nine layers, each 6 km thick, with ozone density assumed constant in each layer. In order to calculate the light scattered downward into the instrument, the entire mass of air in each layer is assumed to be concentrated at a height of 2 km above the base of the layer. Thus only a single ray is traced for each scattering layer and, in the notation of this study, we have for the ozone absorbing mass

$$\ell_i = \sum_{j=i}^{9} \overline{[(\sec\zeta)-1]}_{ij} x_j \qquad (13)$$

for light scattered downward from the ith layer. In this case, as opposed to method A, the layer number increases upwards. The quantity L_i is determined from Wilkes tabulation and we get the equivalent of (10) to be

$$Q(\theta) = \sum_{i=1}^{10} m_i e^{-\alpha\ell_i - \beta L_i} \qquad (14)$$

where m_i is the mass of air in the ith layer, and the 10th layer embraces the entire atmosphere above 54 km. The final quantities to be compared are

$$\eta(\theta_k, x_1, \ldots, x_9) = 100 \left\{ \log \frac{Q'(\theta_k)}{Q(\theta_k)} - \log \frac{Q'(\theta_o)}{Q(\theta_o)} \right\} \qquad (15)$$

and the observed quantity

$$N(\theta_k, x_1, \ldots, x_9) = 100 \left\{ \left(\log \frac{I'}{I} \right)_{\theta_k} - \left(\log \frac{I'}{I} \right)_{\theta_o} \right\} . \qquad (16)$$

Ramanathan and Dave present tables to assist in the computation of η for $(\theta_o, \ldots, \theta_7) = (60°, 70°, 75°, 80°, 84°, 86.5°, 88°, 90°)$. An additional requirement is, of course, that the sum of the layer amounts equal the observed total amount of ozone. In the suggested method of solution, a trial distribution is assumed and the associated Umkehr curve is calculated and compared with the observed one. Then adjustments are made in the distribution until the calculated and observed curves agree within experimental error.

To facilitate this adjustment process, Mateer (1960) calculated values of $\eta_k = \eta(\theta_k, x_{1s}, \ldots, x_{9s})$ and of the first order partial derivatives $\partial\eta_k/\partial x_i$ for three "standard" vertical distributions of ozone. (The subscript s refers to layer ozone amounts in the standard distribution of ozone.) The evaluation then consisted of solving, by hand relaxation, a set of eight linear equations in nine unknowns, viz.,

$$\sum_{i=1}^{9} \delta x_i = \Omega - \Omega_s$$

$$\sum_{i=1}^{9} \frac{\partial \eta_k}{\partial x_i} \delta x_i = N_k - \eta_k \quad . \qquad k=1,\ldots,7 \tag{17}$$

where $\delta x_i = x_i - x_{is}$ represents the deviation of the solution from the standard distribution. This method has also been used by Muramatsu (1961) who calculated similar tables for three additional standard distributions.

Since the above system of equations is underdetermined, method B is a subjective one and "unique" solutions are not possible, regardless of whether the approximate linear method or the successive approximations method is used. This nonuniqueness was clearly recognized by Götz et al., in the original paper on this method. They noted, for example, "we may conclude that the shape of the Umkehr curve depends mainly on the value of" Ω. Moreover, they found that there was no advantage in using many points from the Umkehr curve because "more than six points would be much more interdependent." They worked mainly with mean Umkehr curves appropriate to a specific small range of values of total ozone, thereby minimizing random errors. Using fewer layers than Ramanathan and Dave, they essentially attempted to obtain five unknowns from seven equations by a "least square" solution method. For a single Umkehr curve, they note that "the probable errors of values of x_i... are so large that the resulting ozone distribution is almost meaningless." These "words of warning" should be kept in mind when reading the later chapters of this

report.

2.4 METHOD OF DÜTSCH

In a series of reports, Dütsch (1957, 1959a, 1959b, 1963) has introduced a measure of objectivity into Umkehr evaluations by method B. In fact, the method is completely objective once the basic solution system has been selected. Dütsch divided the atmosphere up into layers approximately 2.5 km thick, such that the pressure at the bottom of each layer was $\sqrt{2}$ times that at the top. He used three standard vertical distributions of ozone, with ozone in each layer up to 72 km. The ozone amounts in the upper layers were based on his photochemical calculations. With the assumption that ozone density was constant in each layer, and using Bemporad's function, his quadrature formula was

$$I = I_o K\beta(1+\cos^2\theta) \sum_{i=1}^{n} \frac{\Delta p_i}{p_o} e^{-\beta L} \exp\left[-\alpha\left\{\sum_{k=1}^{i} x_k + \sum_{k=i+1}^{n} a_{ik}x_k\right\}\right] \quad (18)$$

where a_{ik} is the relative slant path through the kth layer for the ray scattered downward in the ith layer, Δp_i is the pressure difference between the top and bottom of the ith layer, and p_o = 1013.250 mb, the surface pressure in the standard atmosphere.

In calculating values of η_k for comparison with the observations N_k, Dütsch does not eliminate the instrumental constant but estimates it empirically. Moreover, he does not use directly in the solution system the requirement that the vertical distribution be exactly equivalent to the

measured total amount of ozone. Instead, he uses the comparison between computed total ozone and observed total ozone as a check on the accuracy of his solution.

He defines

$$f_i = \frac{x_i}{x_{is}}$$

and

$$\Delta f_i = f_i - 1 = \frac{x_i - x_{is}}{x_{is}} \quad . \tag{19}$$

Then, using Taylor's expansion, we have

$$N_k \cong \eta_k + \sum_{i=1}^{n} \frac{\partial \eta_k}{\partial f_i} \Delta f_i + \frac{1}{2} \sum_{i=1}^{n} \sum_{j=1}^{n} \frac{\partial^2 \eta_k}{\partial f_i \partial f_j} \cdot \Delta f_i \cdot \Delta f_j \quad . \tag{20}$$

If we ignore the last term on the right-hand side of (20), the problem is reduced to one of finding the solution of a set of simultaneous linear algebraic equations. Assuming such a solution exists, using superscript m to denote the mth iteration, and defining,

$$S_k^{(o)} = 0$$

$$S_k^{(m)} = \frac{1}{2} \sum_{i=1}^{n} \sum_{j=1}^{n} \frac{\partial^2 \eta_k}{\partial f_i \partial f_j} \cdot \Delta f_i^{(m)} \cdot \Delta f_j^{(m)} \quad . \tag{21}$$

then we have

$$\sum_{i=1}^{n} \frac{\partial \eta_k}{\partial f_i} \Delta f_i^{(m)} = N_k - \eta_k - S_k^{(m-1)}, \qquad k=1,\ldots,12 \tag{22}$$

as the basis for an iterative solution procedure. The iteration may be stopped whenever

$$\sum_{k=1}^{12} \left| S_k^{(m)} - S_k^{(m-1)} \right| \leq \epsilon \qquad (23)$$

where ϵ is some suitably small number. Dütsch found that the tropospheric layers could not be subdivided because the derivatives were too similar for these layers. He found the same to be true for the layers above 2 mb. Hence, he combined the tropospheric derivatives into a set for a single layer and did the same thing for the layers above 2 mb. In these combined layers, he assumed that ozone always appeared in the same relative proportions as in the standard distribution. This left the unknown vertical distribution as a set of nine quantities to be determined.

Dütsch used a total of 12 zenith angles (60, 65, 70, 74, 77, 80, 83, 85, 86.5, 88, 89, 90) and computed η_k, $\frac{\partial \eta_k}{\partial f_i}$, and $\frac{\partial^2 \eta_k}{\partial f_i \partial f_j}$, for these 12 zenith angles and for each of three standard distributions. In attempting to solve for the vertical distribution in the nine layers directly from a set of nine linear equations, he obtained physically unrealistic results, including negative ozone densities in certain layers, and solutions that exhibited large variations in ozone concentration from one layer to the next. He attributed this difficulty to the inaccuracies of the measurement and to the linearity imposed on a nonlinear problem. To get around these difficulties, he gradually evolved a system whereby the nine atmospheric layers were combined into sets and subsets of over-

lapping layers. In each overlapping layer, he assumed that the fractional change in ozone content was the same in each of the original layers comprising the larger overlapping layer. In each subset, he effectively had a set of at most five linear equations in five unknowns. The solutions for the subsets were averaged to get an average for each set and, finally, the set solutions were averaged to obtain the final solution for the linear system. The second order derivative corrections $S_k^{(1)}$ were then calculated, the right-hand side of (22) adjusted, and the linear solution repeated, the iteration being stopped when the condition of (23) was met. The entire solution procedure as now used requires approximately 1.5 seconds of computer time on the IBM 7090, most of the time being taken up in the computation of the $S_k^{(m)}$. Further details of the Dütsch method are given in Appendix B.

The procedure is clearly an objective one, once the basic systems of overlapping layers have been selected, and provides a smoothed picture of the vertical distribution.

2.5 SOURCES OF ERROR

2.5.1 Multiple Scattering and Reflected Light

Quite apart from the fundamental mathematical difficulties in the solution of Eq. (22), which will be discussed later, there are a number of errors inherent in the physical-mathematical model used to compute the synthetic Umkehr curves. The major source of error, which has received much attention during the past decade, is the effect of multiple scattered

light which contributes to the intensity of the light entering the instrument.

Following Ramanathan and Dave, if we let P, P' be the intensities of primary scattered light and M, M' the intensities of multiple scattered light for the short and long wavelengths of a pair, then we have that

$$\frac{I'}{I} = \frac{P'+M'}{P+M} = \frac{P'}{P}\left(\frac{1+\frac{M'}{P'}}{1+\frac{M}{P}}\right) \quad . \tag{24}$$

Hence, if M/P and M'/P' were known, the observed Umkehr curve could be "corrected" to a basis of primary scattering and the computation, using P, P', could proceed as previously.

Walton (1953) calculated the ratios S/P, S'/P', where S,S' are the intensities of secondary scattered light. He assumed a plane parallel atmosphere with the total atmospheric ozone content concentrated in a thin layer at the center of gravity of the ozone distribution. He found that the corrections varied with solar zenith angle but were nearly constant for zenith angles between 80 and 88°. The effect of the secondary scattering correction was to decrease the computed amount of ozone at higher levels and to increase it at lower levels. That is to say, the center of gravity was lowered by some 2-3 km. Walton's corrections are given in the first column of Table 1.

Ramanathan, Moorthy, and Kulkarni (1952) used simultaneous Umkehr curves for two pairs of wavelengths (3112/3323 A) and (3075/3278 A), to

TABLE 1

HIGHER ORDER SCATTERING CORRECTIONS TO BE SUBTRACTED
FROM OBSERVED N-VALUES AT VARIOUS ZENITH ANGLES

Investigator:	Walton	Ramanathan & Dave	Dütsch				Larsen	Sekera & Dave
Wavelengths:	C	C	A	C	D	C	C	C
Total Ozone: (m atm-cm)	400	---	336	336	336	336	360	250
Zenith Angle (degree)								
60	0	0	3.6	0.5	-1.8	0.4	3	2
70	1.5	1	5.9	0.3	-3.0	0.3	4	4
75	3	2	10.7	1.5	-3.6	0.6	5	6
80	6	4.5	18.2	6.0	-3.2	2.3	10	11
84	6	6	22.2	13.6	1.1	5.0	--	14
86.5	6	6	21.7	16.2	4.9	6.2	10	13
88	-	6	20.1	15.6	6.9	6.2	--	11
90	-	6	13.7	8.6	2.2	4.0	--	--

deduce an Umkehr curve for (3075/3112 A) by eliminating the effects of (3278/3323). They do not state how the effects of the latter pair were eliminated, but it appears likely that they used the "double" wavelength pair obtained by subtracting the N-values for the first pair from those for the second and assumed this to be equivalent to using (3075/3112 A). They reasoned that (3075/3112) are both strongly absorbed by ozone and, hence, that the effects of multiple scattering would roughly balance out. Similar considerations should apply when the weakly-absorbed wavelengths (3278/3323) are compared. They concluded that vertical distributions calculated from (3075/3112) should, therefore, eliminate much of the effect of multiple scattering. They show results for Umkehr curves on three days and confirm Walton's result, namely that the effect of correcting for the higher order scattering is to lower the center of gravity of the derived vertical distribution. The corrections suggested for secondary scattering by Ramanathan and Dave are listed in the second column of Table 1.

Dütsch has also incorporated corrections for higher order scattering in his evaluation procedure, the effect being incorporated both in the standard Umkehr curves and in the first order partial derivatives. His quadrature formulation for computing the secondary scattering is given in Appendix B. If we let I_k represent the contribution to I due to kth order scattered light, then Dütsch assumed $I_k/I_{k-1} = C$, a constant being determined as I_2/I_1. It follows then that

$$I = I_1 + I_2 + \ldots = I_1\left(\frac{1}{1-C}\right) \quad . \qquad (25)$$

Multiple scattering corrections based on this assumption for Dütsch's first standard distribution, for the A, C, and D wavelength pairs, are listed in columns 3 to 5 of Table 1. This procedure appears to give too large a correction, that is to say, $I_2/I_1 > I_3/I_4 > \ldots I_k/I_{k-1}$. Dütsch's current procedure is to assume $I = I_1+I_2$ only. These corrections, for the C wavelength pair, are listed in the sixth column of Table 1.

Larsen (1959) has determined values of $(1+M'/P')/(1+M/P)$ based on an empirical analysis of skylight observations at different wavelengths. His results necessarily incorporate the effects of all orders of scattering and are listed in the seventh column of Table 1.

Sekera and Dave (1961) have computed the effects of multiple scattering for a plane parallel atmosphere using the C wavelength pair. They reason that the effective height of secondary scattered light (and also higher orders) is situated very near the ground and that the primary scattered radiation giving rise to the secondary scattering originates from a relatively narrow cone with its axis along the zenith. Consequently, they divide the atmosphere into two layers, viz., an upper layer containing all the ozone in which only primary scattering is considered and a lower layer in which no ozone is present but all orders of scattering are considered. Their results are presented in the last column of Table 1.

In comparing columns 1, 4, 6, 7, and 8 of Table 1, we note that there is fairly good agreement between Walton's results and those of Dütsch, in which only secondary scattering is considered. There is also moderately good agreement between the last two columns in which all orders of scattering seem to be included. There appear, however, to be moderate differences between Dütsch's results and the others for zenith angles between 70° and 80°. However, there is good agreement that the effect of multiple scattering corrections on the derived vertical distribution is to decrease the ozone content at high levels (above about 20 km) and to increase the ozone content of the atmosphere below this level.

Dave and Furukawa (1964) have examined the effect of ground albedo on Umkehr observations. They consider only primary scattering and calculate corrections applicable to the A and C wavelength pairs for a surface albedo of 80%, and total ozone amounts of 260 and 400 m atm-cm. Their corrections are shown in Fig. 6. They also show how the effect of low level clouds can be estimated from these results, when the clouds remain scattered to broken, so that zenith measurements can still be taken on blue sky. The corrections for ground reflection are somewhat smaller than those for higher order scattering and act in the opposite sense in that they are largest at 60° to 70°, and smallest when the sun is near the horizon, whereas the higher order scattering corrections are largest when the sun is near the horizon.

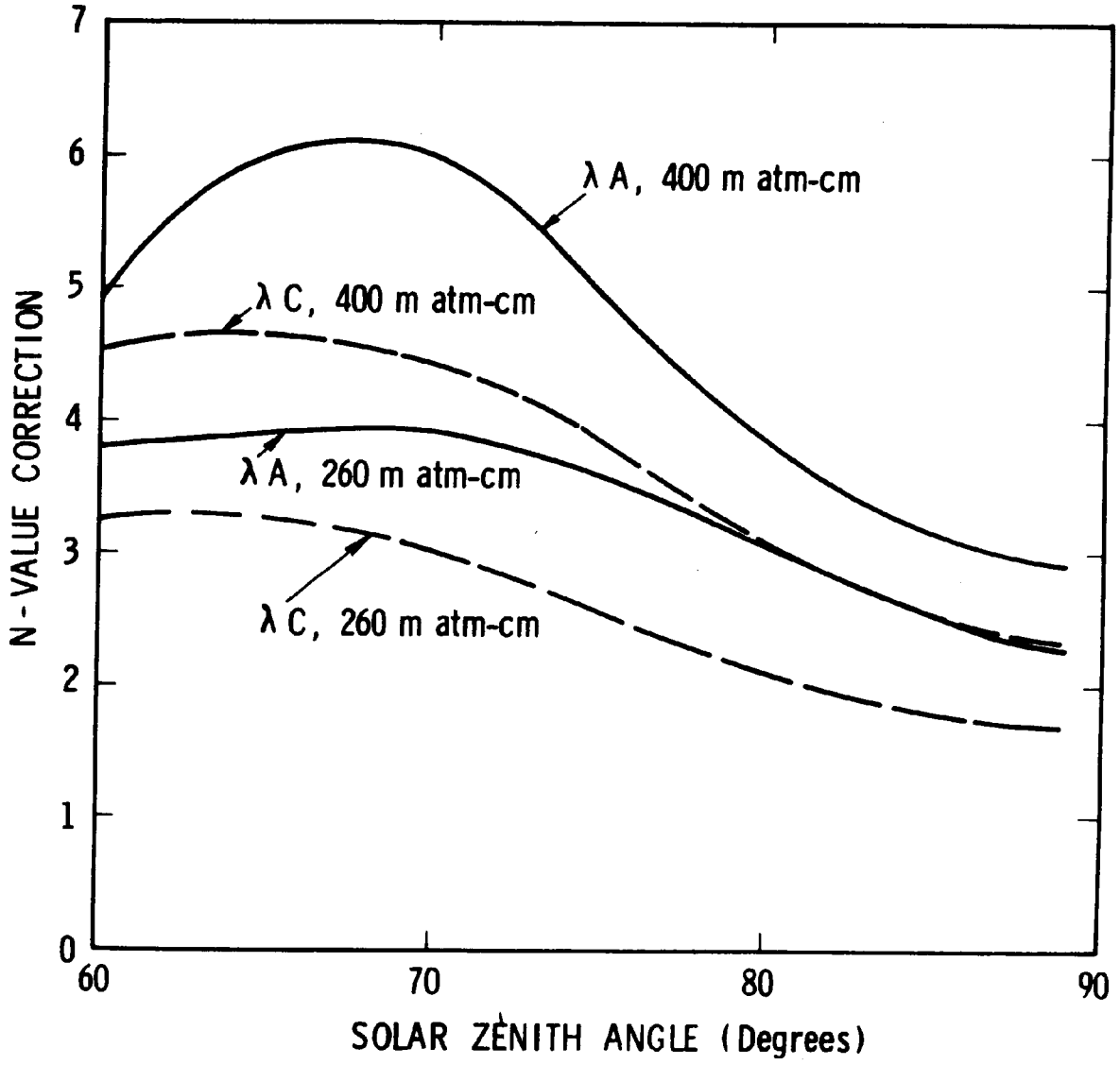


Fig. 6. Corrections (to be subtracted from observed N-values) for ground reflection in the case of 80% albedo. (After Dave and Furukawa.)

2.5.2 Empirical Cloud Corrections and Large Particle Scattering

Dütsch has devised an empirical method for correcting Umkehr curves taken on cloudy zenith sky, based on a comparison of the intensities of visible to ultraviolet skylight. The corrections, which are always subtracted from the observed values, are shown in Fig. 7 as a function of

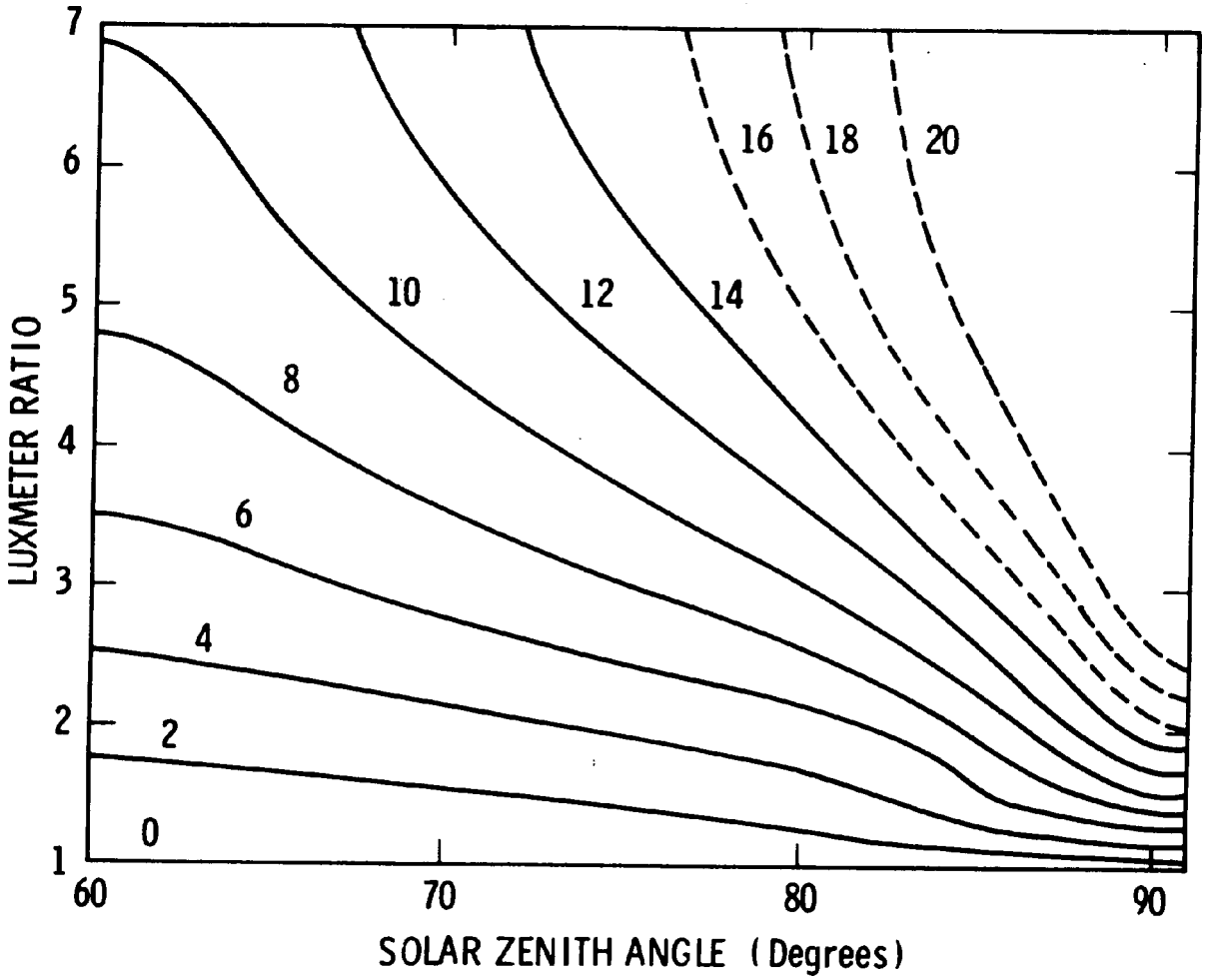


Fig. 7. Cloud corrections (N-units to be subtracted from observed values) as a function of luxmeter ratio and solar zenith angle.

luxmeter reading and solar zenith angle. The luxmeter readings used in the graph are deviations of the observed visible/ultraviolet light ratio from that obtaining under very clear sky conditions at the same zenith angle. The corrections are derived empirically. A sample Umkehr curve showing both the observed and corrected points is plotted in Fig. 8. Dütsch finds this correction procedure satisfactory provided the cloud interference (the magnitude and variability of the corrections) is not too great.

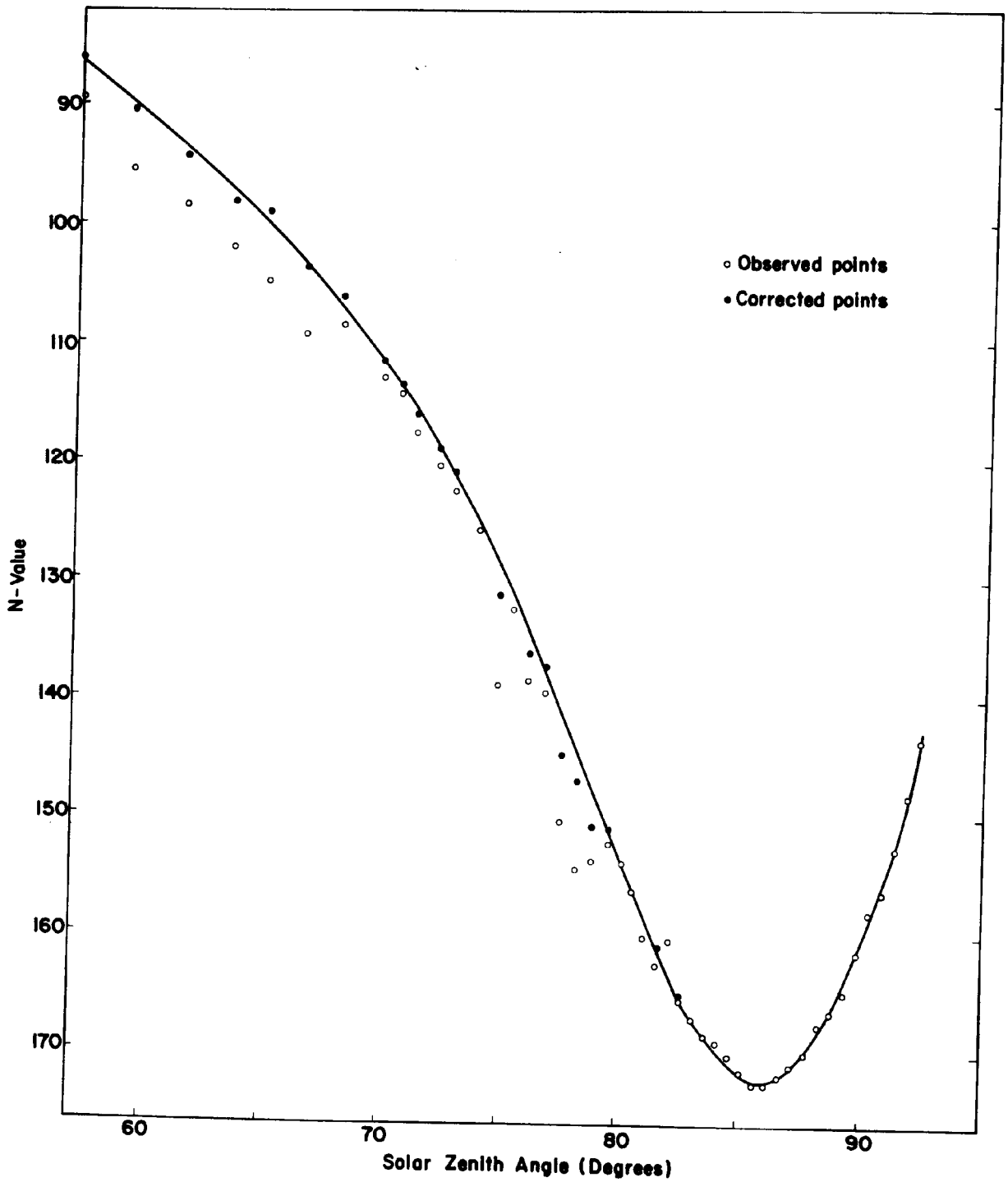


Fig. 8. Sample Umkher curve for Arosa, March 30, 1962, showing observed values and corrected values. Total ozone is 394 m atm-cm.

The effects of large particle scattering on the Umkehr curve have not yet been considered in detail. By comparing Umkehr curves for Oxford and Tromsö, Larsen (1959) found persistent differences of 7 and 8 N-units at sec $\theta = 4$ and 8, respectively. However, at least part of this difference is undoubtedly due to differences in the mean vertical distributions over these two stations. Dütsch's cloud corrections include some large particle scattering effect, since he occasionally should apply a cloud correction on apparently clear sky, according to his luxmeter readings.

3. THE CHARACTERISTIC PATTERNS OF UMKEHR CURVES

3.1 PRELIMINARY REMARKS

It is a natural property of a geophysical variable, which is measured sequentially in time at a network of points, that a high degree of spatial correlation will exist between the individual measurements over the network of points. In addition, a high degree of serial correlation will exist in the individual series of measurements at each of the fixed points. In the case of Umkehr observations, it is natural to inquire into the degree of independence of the individual measurements in a single series of measurements on a given half-day. For example, is the measurement at a solar elevation of 1° independent of the observations at 0° and 2°? As noted earlier, Götz *et al.* recognized a strong degree of interdependence between the points on the Umkehr curve and also remarked that the main features of its shape seemed strongly related to the total amount of ozone. There were, however, certain variations in the curve, total ozone remaining constant, that suggested a variability in the vertical distribution.

The question of interdependence also arises in the formulation of a purely statistical technique for evaluating the Umkehr effect. Suppose we let $p_1,\ldots,p_9$ be the mean ozone partial pressures in nine layers of the atmosphere, such that these nine numbers specify the complete vertical distribution. Suppose further than we have measurements at 12

points on the Umkehr curve $u_1,\ldots,u_{12}$. If we have a number of sets of observations of both these quantities, we may attempt to derive a linear statistical transformation to predict the p_i from the u_j. Thus

$$\hat{p}_i = \sum_{j=1}^{12} a_{ij}u_j \tag{26}$$

where the $\hat{p}_i$ are the estimates of the mean ozone partial pressures in the nine atmospheric layers and the a_{ij} are the elements of the coefficient matrix of the transformation. In matrix notation

$$\hat{P} = AU \tag{27}$$

where the elements of $\hat{P}$ are $\hat{p}_{ik}$ representing the estimate for the ith layer and the kth observation and the elements of U are u_{jk} representing the jth point on the kth Umkehr curve. There is no loss in generality in letting the p_i and u_j be measured from their respective means, in which case the least squares solution for A is simply

$$A = (PU^*)(UU^*)^{-1} \tag{28}$$

where U* is the transpose of U. The transformation matrix A exists if and only if the inverse of UU* exists, that is to say, UU* must be non-singular. If there are strong linear interdependencies between the points on the Umkehr curve, the matrix UU* will be singular or very nearly so and the matrix A will, for all practical purposes, not exist.

3.2 THE STATISTICAL PROCEDURE

To investigate the degree of independence of the observations, we shall use the empirical orthogonal functions introduced to meteorologists by Lorenz (1956). According to Lawley and Maxwell (1963), the technique was put forward by Pearson in 1901, and later developed by Spearman in 1904 as Factor Analysis, which is much used by psychologists, and by Hotelling in 1933 as Principal Component Analysis. There is evidence of some disagreement between statisticians (compare, for example, Kendall (1957) and Lawley and Maxwell) as to the precise differences between these analysis techniques. These differences need not concern us here and, following meteorological practice, we shall use the terms "empirical orthogonal functions" (Lorenz) or "characteristic patterns" (Grimmer, 1963).

What we seek to do in this procedure is to effect a reduction in the number of variables required to describe the Umkehr curve so that the main features of the curve are retained and the random errors of measurement, the noise of the curve, are eliminated. This is essentially a filtering problem. To achieve this, we seek linear transformations, to a new set of variables y_i, of the form

$$y_{ik} = \sum_{j=1}^{12} b_{ij} u_{jk} \qquad (29)$$

where, as before, k represents the kth set of observations. In matrix notation

$$Y = BU \quad . \tag{30}$$

It follows immediately that, if $\bar{u}_j = 0$, then also $\bar{y}_i = 0$. We shall now require that the new variables y_i be uncorrelated. In matrix notation, this requirement may be written as

$$YY^* = \Lambda \tag{31}$$

where Λ is a completely diagonal matrix having nonzero elements on the diagonal only. Introducing (30) into (31), we have

$$B(UU^*)B^* = \Lambda \quad . \tag{32}$$

This is the well-known problem of determining the eigenvalues and vectors (latent roots and vectors or characteristic roots and vectors) of the real symmetric matrix UU^*, in which the elements are proportional to those in the covariance matrix of the points on the Umkehr curve. It can be shown that a solution exists in which the eigenvalues, the diagonal elements of Λ, are all real and nonnegative and the eigenvectors are stored in the rows of B. There is no loss in generality in assuming that the eigenvalues, λ_i, $i = 1,\ldots,12$, are stored in the diagonal elements of Λ in order of decreasing magnitude, provided that the rows of B are arranged accordingly, nor in requiring that the eigenvectors, which are orthogonal, be also orthonormal. That is to say,

$$BB^* = B^*B = I \tag{33}$$

where I is the identity matrix. These eigen, or characteristic, vectors are the spatial empirical orthogonal functions of Lorenz and have been dubbed "characteristic patterns" by Grimmer. We shall hereinafter refer to them as the characteristic patterns (C. P.'s) of the Umkehr curve. The reason for this nomenclature becomes clear if we expand the vector of points from each Umkehr curve in terms of these characteristic patterns. Thus, from (30) and (33), we have

$$U = B^{*}Y \quad . \tag{34}$$

It is useful now to introduce the concept of the "total variance" of the Umkehr curve as

$$v_k^2 = \sum_{j=1}^{12} u_{jk}^2 \quad . \tag{35}$$

It follows directly, from (33) and (34), that

$$v_k^2 = \sum_{i=1}^{12} y_{ik}^2 \quad . \tag{36}$$

Since y_{ik} is the coefficient of the ith pattern vector of B in the expansion (34), we have the result that the ith pattern "explains" y_{ik}^2/v_k^2 of the total variance of the Umkehr curve. Moreover, since

$$\sum_{k=1}^{n} y_{ik}^2 = \lambda_i \tag{37}$$

and

$$V = \sum_{k=1}^{n} v_k^2 = \sum_{k=1}^{n} \sum_{j=1}^{12} u_{jk}^2 = \sum_{k=1}^{n} \sum_{i=1}^{12} y_{ik}^2 \tag{38}$$

we may say that the fraction of the total variance, V, of the Umkehr curves explained by the ith pattern is just λ_i/V. Hence the patterns occur in B in the order of their ability to explain total variance of Umkehr curves. It can be shown (see Lorenz, 1956 or 1959, or Kendall, 1957) that the representation is an optimum one in the sense that among all possible linear combinations of the points on the Umkehr curve, these patterns account, successively, for the largest possible proportions of the total original variance.

3.3 THE APPLICATION OF THE STATISTICAL PROCEDURE

It was noted above that the solution procedure of Dütsch involves the selection of 12 points, $u_1,\ldots,u_{12}$, from each Umkehr curve. It was further noted that the more usual solution procedure of others would be, if u_{12} is the curve point corresponding to the greatest solar elevation, to use u_1-u_{12}, $u_2-u_{12},\ldots,$ $u_{11}-u_{12}$, with the total amount of ozone as the last number. Both of these procedures are used to represent the Umkehr curve in the present study. In addition, there are two possible choices for the matrix UU*, viz., the covariance matrix or the correlation matrix of the points of the Umkehr curve. The covariance matrix is UU* with each element divided by n, the number of Umkehr curves used. The correlation matrix is obtained from the covariance matrix by dividing the (i,j) element of the latter by the quantity

$$\left(\frac{1}{n}\sum_{k=1}^{n} u_{ik}^2\right)^{1/2}\left(\frac{1}{n}\sum_{k=1}^{n} u_{jk}^2\right)^{1/2}.$$

When the covariance matrix is used and total ozone is one of the "points" of the Umkehr curve, some choice must be made with respect to the weight with which total ozone enters. In the studies reported here, total ozone was entered in m atm-cm and the Umkehr curve points in 1000 log-units (as opposed to the customary 100 log-units).

Two basic data samples have been used. The first sample is from observations taken at North American stations, viz., Edmonton, Moosonee and Toronto, Canada, and Sterling, Virginia, in the United States. The sample comprises data for 98 Umkehr curves on wavelength pairs A, C, and D. The second sample is from Arosa, Switzerland, and comprises 100 Umkehr curves for wavelength pair C. Both data sets cover a wide range of total ozone amounts. The North American total ozone data are based on AD double-pair direct-sun measurements, while those from Arosa are based on direct-sun measurements with the C wavelength pair. To make these data comparable, the Arosa measurements have been increased by 6% (a value suggested by Dütsch as appropriate for Arosa measurements), where it was necessary to do so. Both sets of data have been carefully scrutinized (the former by the writer, the latter by Dütsch) to eliminate the spurious clerical errors which often arise in processing the instrument readings through to the final data forms. In the case of the North American curves, the sample represents virtually all of the available data for three wavelength pairs when measurements were possible on all 12 zenith angles. In the case of the Arosa sample, curves were selected from

a large sample of over 500 taken during the period March, 1961, through July, 1962, inclusive. The curves were selected to include most of the low and high ozone cases from the larger sample. Finally, cards having odd numbers in the last position of two of the measurements were selected to represent intermediate ozone values.

The determination of the eigenvalues and vectors of the correlation and covariance matrices were carried out by the Jacobi method, more specifically using subroutine EIGN, which is directly available as a system subroutine on the IBM 7090, Computing Center, The University of Michigan.

The first eight eigenvalues, for the correlation matrices obtained when the entire Umkehr curve is used (i.e., without total ozone), are listed in Table 2. The computations have been carried out for the Arosa sample, for the North American sample on each wavelength pair separately, and for the latter sample with the wavelength pairs combined into one vector of 36 elements. The result is quite clear: some 95% or more of the normalized variance of the Umkehr curves is explained by a single characteristic pattern. Moreover, this pattern is in all cases nothing more than a simple shift of the entire Umkehr curve. The correlation between total ozone and the coefficients of the characteristic patterns (when the Umkehr curve is expanded with respect to these patterns) is also given in Table 2 in brackets. We note that the coefficient of the first C. P. is highly correlated with total ozone and, hence, the amount that the Umkehr curve is shifted depends strongly on total ozone. Thus the statement of Götz *et al.*, that the shape of the curve depends mostly on the to-

TABLE 2

THE FIRST EIGHT EIGENVALUES OF THE CORRELATION MATRIX OF THE POINTS ON THE UMKEHR CURVE, INCLUDING (IN PARENTHESES) CORRELATIONS BETWEEN THE EIGENVECTOR COEFFICIENT AND TOTAL OZONE

Eigen-value Number	North America				Arosa
	A	C	D	A-C-D	C
1	.96716 (.916)	.96922 (.887)	.96518 (.799)	.94844 (.876)	.97767 (.988)
2	.02131 (-.279)	.01870 (-.317)	.02225 (-.030)	.02088 (-.430)	.01505 (-.056)
3	.00858 (.098)	.00814 (-.106)	.01007 (.485)	.01258 (.012)	.00529 (-.074)
4	.00144 (.058)	.00264 (.191)	.00110 (.016)	.01002 (-.105)	.00114 (-.032)
5	.00063 (-.041)	.00050 (.013)	.00055 (-.022)	.00264 (.002)	.00034 (.008)
6	.00029 (.092)	.00023 (-.014)	.00023 (.021)	.00234 (-.077)	.00020 (.014)
7	.00016 (-.023)	.00018 (-.044)	.00018 (.000)	.00076 (.039)	.00009 (-.026)
8	.00016 (.003)	.00011 (-.021)	.00017 (-.025)	.00045 (.005	.00007 (-.015)

tal amount of ozone, is quantitatively confirmed. The essential result of this analysis is shown graphically in Fig. 9 as "standard" Umkehr curves for the C wavelength pair for total ozone amounts of 300, 350, and 400 m atm-cm. The correction of 6% has been applied to obtain the Arosa curves, and the curves for 350 m atm-cm have been made to coincide at a zenith angle of 60°.

In examining Fig. 9, we note in particular the difference in the position of the reversal which occurs, at Arosa, when the sun is closer to the horizon. This suggests that there is a difference in the mean vertical distribution of ozone over Arosa compared to North American. However, neither of the two samples is completely representative. In particular, we note from Figs. 16 and 17 that although the two samples have about the same mean total ozone (near 350 m atm-cm), the standard deviation is 63 m atm-cm for the Arosa sample compared to only 42 m atm-cm for the North American one. This undoubtedly plays some role in determining the difference in the mean curves and, as noted earlier, the curves of Fig. 9 are relatively simple shifts of the mean curves.

Results for the Umkehr curves with the instrument constant removed (i.e., including total ozone) and using correlation matrices are given in Table 3. In this case the correlations between total ozone and the pattern vector coefficients have not been computed. Results are included for the "double" pairs, AD, AC, and CD. A somewhat different picture emerges now because the variability of total ozone has been added to that of the Umkehr curve, but shifts of the entire curve have been eliminated.

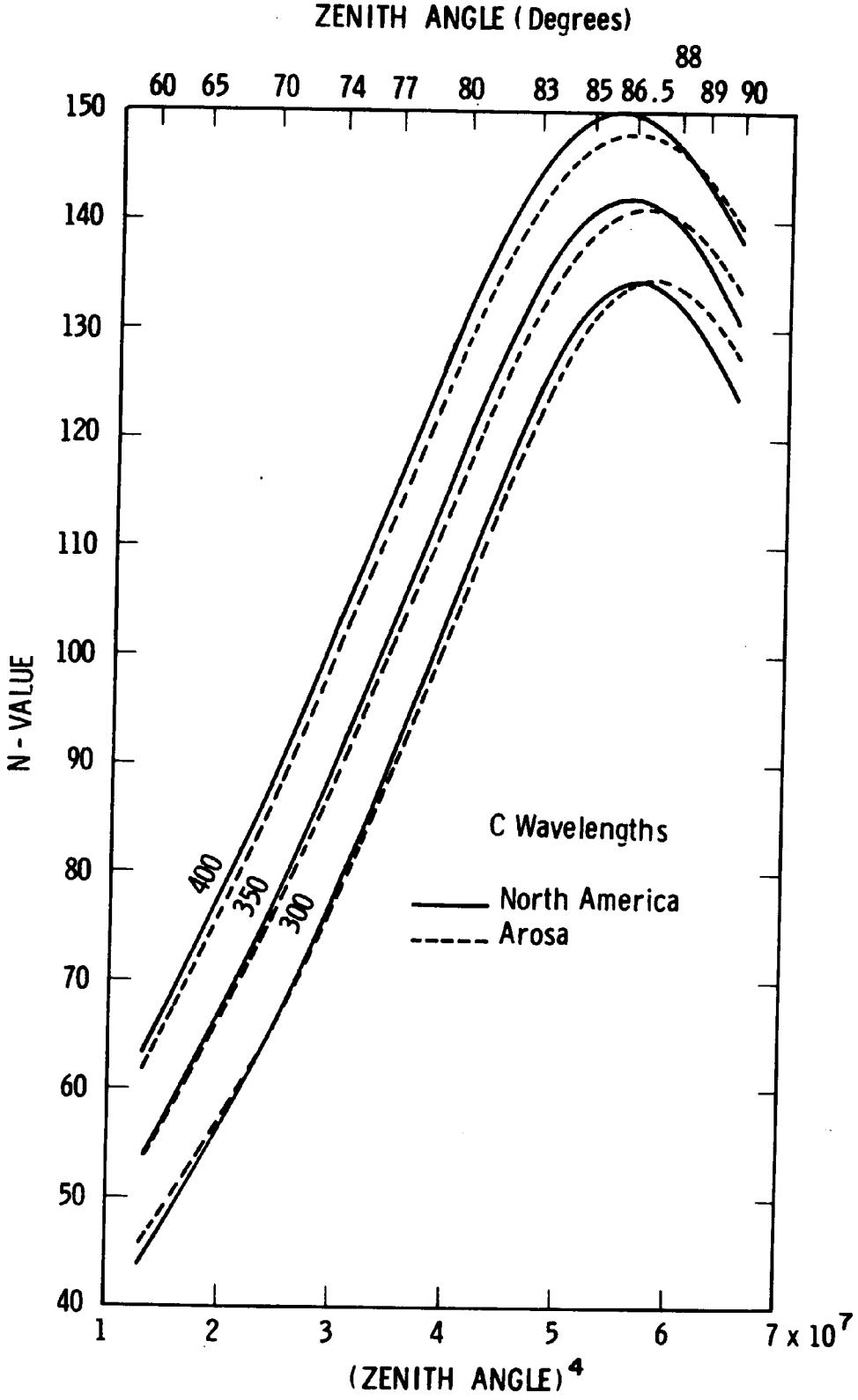


Fig. 9. "Standard" Umkehr curves for Arosa and North America for the C wavelength pair.

TABLE 3

THE FIRST EIGHT EIGENVALUES FOR THE CORRELATION MATRIX OF THE POINTS ON THE UMKEHR CURVE WHEN THE INSTRUMENT CONSTANT IS ELIMINATED AND TOTAL OZONE IS USED

Eigen-value Number	North America							Arosa
	A	AC	C	CD	D	AD	A-C-D	C
1	.73729	.76477	.62100	.68504	.67945	.75385	.59495	.71067
2	.20098	.12204	.31185	.15550	.25814	.15581	.29177	.21543
3	.03175	.06311	.03093	.08378	.02729	.05029	.02876	.05687
4	.01453	.03098	.02173	.04386	.01553	.02288	.02563	.00530
5	.00599	.00768	.00555	.01148	.00789	.00796	.01295	.00441
6	.00482	.00539	.00289	.00660	.00503	.00442	.01157	.00286
7	.00202	.00257	.00210	.00492	.00284	.00219	.00909	.00177
8	.00149	.00162	.00132	.00312	.00135	.00140	.00602	.00093

We find that three C. P.'s are required to explain 97% of the normalized variance of the single pair curves. The first three C. P.'s for each data batch are shown in Figs. 10-12, inclusive (excluding the cases where the A, C, and D wavelength pairs are combined and the double pairs). In order to have something interpretable in terms of N-values, the pattern vector elements have been multiplied by the standard deviation of the appropriate curve point and then the entire vector has been multiplied by the root mean square coefficient the C. P. would have if the Umkehr curves were expanded in terms of these patterns. The "point" corresponding to total ozone is not plotted on these diagrams. The dot product of the original orthonormal pattern vectors for the two C wavelength pair samples is shown on each of the figures. The high values of this product indicate that the patterns are essentially the same and strongly suggest that these patterns are fundamental properties of the Umkehr curve.

Finally, results for the Umkehr curves with the instrument constant removed (total ozone included) and using the covariance matrices are given in Table 4. In this case, the Arosa total ozone values were increased by 6% so that the results would be more nearly comparable. The mean Umkehr curve variance and the root mean square curve-point deviation from the mean are also listed in Table 4. It should be remembered that these deviations have to do with the shape of the curve since the shift of the entire curve with total ozone has been eliminated except insofar as total ozone itself is concerned.

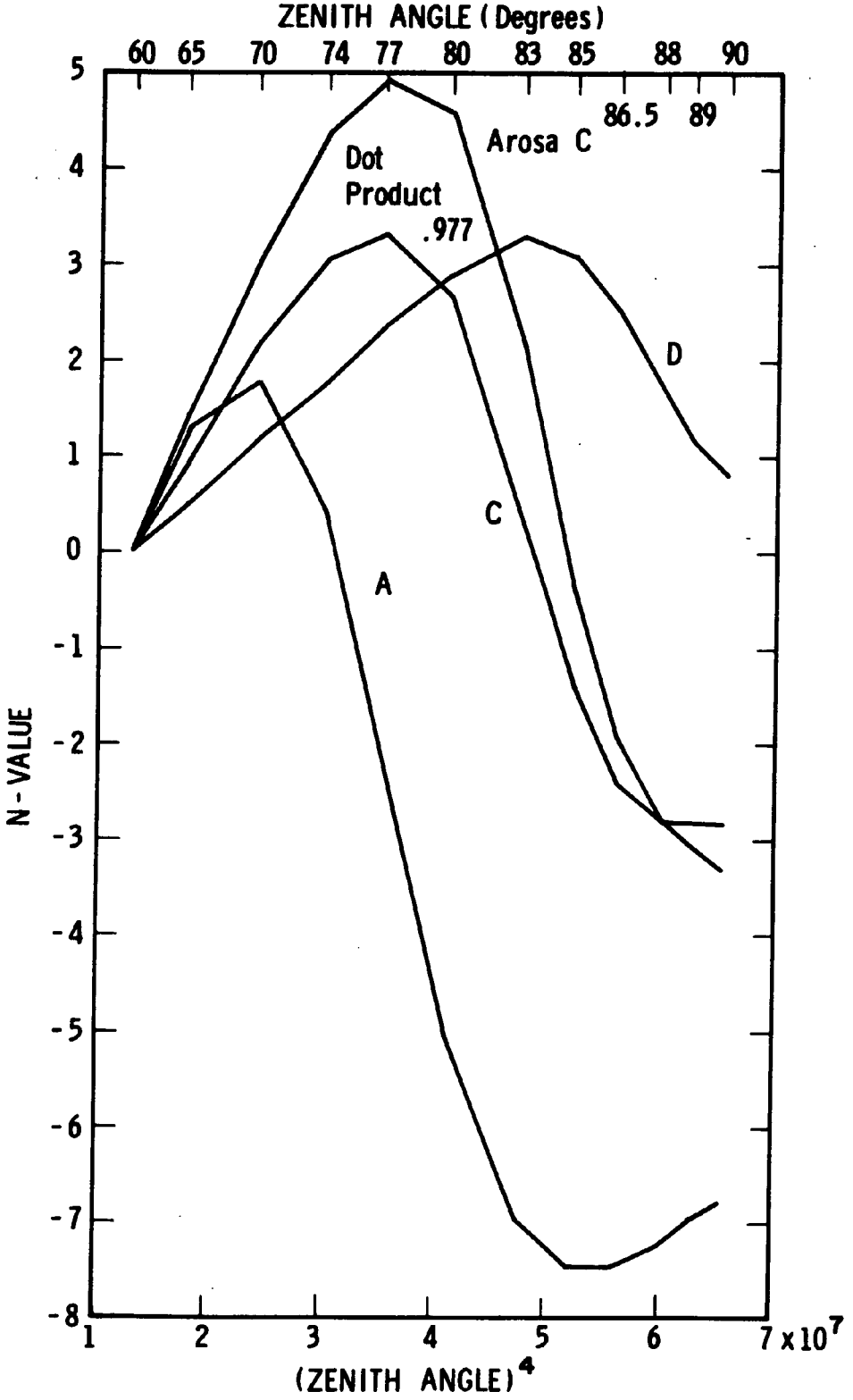


Fig. 10. First Characteristic Pattern of the correlation matrix, with the instrument constant eliminated.

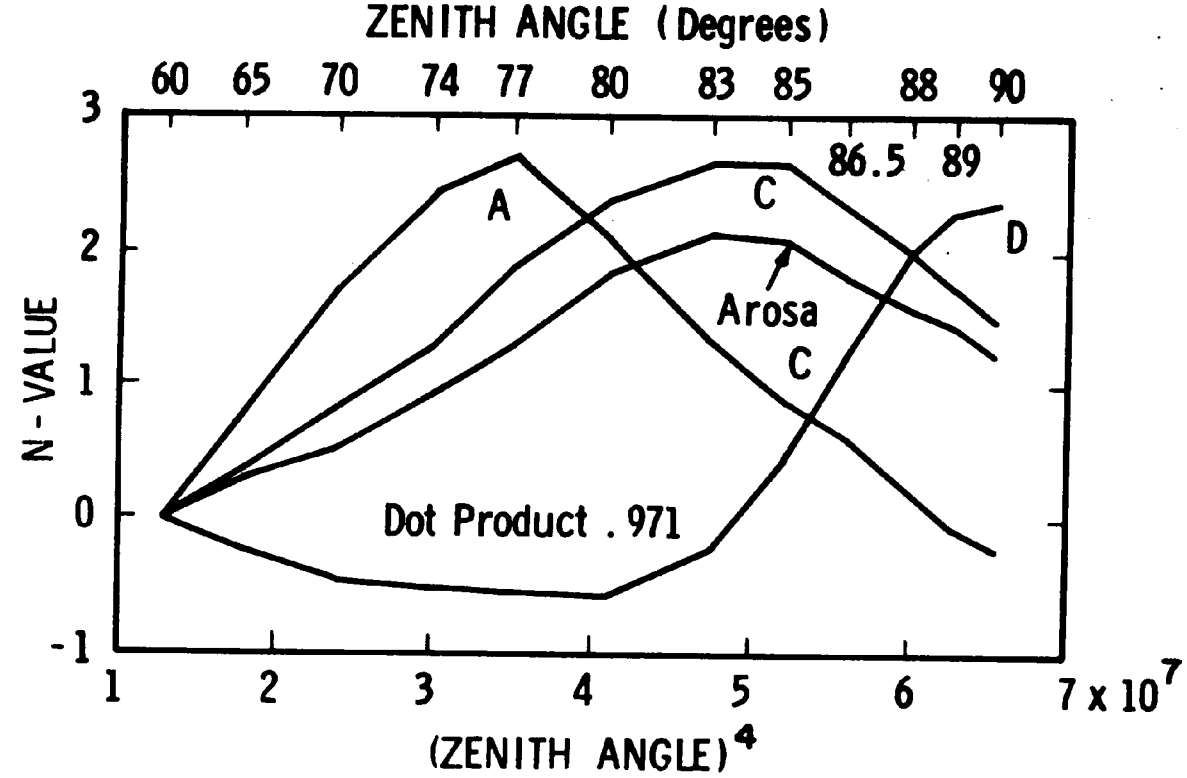


Fig. 11. Second characteristic pattern of the correlation matrix, with the instrument constant eliminated.

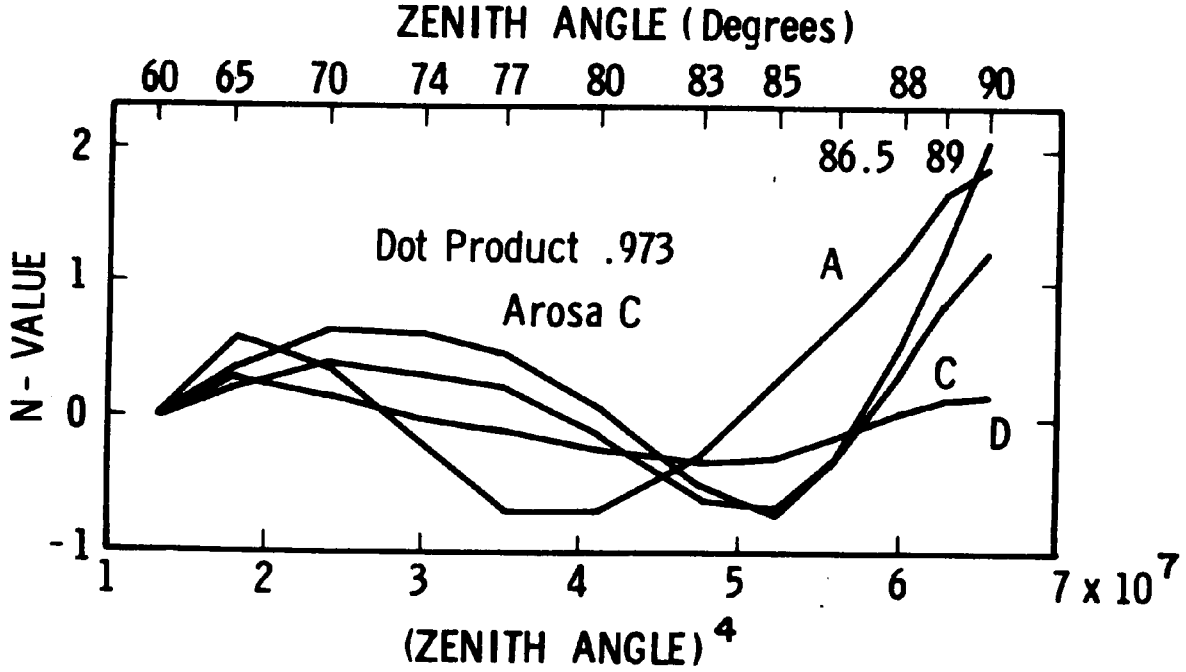


Fig. 12. Third characteristic pattern of the correlation matrix, with the instrument constant eliminated.

TABLE 4

THE FIRST EIGHT EIGENVALUES FOR THE COVARIANCE MATRIX OF THE POINTS ON THE UMKEHR CURVE WHEN THE INSTRUMENT CONSTANT IS ELIMINATED AND TOTAL OZONE IS USED

Eigen-value Number	North America				Arosa
	A	C	D	A-C-D	C
1	.90699	.65569	.70521	.77319	.80605
2	.06070	.29271	.25587	.15858	.13376
3	.02022	.02975	.01858	.02765	.04425
4	.00449	.00890	.00903	.01633	.00849
5	.00239	.00570	.00446	.00715	.00289
6	.00202	.00192	.00190	.00330	.00143
7	.00114	.00180	.00152	.00246	.00100
8	.00082	.00118	.00127	.00214	.00067
Mean Curve Variance $(\text{N-units})^2$	408.8	124.2	89.5	589.5	185.9
RMS Point Deviation (N-units)	5.8	3.2	2.7	4.2	3.9

As before, we find that most of the curve variance is explained by the first three pattern vectors. These patterns, suitably scaled, are shown in Figs. 13, 14, and 15, respectively. The dot product of the

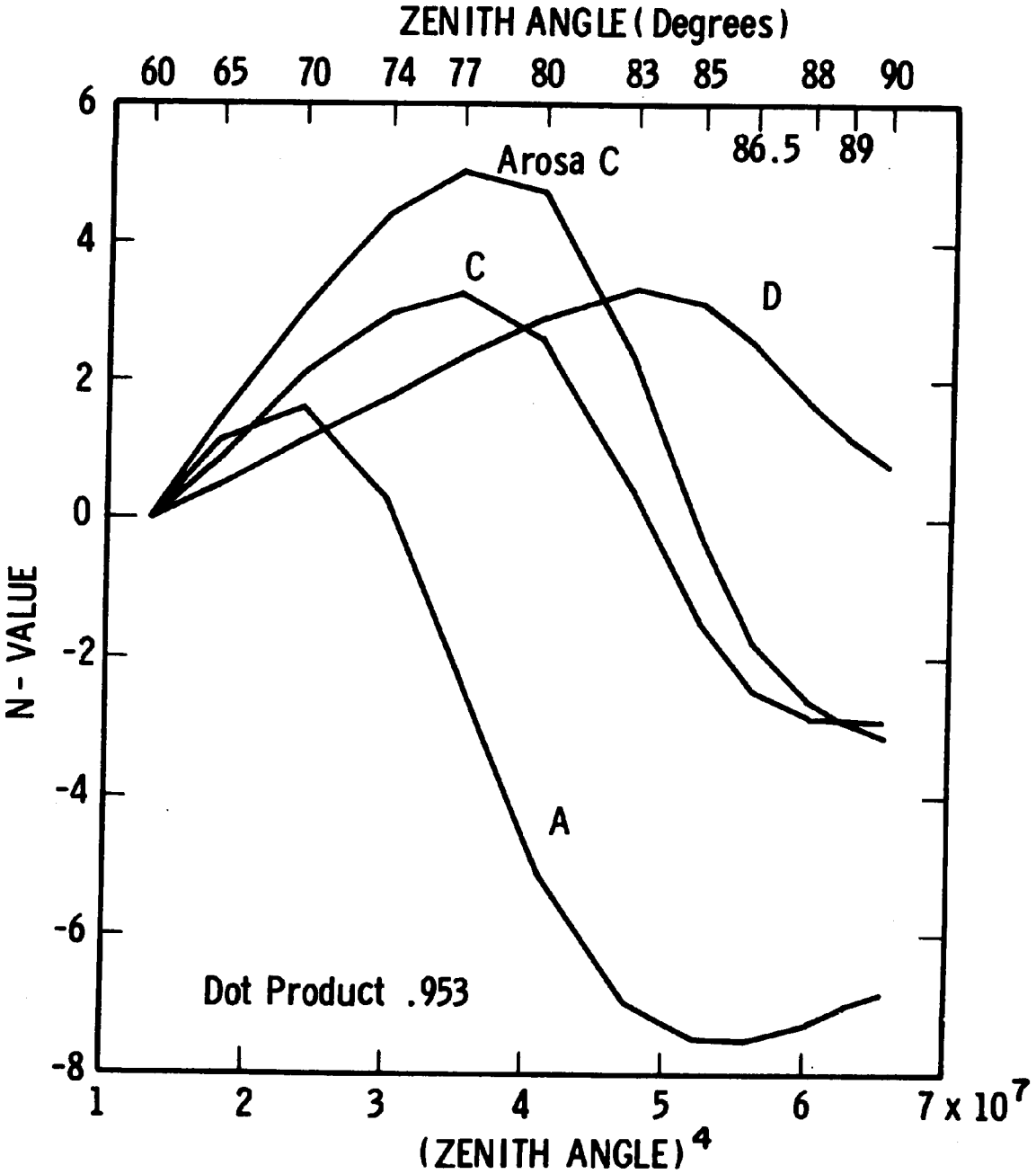


Fig. 13. First characteristic pattern of the covariance matrix, with the instrument constant eliminated. Compare with Fig. 10 but note difference in scale.

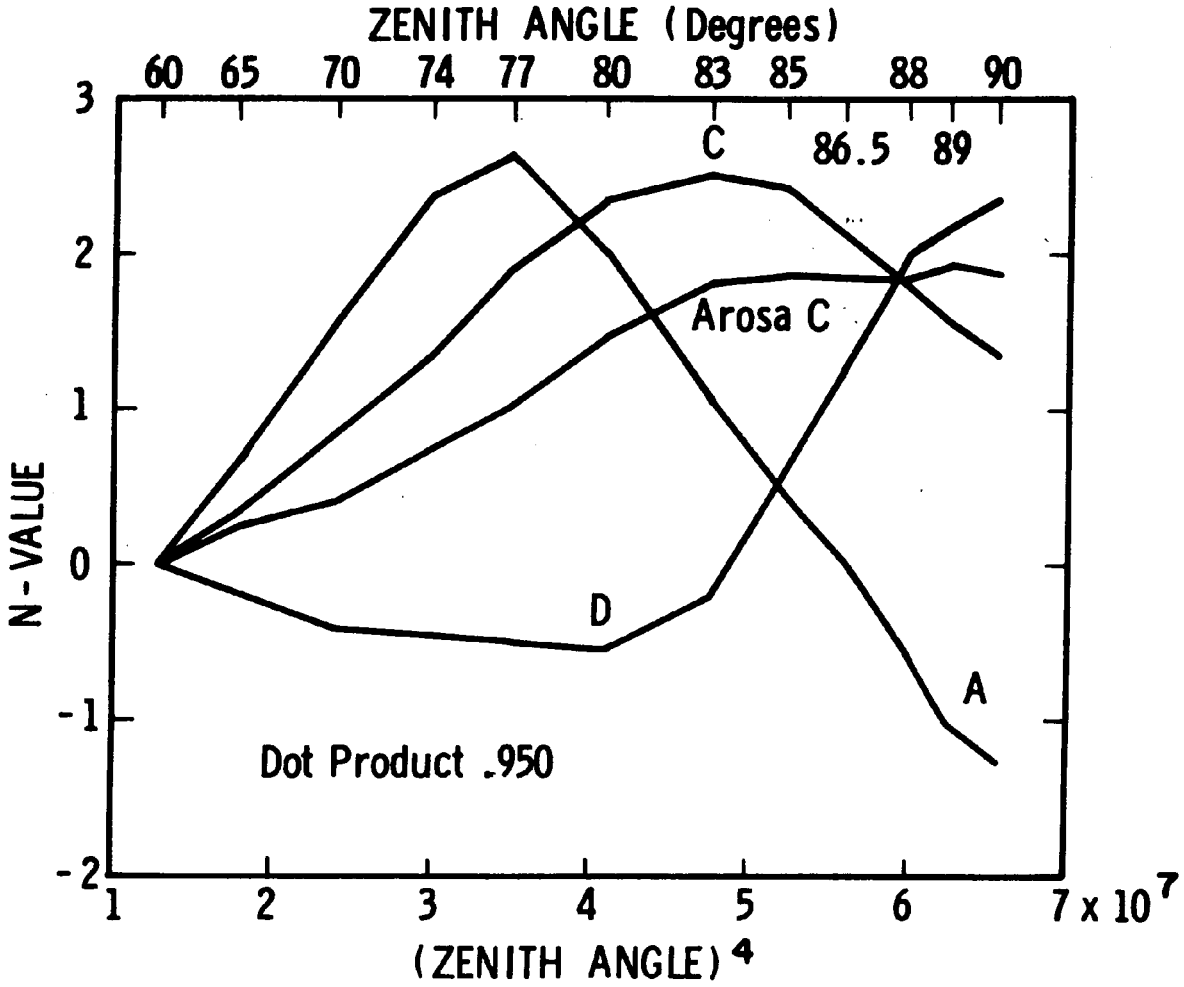


Fig. 14. Second characteristic pattern of the covariance matrix, with the instrument constant eliminated.

original orthonormal pattern vectors for the two C wavelength pair samples is shown on each of the figures. The high values of the product again attest to the similarity of the respective patterns. We note further that the patterns are much the same, regardless of whether the correlation or covariance matrices are used. As a matter of interest, the complete set of 12 characteristic patterns for the covariance matrix of the North American data sample C wavelengths are given in Table 5.

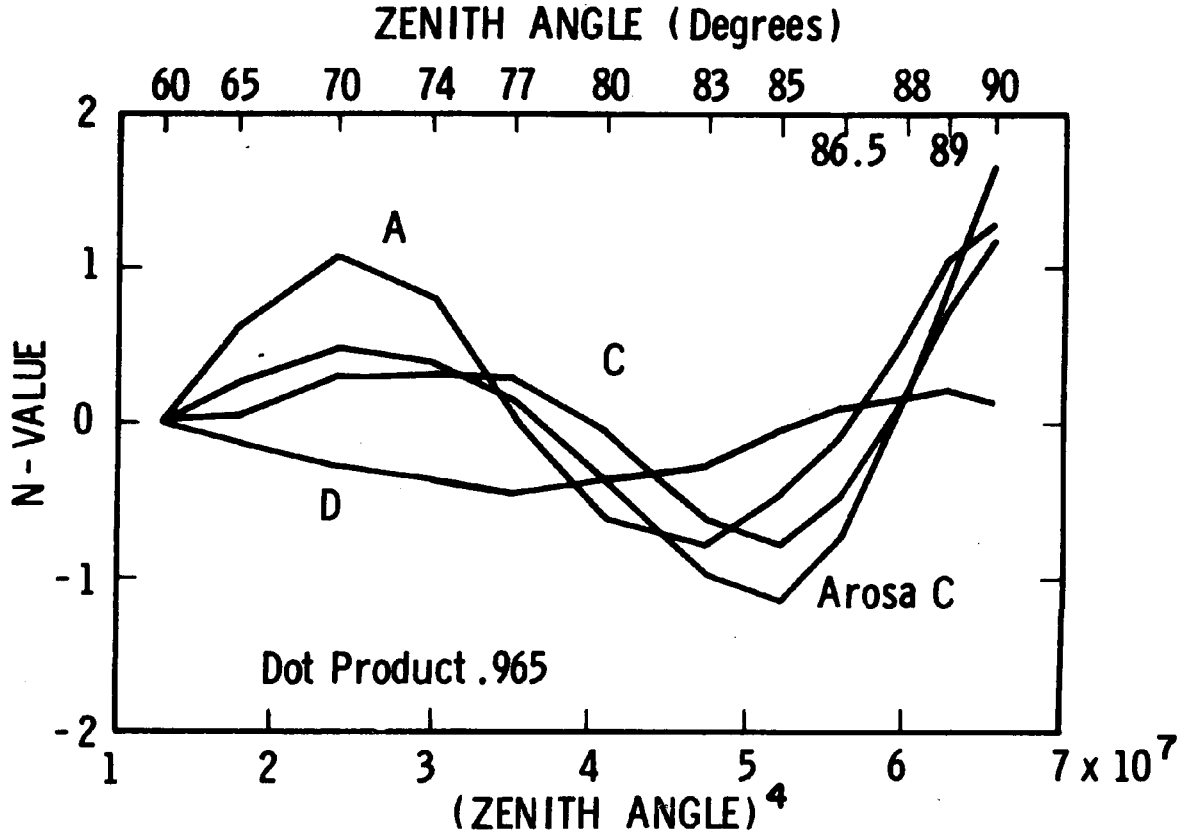


Fig. 15. Third characteristic pattern of the covariance matrix, with the instrument constant eliminated.

In the 12 columns are listed the vector points corresponding to total ozone, and θ = 90, 89,..., 65°, respectively. The root mean square coefficient for each vector is obtained by multiplying the mean curve variance (second last item of third column, Table 4), by the appropriate fractional eigenvalue, then taking the square root. For example, the rms coefficient for the first pattern vector is $[(.65569)(124.2)]^{1/2}$ = 9.02. If we multiply the element of the first C. P. corresponding to 77°, by this number we get (9.02)(.36049) = 3.25, which is the value plotted in Fig. 13.

TABLE 5

CHARACTERISTIC PATTERNS FOR THE COVARIANCE MATRIX OF THE POINTS ON THE UMKEHR CURVE WHEN THE INSTRUMENT CONSTANT IS ELIMINATED AND TOTAL OZONE IS USED FOR THE NORTH AMERICAN C WAVELENGTH DATA SAMPLE

Pattern Number	Characteristic Pattern Points											
	1	2	3	4	5	6	7	8	9	10	11	12
1	.44756	-.32217	-.31989	-.31970	-.27332	-.16005	.04732	.28913	.36049	.33195	.23608	.09660
2	.11456	.22497	.25767	.29777	.34968	.40192	.41605	.38990	.31687	.22026	.14114	.05846
3	.19679	.62426	.37491	.09812	-.24682	-.42012	-.32447	-.01912	.14929	.16852	.16520	.01834
4	.84447	.08037	.04244	-.01011	.08099	.17243	.04745	-.12274	-.31746	-.24298	-.21075	-.14372
5	.13689	-.27764	.10991	.25992	.19351	.05772	-.16470	-.41511	-.17384	.16730	.47192	.55082
6	-.01676	-.15652	.23137	.14620	-.23669	-.41933	.47743	.35080	-.35800	-.34570	.21730	.15018
7	.07968	-.47737	.20370	.43829	.24123	-.33606	-.19566	.05730	.08888	.18600	-.09816	-.51707
8	-.02278	-.00295	.16477	-.08376	-.20654	-.10094	.59317	-.53735	-.02567	.46931	-.19050	-.12107
9	.06549	-.21388	.20688	.26346	-.35352	.09671	-.00304	-.16955	.56319	-.38551	-.35171	.29185
10	-.03752	-.07109	.16233	-.05963	-.31720	.35684	.00487	-.19240	.10720	-.23969	.60575	-.51260
11	.05274	.16239	-.29131	-.06523	.47262	-.40744	.25722	-.30743	.37848	-.37397	.20989	-.06726
12	-.01849	-.20686	.63297	-.65888	.30375	-.04018	-.07569	.03552	.08780	-.07478	-.04586	.07628

The Umkehr curves have been expanded in terms of the C. P.'s of the covariance matrix in an attempt to find out how many patterns are required to "explain" everything but the experimental error which might be expected in the data. In the present case, it was assumed that, when the total residual curve variance was less than 6.0 $(\text{N-units})^2$, we were down to the level of experimental error. (The total ozone residuals were in units of 10 m atm-cm.) In each expansion, the coefficients of all patterns and the variance explained by each were computed and the total variance explained was summed. The sum was tested after the addition of the variance explained by each C. P. and the series expansion was truncated when the residual variance was less than 6.0. In the case of the A wavelength pairs, a value of 12.0 $(\text{N-units})^2$ was used and, for the combined pairs (A-C-D), a value of 34.0 $(\text{N-units})^2$ was used for testing purposes. These higher testing values were used in the latter cases because of an apparently higher noise level. In addition, for the C wavelength pairs, the Arosa curves were expanded in terms of the North American patterns, and vice versa. The results are listed in Table 6, which gives the frequency distributions of truncation levels for the various expansions. The bracketed numbers in the C columns are the truncation levels when the Arosa curves are expanded in terms of the North American patterns, and vice versa. In general, most of the curves require only three characteristic patterns to explain all the variance except that attributable to experimental error. Most of the remaining curves require only one additional characteristic pattern.

TABLE 6

FREQUENCY DISTRIBUTIONS OF TRUNCATION LEVELS FOR EXPANSIONS OF UMKEHR CURVES IN TERMS OF THEIR CHARACTERISTIC PATTERNS

Characteristic Pattern Number	North America				Arosa
	A	C	D	A-C-D	C
1	25	14 (0)	21	10	9 (7)
2	40	46 (8)	61	43	29 (12)
3	25	29 (73)	13	26	50 (59)
4	6	6 (15)	3	13	11 (19)
5	2	3 (1)	0	4	1 (3)
6	0	0 (0)	0	1	0 (0)
7	0	0 (1)	0	1	0 (0)
8	0	0 (0)	0	0	0 (0)

We may conclude from the above results that at most four characteristic patterns are required to explain variations in the shape of the Umkehr curve when the instrument constant is eliminated and total ozone is included. The first three patterns at least are fundamental properties of the Umkehr curve and there is some possibility that the fourth pattern is also important. The remaining patterns are mostly noise, particularly the higher order vectors, which exhibit sign changes from one angle to the next and explain virtually no variance. If we assume that the main information content of the Umkehr curve has to do with variations in the vertical distribution of ozone, then we may further conclude that there are, at most, four pieces of information about these variations that may be inferred from Umkehr observations. From the evidence presented here, it appears that little or no additional information is to be obtained from observations on more than a single wavelength pair,

at least when observations are available for all 12 zenith angles. Thus the existence of strong interdependence between the points on the Umkehr curve, first recognized by Götz et al., has been quantitatively confirmed. Pictorial evidence is presented in Figs. 16 and 17 for the strong control of total ozone in determining the shape of the Umkehr curve. These figures are scatter diagrams in which the coefficients of the first C. P. (of the covariance matrix with total ozone included) are plotted against total ozone for the C wavelengths and for the North America and Arosa data samples, respectively. There is some redundancy here in that total ozone is also included in the first "point" of the pattern vector. However, total ozone does not dominate this pattern vector, and the high degree of correlation between the coefficient and total ozone could not exist unless total ozone also played a dominant role in determining the shape of the Umkehr curve.

3.4 PHYSICAL EXPLANATION

A simplified explanation of the above results, viz., the strong colinearities existing between the points on the Umkehr curve, may be found by referring to the development of Section 2.1, which considers only primary scattering. We may perform the numerical integration indicated by Eq. (7) and plot the "source function" $\chi(\Theta,z)$ as a function of height to see how broad a layer of the atmosphere actually contributes to the primary scattered intensity at the ground for each wavelength. This has been done for each of the 12 zenith angles used by Dütsch, for each of the wave-

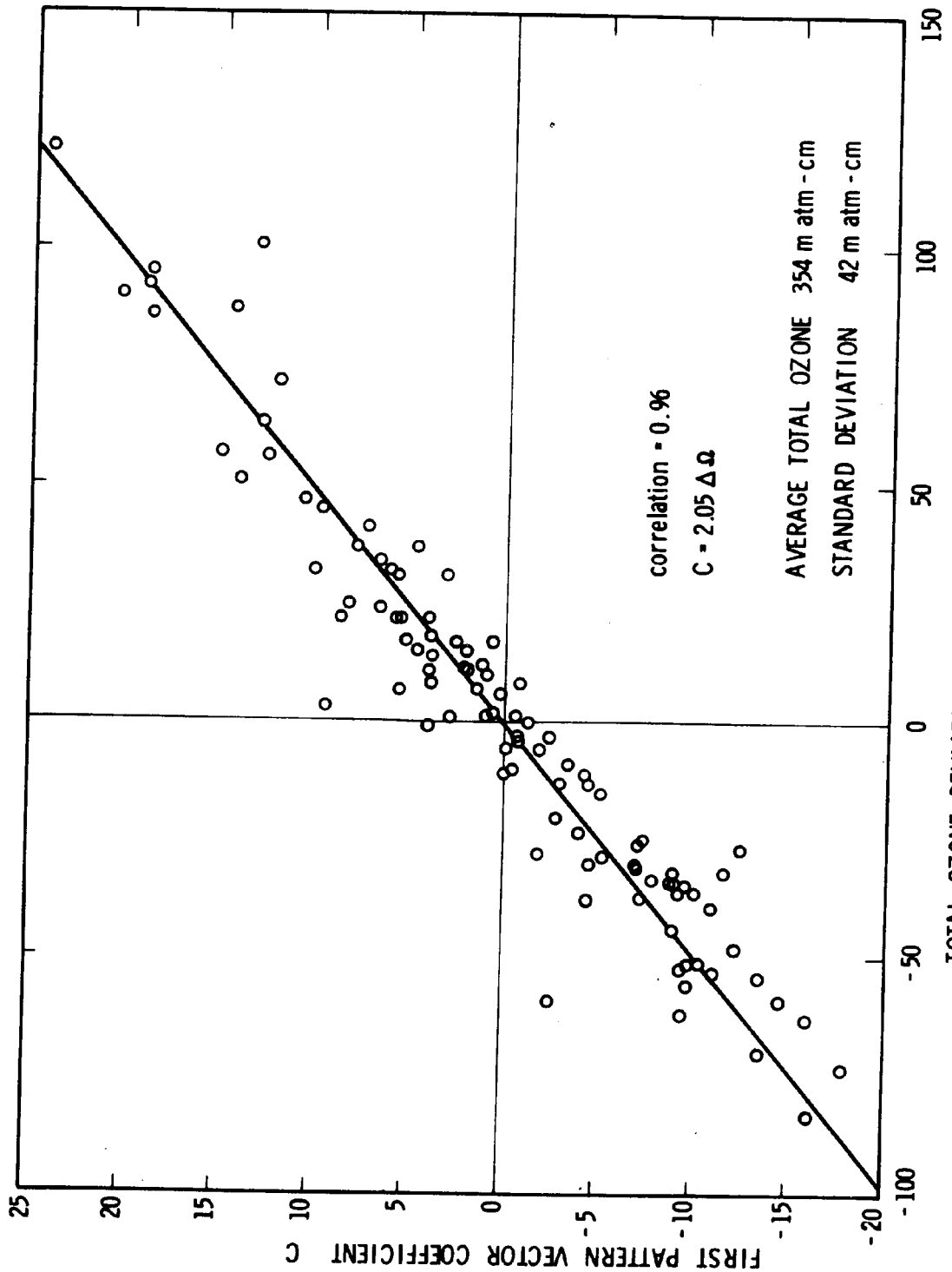


Fig. 16. Scatter diagram of first pattern vector coefficient plotted against total ozone deviation from mean for C wavelength pair, North America sample.

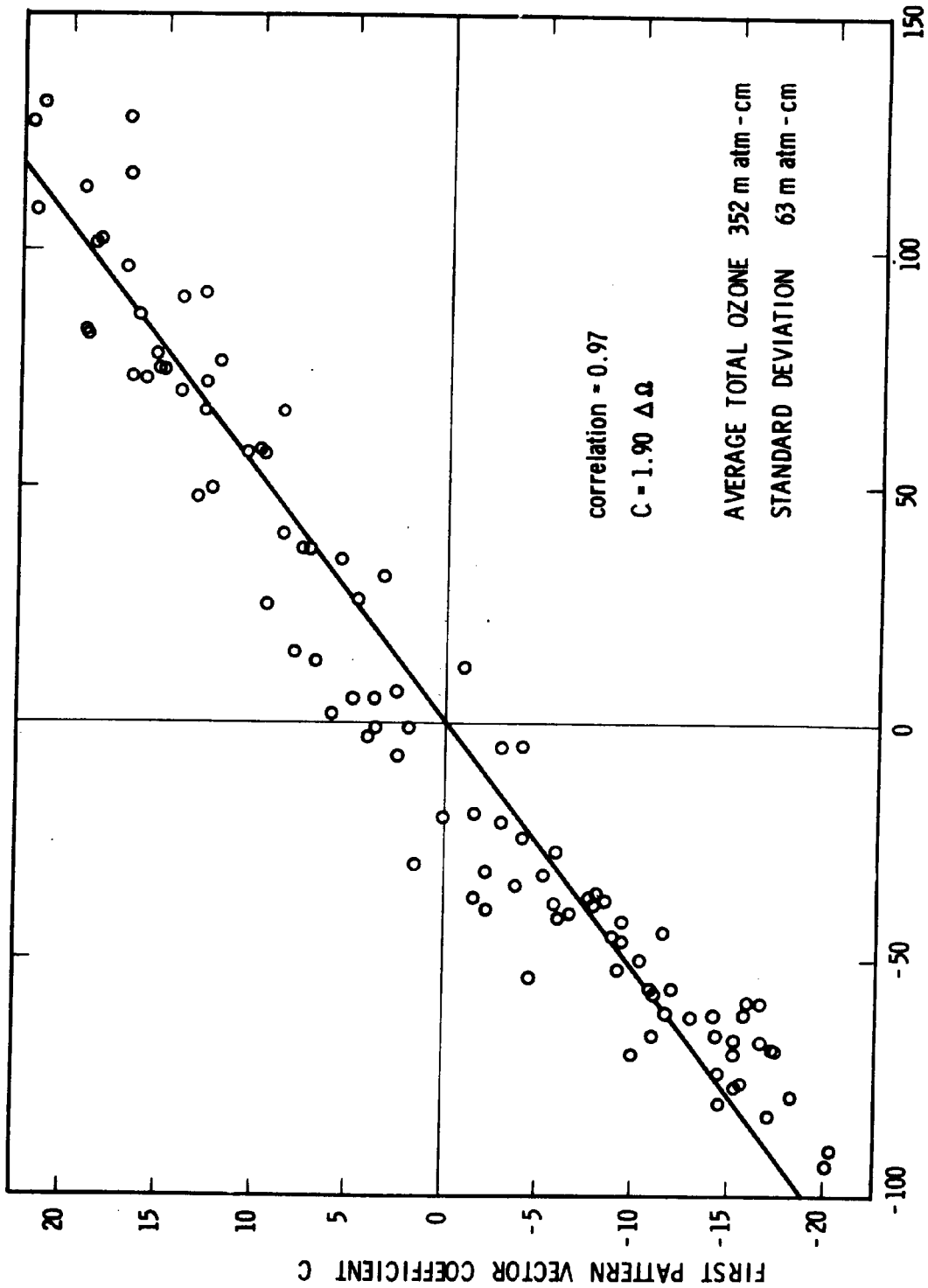


Fig. 17. Scatter diagram of first pattern vector coefficient plotted against total ozone deviation from mean for C wavelength pair, Arosa sample.

lengths of the three pairs A, C, and D, for the vertical distribution of ozone shown in Fig. 18, which corresponds to about 360 m atm-cm of ozone. The quadrature formulation used is described in Appendix C. It will suffice here to note that both refraction and the sphericity of the atmosphere have been taken into account in the calculations. The results are plotted in Figs. 19-21, inclusive, wherein the source functions have in each case been normalized so that the greatest computed value is unity. Since the source function curves overlap so strongly, only seven of each have been drawn. The resulting relative Umkehr curves and the relative intensities of the individual wavelengths are plotted in Fig. 22.

Referring to the source function curves we note that, as stated earlier, the "return" does indeed come from a definite layer of the atmosphere. However, the layer is an extremely broad one, the half-height (abscissae = 0.5) points on each curve being separated by at least 10 km and as much as 30 km. On this basis, we could say that at most three zenith angles provide return from the entire layer of atmosphere that is "sensed" in the zenith angle range $60° \leq \theta \leq 90°$. If we are more liberal and take the 3/4 height points, we might say that at most five zenith angles are required. Since the long and short wavelength curves for 60° very nearly coincide, we may conclude that variations in the vertical distribution have little effect on the intensity ratio at 60°.

In view of the classical explanation for the Umkehr effect of Götz *et al.*, in Section 1.2, it is interesting to note the essentially double peaked nature of the source function curves for 70° and 74° for

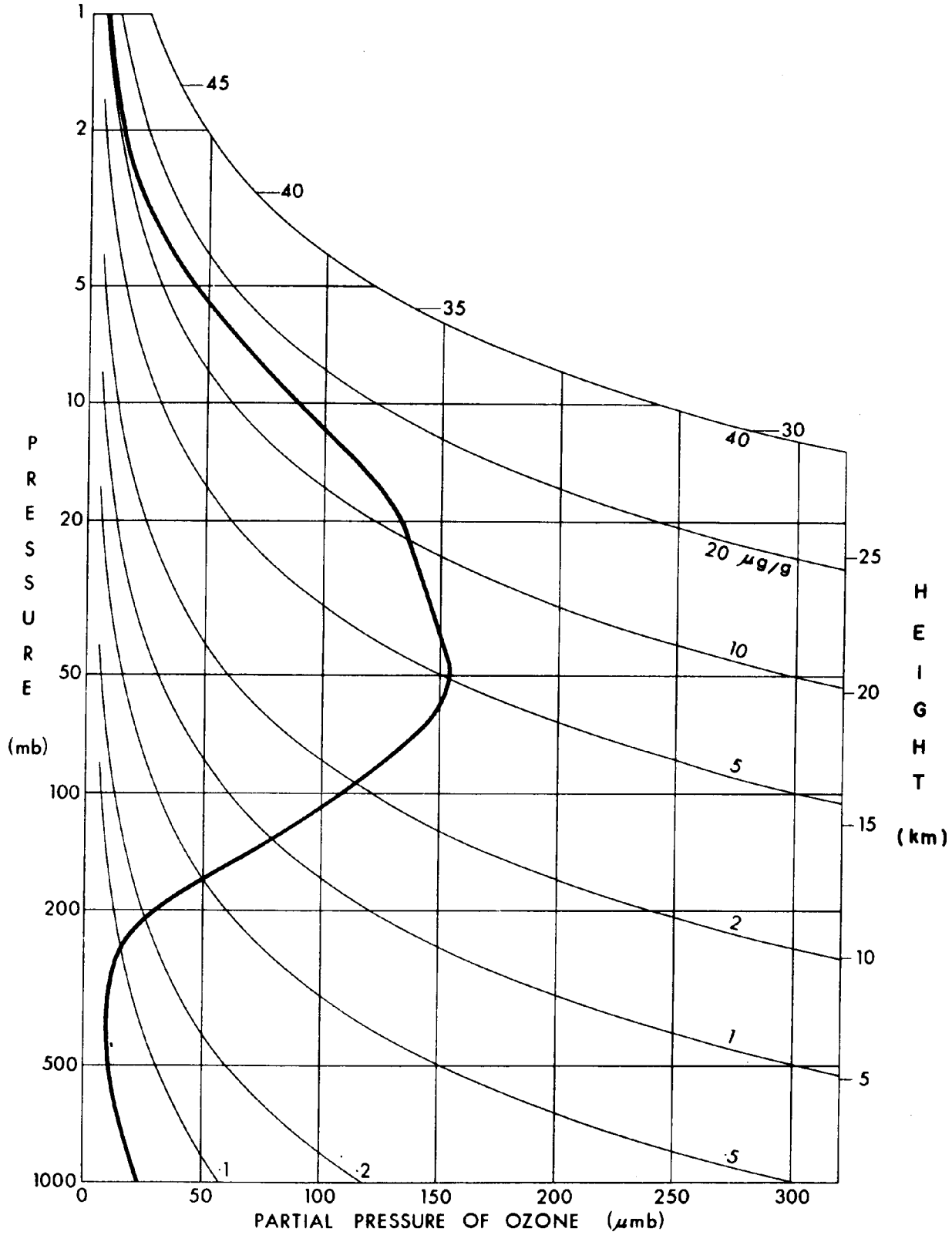


Fig. 18. Vertical distribution of ozone used in the computation of source function $\chi(\Theta,z)$.

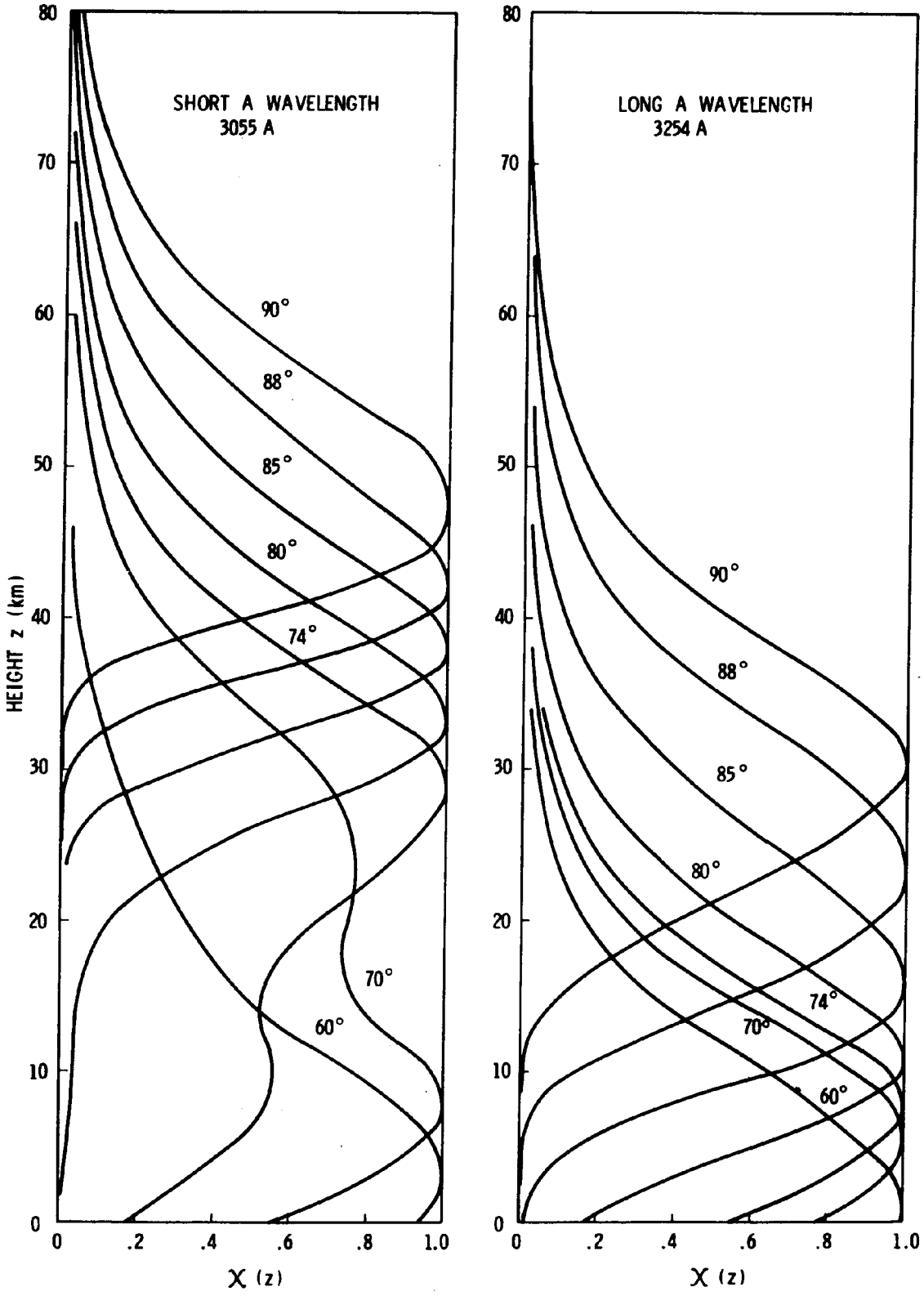


Fig. 19. Source functions $\chi(\Theta,z)$ plotted against height for various zenith angles for the A wavelengths.

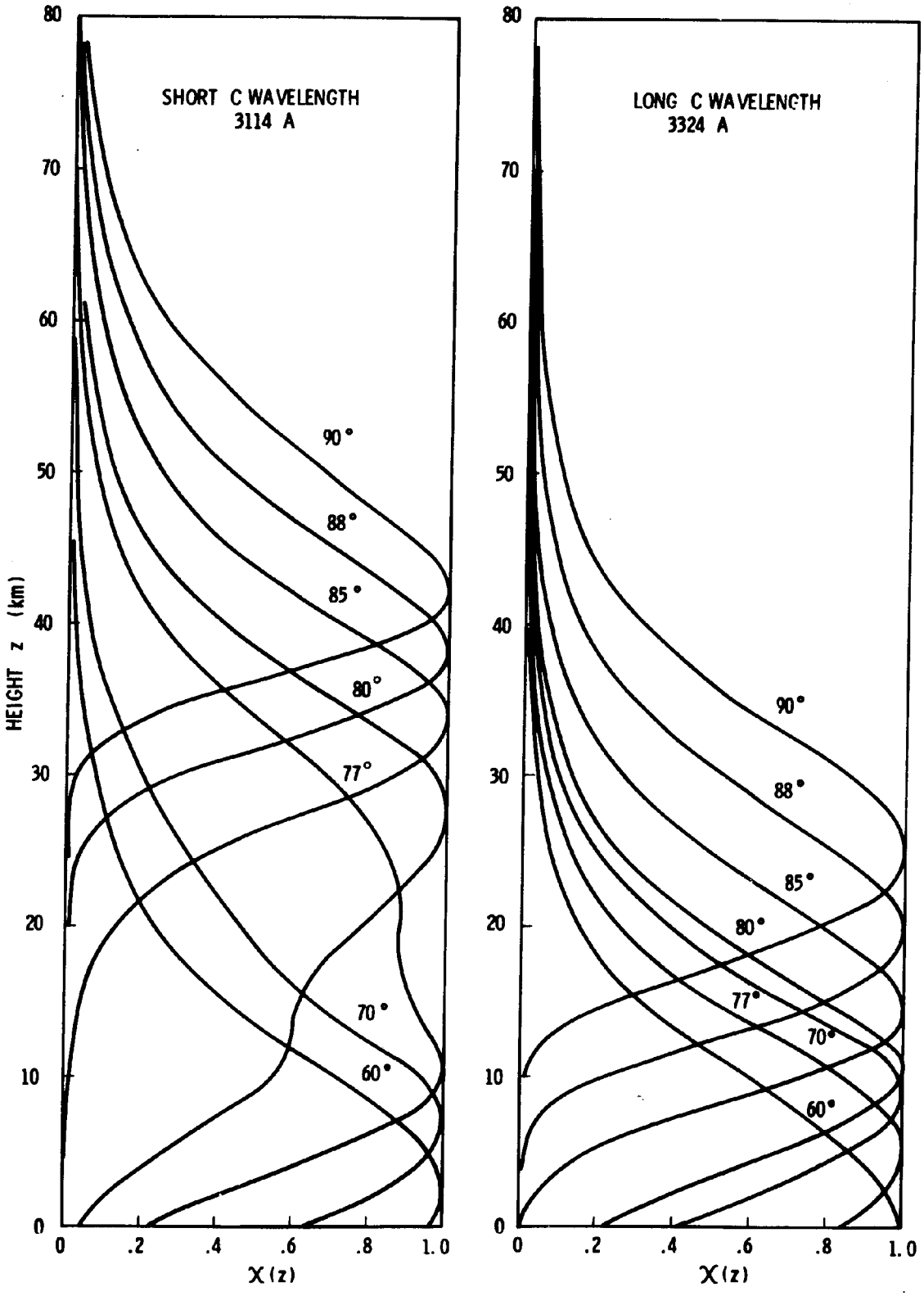


Fig. 20. Source function $\chi(\Theta,z)$ plotted against height for various zenith angles for the C wavelengths.

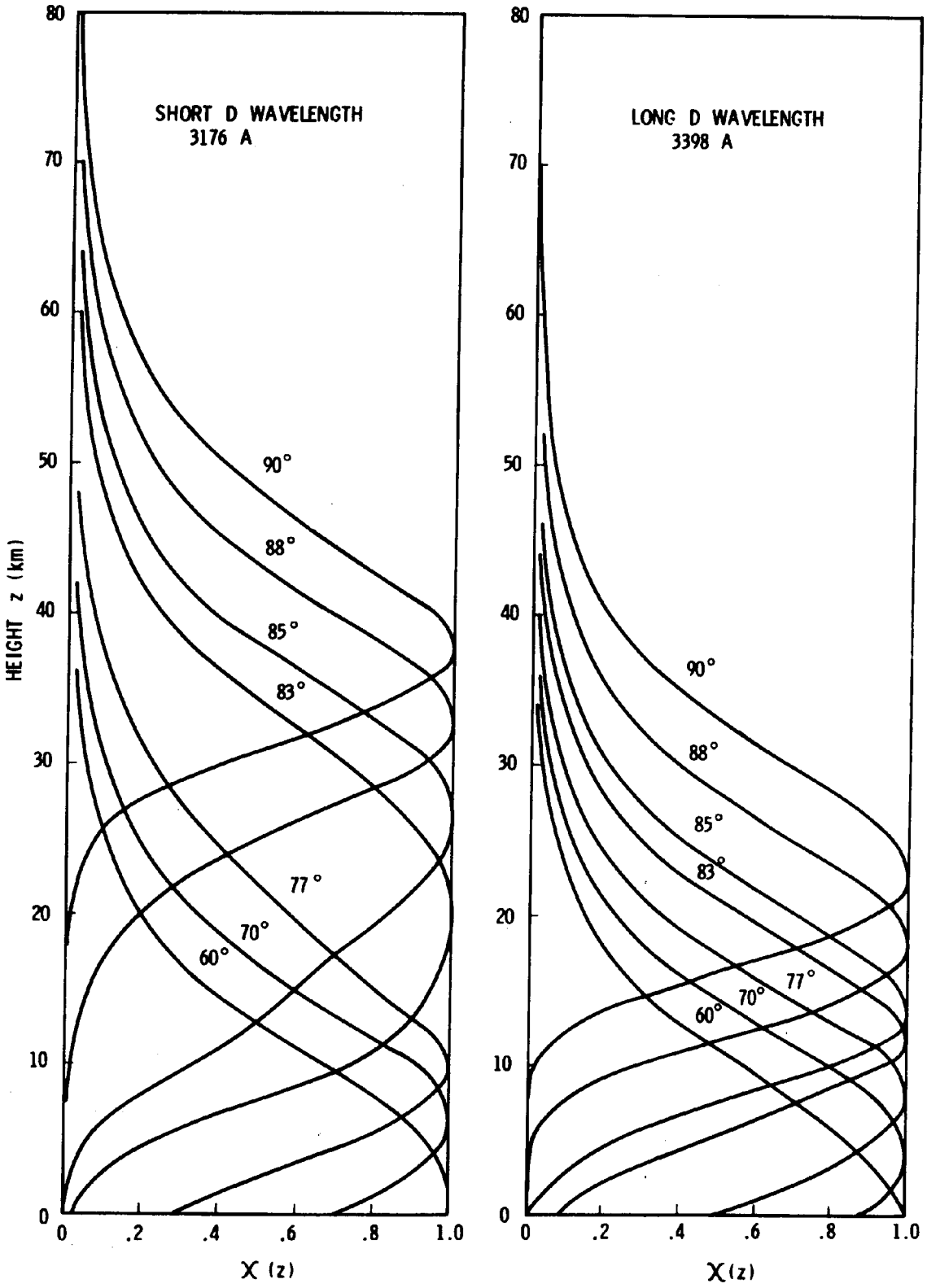


Fig. 21. Source functions $\chi(\Theta,z)$ plotted against height for various zenith angles for the D wavelengths.

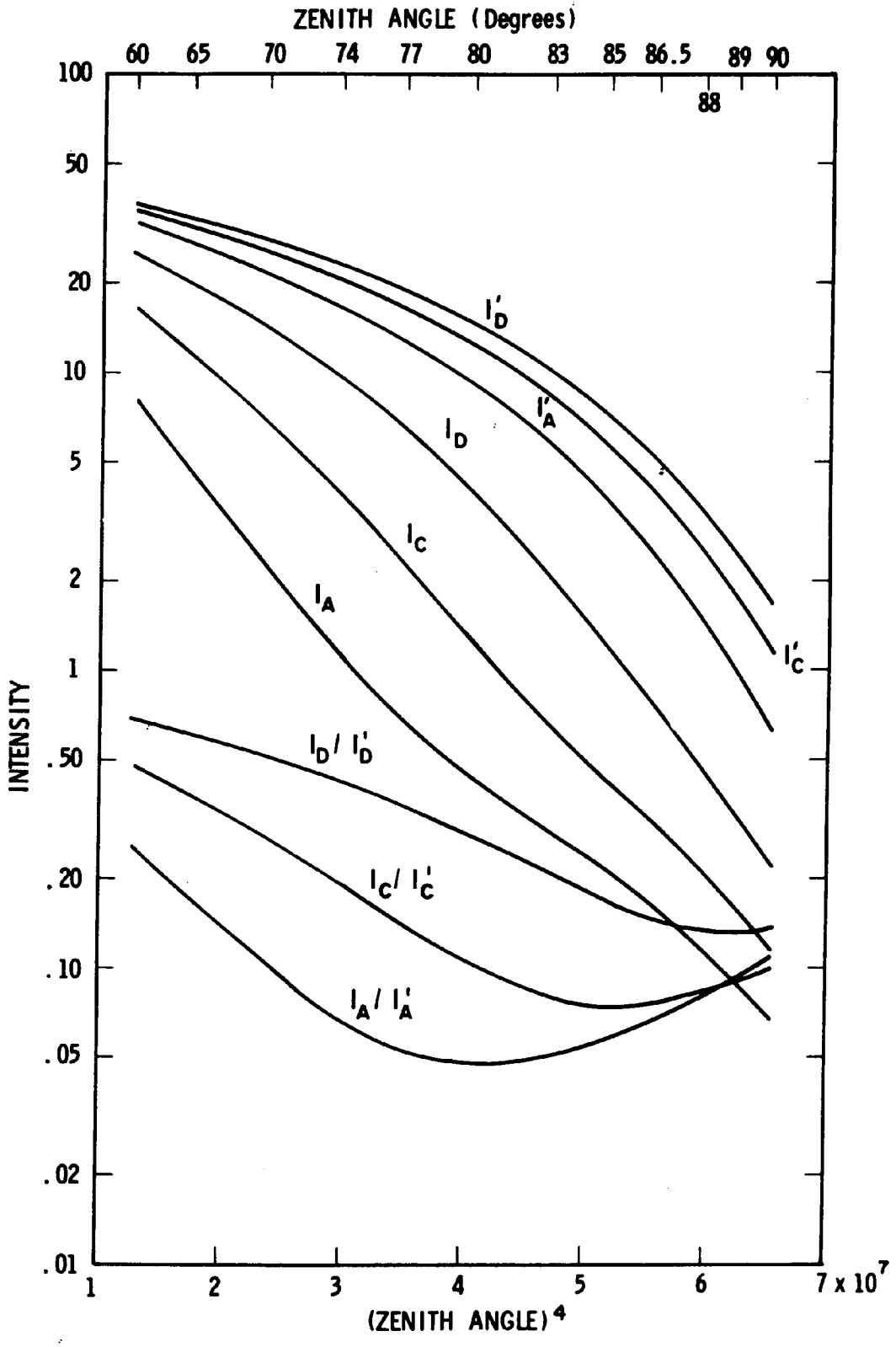


Fig. 22. Relative intensities and intensity ratios for wavelengths A, C and D plotted on a logarithmic scale against solar zenith angle.

the short A wavelength. The upper peak of these undoubtedly represents the predominating effect of decreased absorption path, whereas the lower one represents the predominating effect of greater atmospheric density. This effect is also to some extent observed on the 77° and 80° curves for the short C wavelength, but is heavily smoothed out on the short D wavelength curve. We may note further that the Umkehr effect does not occur until the scattering layer for the short wavelength is almost completely above the ozone maximum.

Because of the great similarity in the shape of the source function curves and the strong overlapping, it is not at all surprising that strong colinearities exist between the points on the Umkehr curve. Looking at it in another way, we may say that the Umkehr effect is an integrating effect and, since information is always lost when we integrate, the Umkehr effect can inevitably provide us with no more than a smoothed vertical distribution of ozone. A measure of the vertical resolution attainable in these solutions is obtained from the half-width of the source function curves.

We may note that measurements on the A wavelength pair are probably equivalent to observing on the C pair when the sun is about 2° below the horizon and that measurements on the D pair are equivalent to stopping C observations when the sun is still 2° above the horizon. Since the "return" for the C pair at 90° is already giving information about ozone content in an atmospheric layer which is very nearly in photochemical equilibrium, we may expect that the ozone layer sensed by the A pair at

90° will have an ozone content considerably dependent on the ozone content of the lower layer sensed by the C pair at 90°. Hence, in effect, there is likely very little additional information to be gained by A pair measurements. The possibility of obtaining additional information by taking observations on more than one wavelength pair is discussed in a later section.

Since multiple scattered radiation originates mostly in the troposphere from primary scattered radiation arriving from the ozone layers above (Sekera and Dave, 1961), we may conclude that the incorporation of multiple scattering in the source function curves will certainly not improve the independence of the points on the Umkehr curve. This is confirmed by the statistical analysis of the previous section.

4. DISCUSSION OF THE LINEARIZED EVALUATION METHOD

4.1 PRELIMINARY REMARKS

In the preceding chapter, it was shown that a linear statistical transformation between points on the Umkehr curve and the ozone content in a number of atmospheric layers can yield information on not more than four layers which should encompass the entire atmosphere up to about 50 km. We saw also that, at least qualitatively, such a result is to be expected from consideration of a simple physical-mathematical model in which only primary scattering is considered. Moreover, we considered that the inclusion of multiple scattering was not likely to improve the resolving power, even though an increase in absolute accuracy might be expected. We may, therefore, anticipate some difficulty with the linearized evaluation equations of Dütsch, which may be written

$$\sum_{j=1}^{9} d_{ij}p_j = u_i, \qquad i=1,\ldots,12 \tag{39}$$

where p_j is now the layer-mean ozone partial pressure deviation from the standard distribution value in layer j, u_i is the difference, $N(\Theta_i)-\eta(\Theta_i)$, between the observed N-value and the standard distribution N-value at zenith angle Θ_i, and d_{ij} is $\partial\eta_i/\partial p_j$.

In practice, the u_i are not known exactly because of instrumental and "modeling" errors. The latter will include inadequate allowances for multiple scattering, no allowance for aerosol effects, errors due to

truncation of the Taylor expansion leading to Eq. (39) (these may be considered as errors due to the linearization of the basically nonlinear problem), errors in the quadrature formulation, and changes in the vertical distribution over the period of observation. If we represent the instrumental errors by ϵ_i and the modeling errors by δ_i then we have

$$\sum_{j=1}^{9} d_{ij}p_j = u_i - \epsilon_i - \delta_i \quad . \tag{40}$$

On the surface, it would appear reasonable to assume that the ϵ_i are random variables with zero mean and are uncorrelated. We should note, however, that ϵ_i is not the instrumental error for a single observation. Each Umkehr curve consists of from 50 to 150 observations, and considerable smoothing of random errors is effected in the process of selecting the N-values for the 12 zenith angles to represent the curve. In addition, some of the random effects of aerosol scattering will be smoothed out in this process. If we lump together these residual errors into one error vector, $e_{ik} = \epsilon_{ik}+\delta_{ik}$, where k, as previously, represents the kth of n Umkehr curves, then it does not necessarily follow that

$$\sum_{k=1}^{n} e_{ik} = 0$$

or that

$$\sum_{k=1}^{n} (e_{ik}-\bar{e}_i)(e_{jk}-\bar{e}_j) = 0, \qquad j \neq i \quad . \tag{41}$$

We may, of course, consider that some of the nonlinear effects are in-

cluded in our system, at least in the final iterative solution of the equivalent of Eq. (22), where an allowance is made for the second order derivative terms in the Taylor expansion.

4.2 THE "COMPLETE" SOLUTION OF THE LINEAR EQUATIONS

Let us now write Eq. (39) in matrix notation as

$$\underset{\sim}{D}\underset{\sim}{p} = \underset{\sim}{u} \quad . \tag{42}$$

In the Dütsch system, this is a set of 12 equations in nine unknowns, and the least squares solution may be written directly as

$$\underset{\sim}{p} = (D^*D)^{-1}D^*\underset{\sim}{u} \quad . \tag{43}$$

A unique solution exists if and only if the matrix D*D is nonsingular. In practice, however, difficulties arise when the matrix is nearly singular. In a recent paper of fundamental importance to the present discussion, Twomey and Howell (1963) have discussed the stability of solutions of equations of this type, which arise in the attempt to evaluate indirect soundings of the atmosphere. They show, as found by Dütsch (1957), that the complete solution of the system leads to wildly oscillating solutions, including the physically unacceptable result of negative ozone concentrations in some layers of the atmosphere.

In arriving at the result of Twomey and Howell, we shall follow a somewhat different procedure. First, we shall "normalize" or scale the solution vector by setting

$$\underset{\sim}{p} = \Sigma\underset{\sim}{\pi} \tag{44}$$

where Σ may be considered as a completely diagonal matrix, having as its diagonal elements the standard deviations of the ozone partial pressures in the appropriate layers. Then we have that

$$D\Sigma\underset{\sim}{\pi} = \Delta\underset{\sim}{\pi} = \underset{\sim}{u} \tag{45}$$

where $\Delta = D\Sigma$. The need for such a normalization or scaling is discussed later. Next, we shall expand the normalized solution vector in terms of a set of orthonormal vectors as follows:

$$\underset{\sim}{\pi} = W^{*}\underset{\sim}{b} \tag{46}$$

where the orthonormal vectors are in the rows of the matrix W and $\underset{\sim}{b}$ is the vector of coefficients of the vectors in the expansion. This is perfectly general in the sense that any arbitrary vertical distribution of ozone (expressed in terms of the mean partial pressures in nine layers) can be expanded exactly in terms of such a set of vectors.

If we now substitute (46) into (45), we have that

$$\Delta W^{*}\underset{\sim}{b} = \underset{\sim}{u} \tag{47}$$

which has the least squares solution for the vector coefficients

$$\underset{\sim}{b} = (W\Delta^{*}\Delta W^{*})^{-1}W\Delta^{*}\underset{\sim}{u} \quad . \tag{48}$$

Let us next require that the contribution to the solution by each vector

shall also "explain" an independent portion of the total variance of the Umkehr curve.

The residual variance of the Umkehr curve is just

$$(\underset{\sim}{u}-\Delta W^{*}\underset{\sim}{b})^{*}(\underset{\sim}{u}-\Delta W^{*}\underset{\sim}{b}) = \underset{\sim}{u}^{*}\underset{\sim}{u} - \underset{\sim}{b}^{*}(W\Delta^{*}\Delta W^{*})\underset{\sim}{b} \qquad (49)$$

when we make the substitution of (47) for $\underset{\sim}{u}$ and note that each term in the expansion is a scalar, and that the transpose of a scalar is just the scalar itself. Thus, the solution contribution of each vector will explain an independent portion of the total variance of the Umkehr curve provided that

$$W(\Delta^{*}\Delta)W^{*} = \Lambda \qquad (50)$$

where Λ is a completely diagonal matrix. As in the previous chapter, this is just the problem of determination of the eigenvalues and vectors of the real symmetric matrix $\Delta^{*}\Delta$. As before, we shall specify that the eigenvalues, λ_i, $i = 1,\ldots,9$, occur on the diagonal of Λ in order of decreasing magnitude and that the rows of W are numbered accordingly. Equation (48) now becomes

$$\underset{\sim}{b} = \Lambda^{-1}W(\Delta^{*}\underset{\sim}{u}) \quad . \qquad (51)$$

We note further that the coefficients b_j are determined independently of each other, being just the product of the reciprocal of the corresponding eigenvalue, λ_j, and the dot product of the vectors $\underset{\sim}{w}_j$ and $(\Delta^{*}\underset{\sim}{u})$, where $\underset{\sim}{w}_j$

is the jth row of W. That is to say,

$$b_j = \lambda_j^{-1} \underset{\sim}{w}_j (\Delta^* \underset{\sim}{u}) \quad . \tag{52}$$

In addition, it follows directly from (49) and (50) that the variance explained by the jth vector is $\lambda_j b_j^2$.

The eigenvalues and vectors for $\Delta^*\Delta$ for one configuration of Dütsch's first derivative matrix, in which the instrument constant is eliminated, total ozone is used, and the scaling vector CI shown in the first column of Table 17 is used in the diagonal of Σ, are shown in Table 7. We note the following:

(i) There is a tremendous range in the eigenvalues of the matrix, from 46.8 to about 10^{-5}, the ratio being 4.5×10^6.

(ii) The low order eigenvectors, corresponding to the larger eigenvalues, exhibit very few changes in algebraic sign from one element to the next. Thus their contributions to the solution vector $\underset{\sim}{\pi}$ will be "smooth."

(iii) The high order eigenvectors, corresponding to the very small eigenvalues, exhibit frequent changes in sign from one element to the next. Their solution contributions will not be "smooth."

It is pertinent to consider what might be termed the "instability ratio" (R_j) for the normalized solution contribution by the jth vector. We may define this as the sum of the squares of the normalized solution contributions divided by the amount of the variance of the Umkehr curve

TABLE 7

EIGENVALUES AND VECTORS FOR ONE CONFIGURATION OF DÜTSCH'S FIRST DERIVATIVE MATRIX FOR HIS STANDARD DISTRIBUTION I

Vector Number	Eigenvalue	Fractional Eigenvalues	Eigenvector Points								
			1	2	3	4	5	6	7	8	9
1	.468C5E 02	.69347	-.17969	-.47106	-.46180	-.40548	-.32145	-.12481	.13566	.30839	.36841
2	.15492E 02	.22953	-.08719	-.02204	.16043	.26205	.37448	.44135	.51507	.39917	.37127
3	.41522E 01	.06152	.33405	.47201	.24817	-.00397	-.23142	-.35635	-.16788	.33450	.53235
4	.917C6E 00	.01359	.68202	.18706	-.21922	-.29723	-.16631	.22658	.46846	-.02005	-.25415
5	.11645E 00	.00173	-.49336	.28229	.26323	-.04507	-.39135	-.26618	.52828	.09560	-.30554
6	.94714E-02	.00014	.26262	-.29892	-.08167	.28847	.34656	-.65079	.17957	.30991	-.28262
7	.158C4E-02	.00002	-.23646	.45609	-.27251	-.48948	.52067	-.03103	-.15579	.31067	-.17138
8	.34137E-03	.00001	-.12243	.37781	-.69850	.50999	-.06399	-.08045	.11768	-.21095	.15926
9	.1C342E-04	.00000	.00895	.00577	-.11505	.30598	-.35605	.33088	-.34529	.62215	-.38791

that is "explained" by this solution contribution. It follows that

$$R_j = \frac{\sum_{i=1}^{9} (b_j w_{ji})^2}{\lambda_j b_j^2} = \frac{1}{\lambda_j} \quad . \tag{53}$$

Thus the vectors corresponding to the large eigenvalues have a relatively small instability ratio, providing a large reduction in Umkehr curve variance for relatively small contributions to the solution. Moreover, as noted above, these solution contributions are "smooth." On the other hand, the vectors corresponding to the very small eigenvalues have a very large instability ratio, providing always a relatively small or negligible reduction in curve variance while introducing very large nonsmooth or oscillatory contributions to the solution. We may conclude that it is the solution contributions of these vectors which introduce the large oscillations into the "complete" solution of Eq. (45).

Looking at the problem in another way, we might consider the "predictability," P_j, of the coefficient of the jth vector as the inverse of the instability ratio. Thus, those vectors which explain little or no curve variance, but contribute much to the solution, are not really predictable from Umkehr observations. That is to say, the eigenvectors associated with the very small eigenvalues represent linear combinations of the unknown variables about which Umkehr observations contain no information (Lanczos, 1956). The problem of deciding where the information ends and the noise begins must be decided by numerical experiment coupled with information about the probable experimental errors.

4.3 THE PROBLEM OF INFORMATION VERSUS NOISE

4.3.1 The Use of the Characteristic Patterns of the Umkehr Curve

In attempting to separate the noise of the Umkehr curve from the basic information, we may use the filtering device of the Characteristic Patterns introduced in Chapter 3. Let us expand the Umkehr curve points u_i in terms of these C. P.'s, truncating the expansion by using only the first four patterns. Thus

$$\hat{\underset{\sim}{u}} = \hat{B}*\underset{\sim}{y} + \bar{\underset{\sim}{u}} \tag{54}$$

where now $\hat{B}$ is a matrix with only four rows each comprising 12 elements, $\hat{\underset{\sim}{u}}$ are the points of the smoothed Umkehr curve, $\bar{\underset{\sim}{u}}$ is the average Umkehr curve for the sample considered and

$$\underset{\sim}{y} = \hat{B}(\underset{\sim}{u}-\bar{\underset{\sim}{u}}) \quad . \tag{55}$$

The noise of the Umkehr curve may be defined as $\underset{\sim}{u}'$ where

$$\underset{\sim}{u} = \hat{\underset{\sim}{u}} + \underset{\sim}{u}' \quad . \tag{56}$$

Substituting in (51) we get

$$\hat{\underset{\sim}{b}} + \underset{\sim}{b}' = \Lambda^{-1}W\Delta'*(\hat{\underset{\sim}{u}}+\underset{\sim}{u}') \tag{57}$$

where

$$\hat{\underset{\sim}{b}} = \Lambda^{-1}W(\Delta*\hat{\underset{\sim}{u}}) \tag{58}$$

and

$$\underset{\sim}{b}' = \Lambda^{-1} W(\Delta^* \underset{\sim}{u}') \quad . \tag{59}$$

The above quantities have been calculated for the Arosa data sample and are given in Table 8 as averages of $w_i \Delta^* \hat{\underset{\sim}{u}}$ (mean smoothed dot product), $\underset{\sim}{w}_i \Delta^* \underset{\sim}{u}'$ (mean error dot product), $\lambda_i \overline{b_i^2}/\overline{v^2}$ (mean fractional variance explained by smoothed curve coefficient), and $\lambda_i \overline{b_i'^2}/\overline{v^2}$ (mean fractional variance explained by error curve coefficient), and $\lambda_i \overline{(b_i+b_i')^2}/\overline{v^2}$ (mean fractional variance explained by combined curve coefficient) for each of the vectors $\underset{\sim}{w}_i$, $i = 1,\ldots,9$. We note that there is certainly no question about the information content of the smooth Umkehr curve as provided by the first three eigenvectors of the matrix $\Delta^*\Delta$. Moreover, the error

TABLE 8

AVERAGES OF SMOOTHED AND ERROR DOT PRODUCTS AND FRACTIONAL VARIANCE EXPLAINED BY EACH AND BY THE COMBINED DOT PRODUCTS

Vector Number i	$\overline{\underset{\sim}{w}_i \Delta^* \hat{\underset{\sim}{u}}}$	$\overline{w_i \Delta^* \underset{\sim}{u}'}$	$\frac{\lambda_i \overline{b_i^2}}{\overline{v^2}}$	$\frac{\lambda_i \overline{b_i'^2}}{\overline{v^2}}$	$\frac{\lambda_i \overline{(b_i+b_i')^2}}{\overline{v^2}}$
1	6.758 (1)	-8.68 (-4)	.51553	.00000	.51552
2	-1.755 (1)	-2.74 (-3)	.25212	.00000	.25214
3	1.718 (1)	-3.53 (-3)	.21634	.00001	.21627
4	-1.379 (0)	2.68 (-3)	.01023	.00008	.01029
5	1.655 (-2)	1.40 (-2)	.00054	.00124	.00179
6	-4.016 (-2)	2.84 (-4)	.00058	.00072	.00129
7	-1.059 (-2)	4.27 (-4)	.00037	.00037	.00076
8	4.450 (-3)	2.77 (-4)	.00017	.00023	.00038
9	-6.191 (-4)	3.84 (-5)	.00012	.00015	.00025

Number in parentheses is power of 10 by which preceding number is to be multiplied.

curve contribution is much smaller than that of the smoothed curve for these eigenvectors. The smoothed curve also provides the bulk of the contribution to the fourth coefficient. However, on the average, the fourth eigenvector explains a rather small fraction of the total curve variance. For the fifth and higher order eigenvectors, the variance explained is negligibly small and more is explained by the error curve than by the smoothed curve. The mean total curve variance is 372.7 $(\text{N-units})^2$; after the first three eigenvectors have been used, the mean residual variance is 6.0, after the first four, it is 1.2. In view of the uncertainties involved, we can certainly expect to obtain no additional real information by explaining this residual variance. We conclude that most of the information content of the Umkehr curve about the vertical distribution of ozone is obtained when we solve for the coefficients of the first three eigenvectors. Perhaps there is some further information to be obtained by solving for the coefficient of the fourth eigenvector; at least we are sure that the fourth vector coefficient is not much contaminated by noise. However, there is no basis for inclusion of the fifth and higher order eigenvectors in the solution system. Thus there are, at most, four pieces of information about the vertical distribution of ozone in the Umkehr observations.

4.3.2 Stepwise Solutions Using the Eigenvectors of $\Delta^*\Delta$

We may, of course, proceed directly from Eq. (52), determining the coefficients b_j and the variance explained $\lambda_j b_j^2$ for each vector in turn.

We test the residual variance after each calculation and, when it drops below some specified limit, truncate the solution procedure, considering that we have extracted all the available information about the vertical distribution. This has been done for the Arosa data sample, using a residual variance testing limit of 6.0 $(\text{N-units})^2$, although the solution contributions and explained variance were computed for all vectors. The frequency distribution of the number of vectors used in the stepwise solution procedure, plus the average fractional curve variance explained by each eigenvector, are given in Table 9. The numbers in the third column of Table 9 represent the same thing as the numbers in the last column of Table 8. In the present case, however, the fraction is taken with each curve and the fractions are averaged. In the previous case, the ex-

TABLE 9

FREQUENCY DISTRIBUTION OF THE NUMBER OF EIGENVECTORS USED IN THE STEPWISE SOLUTION PROCEDURE AND AVERAGE FRACTIONAL UMKEHR CURVE VARIANCE EXPLAINED BY EACH VECTOR

Eigenvector Number	Frequency Distribution of Solution Truncation Levels	Average Fractional Variance Explained by Each Vector
1	0	.4156
2	1	.2241
3	61	.3313
4	33	.0166
5	4	.0035
6	0	.0030
7	1	.0016
8	0	.0013
9	0	.0007

plained variance was summed directly and the fraction taken at the end.

To achieve the selected level for explanation of curve variance, we find that only five cases require more than four vectors, four of these requiring five vectors and the remaining one requiring seven. In the last case, the solution is quite ridiculous, the difficulty apparently being that there is a large residual for $\theta = 65°$, which is not satisfactorily explained by any number of vectors, but the residual variance is brought down just below the limit when the seventh vector is included. In the four cases requiring the fifth vector, there are a few moderately large residuals after four vectors have been used, such that the fifth vector was required to bring the overall residual variance down below the selected limit. As might be expected, all these solutions look a little queer, three of the four having negative tropospheric ozone.

The solution for March 21, 1962, is shown in Table 10. In this particular case, the inclusion of the fifth and sixth vector contributions would still leave a realistic looking solution. However, since very little variance is explained by these contributions, there is no reason for their inclusion. As indicated earlier, the seventh, eighth, and ninth vectors introduce the wild oscillations which must be excluded from the solution system.

The nonuniqueness of the "complete" solution arises from these high order vectors. They represent linear combinations of the unknowns which may be added to the solutions, without affecting, to any appreciable degree, the residuals. Thus we have a triple infinity of solutions that

TABLE 10

STEPWISE SOLUTIONS FOR MARCH 21, 1962, SHOWING INDIVIDUAL SOLUTION CONTRIBUTIONS BY EACH EIGENVECTOR

(Total ozone is 403 m atm-cm)

Eigen-vector Number i	Vector Coefficient b_i	Explained Variance $\lambda_i b_i^2$	Residual Variance	Solution Contributions and Summed Solutions for the Various Vectors — Layer-Mean Partial Pressures (μmb)								
				1	2	3	4	5	6	7	8	9
-	-	-	204.4	23.5	42.1	84.3	132.6	133.9	95.2	53.4	20.1	7.0
1	0.225	2.4	202.0	- 0.5	- 3.2	- 2.5	- 1.6	- 1.0	- 0.3	0.2	0.2	0.1
				23.0	38.9	81.8	131.0	132.9	94.9	53.6	20.3	7.1
2	2.145	71.3	130.7	- 2.2	- 1.4	8.3	10.1	11.2	8.5	6.6	2.6	1.2
				20.8	37.5	90.1	141.1	144.1	103.4	60.2	22.9	8.3
3	5.433	122.5	8.2	21.8	76.9	32.4	- 0.4	- 17.6	- 17.4	-5.5	5.5	4.3
				42.6	114.4	122.5	140.7	126.5	86.0	54.7	28.4	12.6
4	- 2.590	6.1	2.1	-21.2	- 14.5	13.6	13.9	6.0	- 5.3	-7.3	0.2	1.0
				21.4	99.9	136.1	154.6	132.5	80.7	47.4	28.6	13.6
5	1.213	0.2	1.9	- 7.2	10.3	7.7	- 1.0	- 6.6	- 2.9	3.8	0.3	-0.6
				14.2	110.2	143.8	153.6	125.9	77.8	51.2	28.9	13.0
6	0.987	0.009	1.9	3.1	- 8.9	- 1.9	5.1	4.8	- 5.8	1.1	0.9	-0.4
				17.3	101.3	141.9	158.7	130.7	72.0	52.3	29.8	12.6
7	-15.49	0.4	1.5	44	-212	101	136	-113	4	14	-14	4
8	33.87	0.4	1.1	-50	384	-568	311	- 30	- 24	24	-21	8
9	-43.79	0.05	1.0	- 5	- 8	121	-241	218	-130	91	-82	25

are "plausible" from the point of view of explained curve variance by choosing $0 \geq b_7 \geq -15.49$, $0 \leq b_8 \leq 33.87$, and also $0 \geq b_9 \geq -43.79$, in the particular case of Table 10. In general, similar remarks apply to the choice of b_5 and b_6. Since there are at least an infinity of solutions within the above framework that are physically acceptable in that they "look reasonable," we can see clearly why solutions carried out subjectively (by, for example, solving (42) by hand relaxation) are not comparable with each other. Such solutions do not, in fact, obtain from the Umkehr curve the information that is really there, but have "noise" introduced, to an unknown degree, by the personal ideas of the evaluator about what the vertical distribution should look like.

4.4 OBJECTIVE METHODS OF SMOOTHING THE SOLUTION

4.4.1 Truncation of the Eigenvector Expansion

By now it should be clear that the Umkehr observations contain no information about variations in ozone content from one layer to the next. This information must be given by the higher order eigenvectors whose coefficients are not predictable from the observations. As noted in the last section, there is a multiple infinity of solutions which will satisfy Eq. (42). Most of these solutions are physically unrealistic, but there remain at least an infinity of solutions which are physically plausible. It is necessary, therefore, to devise some objective method for selecting a "best" solution, which is consistent with the information that we know we may infer from the Umkehr observations.

One way of obtaining such a solution system is to expand the solution in terms of the eigenvectors of the matrix $\Delta^*\Delta$, truncating the solution with either three or four vectors. It is evident from the preceding discussion that such a procedure will lead to the explanation of a satisfactory amount of curve variance. Moreover, the solutions so obtained are physically plausible when a suitable normalizing procedure has been chosen. A discussion of the scaling problem (i.e., choosing a suitable normalizing procedure) and a more complete discussion of solutions actually obtained by this method are given in the next chapter.

4.4.2 Twomey's Method

In extending a paper by Phillips (1962) which dealt with a similar system of equations, Twomey (1963) introduced a method of objective smoothing which is particularly appropriate to the present case. Twomey and Howell (1963) have also discussed the application of this method in the evaluation of indirect soundings of the atmosphere.

Twomey starts with Eq. (45) with an error vector, $\underset{\sim}{e}$, added as follows

$$\Delta\underset{\sim}{\pi} = \underset{\sim}{u} + \underset{\sim}{e} \quad . \tag{60}$$

He imposes the condition that

$$\sum_{i=1}^{12} e_i^2 = \text{constant} \tag{61}$$

and applies the constraint that the sum of the squares of the solution

deviations from a trial solution shall be a minimum. In our particular problem, an obvious choice for a trial solution is just the standard distribution for which the matrix D of partial derivatives has been calculated. This is equivalent to requiring minimization of the following quantity.

$$\sum_{j=1}^{9} \pi_j^2 + \gamma^{-1} \sum_{i=1}^{12} e_i^2 \tag{62}$$

where γ is an undetermined Lagrange multiplier. To find the minimum, Twomey differentiates (62) with respect to the π_j. Noting from (60) that

$$\frac{\partial e_i}{\partial \pi_j} = \delta_{ij} \tag{63}$$

we get

$$\gamma \pi_j + \sum_{i=1}^{12} e_i \delta_{ij} = 0 \tag{64}$$

or

$$\Delta^* \underset{\sim}{e} = -\gamma \underset{\sim}{\pi} \quad . \tag{65}$$

Premultiplying both sides of (60) by Δ^* and introducing (65), we have

$$(\Delta^* \Delta + \gamma I) \underset{\sim}{\pi} = \Delta^* \underset{\sim}{u} \tag{66}$$

which has the solution

$$\underset{\sim}{\pi} = (\Delta^* \Delta + \gamma I)^{-1} \Delta^* \underset{\sim}{u} \quad . \tag{67}$$

To determine the precise meaning of this equation in terms of our previous discussion, it is instructive to expand the solution in terms of the eigenvectors of the matrix $(\Delta^*\Delta+\gamma I)$. Let

$$V(\Delta^*\Delta+\gamma I)V^* = \Lambda' \quad . \tag{68}$$

But

$$V(\gamma I)V^* = \gamma I$$

whence

$$V(\Delta^*\Delta)V^* = \Lambda' - \gamma I \quad .$$

However,

$$W\Delta^*\Delta W^* = \Lambda$$

and therefore

$$\Lambda' = \Lambda + \gamma I$$

and

$$W = V$$

provided we require that the eigenvectors in the rows of V be orthonormal. Thus we are expanding our solution in terms of the same eigenvectors as before, but now each of the eigenvalues has been increased by γ. The solution for the eigenvector coefficients may now be written

as

$$b_j = (\lambda_j+\gamma)^{-1}\underset{\sim}{w}_j(\Delta^*\underset{\sim}{u}) \quad . \qquad (69)$$

Thus, in the determination of b_j, we now multiply by $(\lambda_j+\gamma)^{-1}$ instead of λ_j^{-1}. The quantity γ is, therefore, a smoothing factor which must be chosen sufficiently large that the high order eigenvector coefficients are effectively reduced to zero, but the low order vector coefficients remain essentially unchanged.

The stepwise solution procedure discussed in Section 4.3.2 and illustrated in Table 10 may now be repeated for Twomey's method. The new vector coefficients are obtained from those in Table 10 upon multiplication by $\lambda_j/(\gamma+\lambda_j)$. The same multiplying factor is required for the variance explained by each vector. In Table 11, the solution of Table 10 is repeated using $\gamma = 0.5$. This value of γ is sufficiently large to eliminate effectively the solution contributions of eigenvectors six through nine, inclusive. The contribution of the fifth vector is decreased to 20% of its original value, that of the fourth to 65%, while the contributions of the first three vectors are relatively unchanged. We may note that the smoothing accomplished by Twomey's method is achieved at the expense of some loss in explained variance. For example, comparing the method of Table 10 with Twomey's, we find the residual curve variance here is 19.6 $(\text{N-units})^2$, whereas three vectors left 8.2 and four vectors 2.1 in the previous method. The variance explained can, of course, be increased by decreasing γ, at some loss in

TABLE 11

STEPWISE SOLUTIONS FOR MARCH 21, 1962, SHOWING THE INDIVIDUAL SOLUTION CONTRIBUTIONS BY EACH EIGENVECTOR USING TWOMEY'S METHOD WITH $\gamma = 0.5$

Eigen-vector Number i	Vector Coefficient b_i	Explained Variance	Residual Variance	Solution Contributions and Summed Solutions for the Various Vectors — Layer-Mean Partial Pressures (μmb)								
				1	2	3	4	5	6	7	8	9
-	-	-	204.4	23.5	42.1	84.3	132.6	133.9	95.2	53.4	20.1	7.0
1	0.224	2.4	202.0	- 0.5	- 3.2	- 2.5	- 1.6	- 1.0	- 0.3	0.2	0.2	0.1
				23.0	38.9	81.8	131.0	132.9	94.9	53.6	20.3	7.1
2	2.078	69.1	132.9	- 2.1	1.4	8.0	9.8	10.9	8.2	6.4	2.5	1.2
				20.9	40.3	89.8	140.8	143.8	103.1	60.0	22.8	8.3
3	4.849	109.3	23.6	19.5	68.6	28.9	- 0.4	-15.7	-15.5	-4.9	4.9	3.8
				40.4	108.9	118.7	140.4	128.1	87.6	55.1	27.7	12.1
4	-1.676	4.0	19.6	-13.7	- 9.4	8.8	9.0	3.9	- 3.4	-4.7	0.1	0.6
				26.7	99.5	127.5	149.4	132.0	84.2	50.4	27.8	12.7
5	0.229	0.03	19.6	- 1.4	1.9	1.5	- 0.2	- 1.2	- 0.5	0.7	0.1	-0.1
				25.3	101.4	129.0	149.2	130.8	83.7	51.1	27.9	12.6
6	0.018	0.00	19.6	- 0.1	0.2	0.1	0.0	- 0.1	- 0.1	0.1	0.0	0.0
				25.2	101.6	129.1	149.2	130.7	83.6	51.2	27.9	12.6
7	-0.049	-	19.6	0.1	- 0.7	0.3	0.4	- 0.3	0.0	0.0	0.0	0.0
8	0.023	-	19.6	0.0	0.1	- 0.2	0.1	0.0	0.0	0.0	0.0	0.0
9	-0.008	-	19.6	0.0	0.0	0.0	0.0	0.0	0.0	0.0	0.0	0.0
				25.3	101.0	129.2	149.7	130.4	83.6	51.2	27.9	12.6

the smoothness of the solution. The example presented here is an extreme one insofar as explained variance is concerned, since about 60% of the curve variance is explained by the third eigenvector. Normally, only about one third of the curve variance is explained by this vector so that the loss is somewhat less.

As will be demonstrated later, Twomey's method is an extremely good one, providing good smoothing of the solution without a too large loss in explained variance. It has the distinct advantage over the method proposed in the previous section that the mathematical constraints applied to the solution are more clearly understood. In particular, the solution contributions by the various vectors are diminished in accordance with the predictability of the vector coefficients. In the method proposed in the last section, we would like to include the fourth vector in the solution, yet the solution contributions seem rather large compared to the amount of variance explained. We should probably eliminate completely the contributions of the fifth and higher order vectors. It also appears reasonable to retain the first three vector contributions without reduction. Thus a combination of the two methods, wherein the first three vector contributions are retained with full weight, the fourth vector contribution is retained at some reduced weight, and the remaining vectors eliminated completely, might prove superior to either of the above methods.

Our main concern here is to determine what information is contained in the Umkehr observations and how this information can best be inter-

preted in terms of the vertical distribution of ozone. It may, therefore, be unwise to weight the eigenvector solution contributions according to the size of the eigenvalue as in Twomey's method, since the linear combinations represented by the eigenvectors almost certainly do not occur in the atmosphere with the same proportionate strength as indicated by the respective eigenvalues. Indeed, there is good numerical evidence, comparing the last columns of Tables 8 and 9 with the eigenvalues of Table 7, that they do not. Solutions computed according to the combined method are presented in the next chapter.

4.5 SOLUTION CONTRIBUTIONS ASSOCIATED WITH THE CHARACTERISTIC PATTERNS OF UMKEHR CURVES

It is of interest to consider the solution contribution associated with each of the Characteristic Patterns. Since these patterns represent deviations from the mean Umkehr curve, we may consider the associated solution contributions as deviations from the mean solution for the sample. If we combine Eq. (34), (44), (46), and (51), the solution contribution vector $\underset{\sim}{\Delta p}_i$ associated with the ith C. P. is given by

$$\underset{\sim}{\Delta p}_i = \Sigma W^* \Lambda^{-1} W \Delta^* \underset{\sim}{\beta^*}_i y_i$$

where $\underset{\sim}{\beta^*}_i$ is the C. P. and y_i is the coefficient of this C. P. when the Umkehr curve is expanded in terms of the C. P.'s. The $\underset{\sim}{\Delta p}_i$ have been computed using the C. P.'s and the derivative matrix configuration used in Section 4.3.2. The truncated eigenvector expansion method of solution has been assumed with four eigenvectors used. Root-mean-square values

were used for the C. P. coefficients, y_i. Results are plotted in Fig. 23 for i = 1,2,3,4. Very similar solution contributions are obtained when Twomey's method is used.

It has to be remembered that the contributions represent deviations from the mean solution. These solution contribution vectors appear with both positive and negative signs and, on the average for the entire sample, each contribution vector has zero mean. Since the coefficient of the first C. P. is strongly correlated with total ozone, we see that above-average ozone results in addition of ozone in the lower stratosphere (layers 2 and 3) and below-average ozone results in subtraction of ozone from the lower stratosphere.

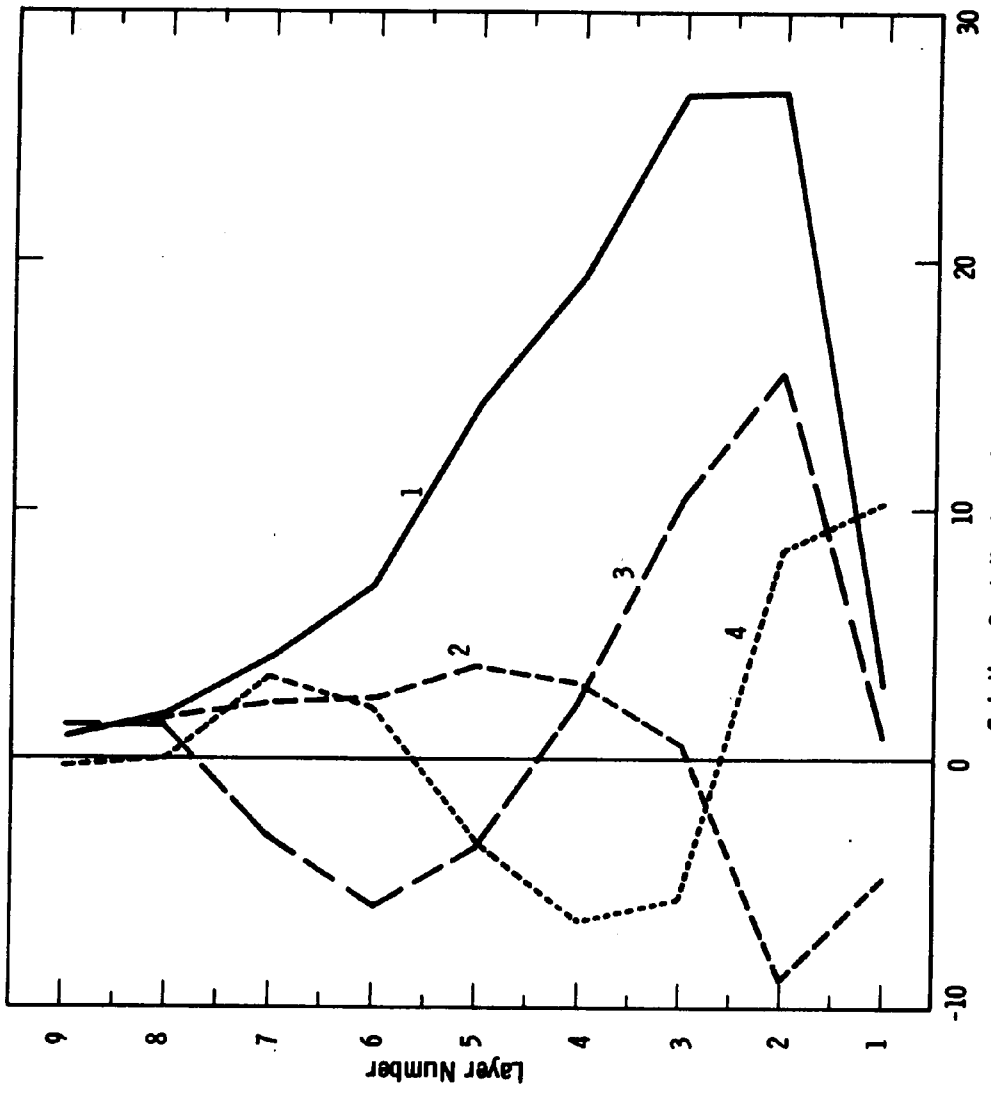


Fig. 23. Solution contribution in the various layers for each of the first four Characteristic Patterns.

5. FURTHER REMARKS ON EVALUATION METHODS AND PRESENTATION OF RESULTS

5.1 THE SCALING PROBLEM

There are two scaling problems to be considered, viz., the weighting vector for the equations (the rows of the matrix D and the corresponding elements of $\underset{\sim}{u}$) and the weighting vector for the variables (the columns of D). In the customary configuration of the matrix D as used in this report, the first equation (row) represents the conservation of ozone, i.e., the requirement that the vertical distribution should be nearly equivalent to the measured total amount. The remaining rows of the matrix D are those of Dütsch's matrix (Tables B-3 to B-7), but with the first row subtracted from each of the others. This is equivalent to elimination of the instrument constant. In addition, since he solves for the fractional ozone change in each layer and we solve for the mean partial pressure change from the standard distribution, the elements of each column have to be divided by the mean ozone partial pressure in the various layers in the standard distribution.

The problem of scaling the ozone conservation equation deserves some discussion. If the equation is used in such a way that the observed residual entered in the vector $\underset{\sim}{u}$ is in m atm-cm, then ozone conservation dominates the solution procedure in such a way that solution total ozone is exactly (to the nearest m atm-cm) the same as the observed total amount. This is equivalent to claiming a priori knowledge that the total

amount of ozone is known without error. However, actual a priori knowledge is that measured total ozone has a standard error of estimate of about 2 m atm-cm. It has been found by numerical experiment that, in the case of the C wavelength pair, agreement within a standard deviation of about 2 m atm-cm is achieved by using a total ozone weighting factor $W_\Omega = 0.1$. In all cases, the weighting factor used will be stated.

Apart from the ozone conservation equation, do we have a need for scaling the problem? There are two simple direct approaches. First, since we are solving for mean partial pressures in each layer, why not solve directly for these without scaling? This is equivalent to choosing column and equation scaling vectors with all elements equal. The average solution and associated statistical data, for the Arosa data sample are given in Table 12. The solutions have been carried out using Twomey's method with a column scaling vector of 10 units, $W_\Omega = 0.1$, a scaling factor of unity for the remaining equations, and $\gamma = 0.5$. The solution residuals are moderately large; moreover the ozone mixing ratios appropriate to layers 8 and 9 indicate a rather large increase of mixing ratio with height, which is not in conformity with photochemical theory.

A second direct approach is to solve, as Dütsch does, for the fractional change in the ozone amount in each layer. This is equivalent to using, in the present context, a column weighting vector having elements proportional to the ozone partial pressures of the standard distribution in the respective layers. The average solution, with associated statis-

TABLE 12

AVERAGE SOLUTION FOR AROSA DATA SAMPLE BY TWOMEY'S METHOD WITH COLUMN SCALING OF 10, $W_\Omega = 0.1$, AND $\gamma = 0.5$

Layer	Layer-Mean Partial Pressures (μmb)	Standard Deviations of Layer-Mean Partial Pressures (μmb)
1	34	13.7
2	48	14.9
3	86	18.4
4	129	19.5
5	123	17.8
6	77	11.8
7	40	6.4
8	18	3.0
9	14	2.6
Mean Residual Variance $(\text{N-units})^2$		4.8
RMS Residual (N-units)		0.63
Mean Total Ozone Residual (m atm-cm)		3.0
RMS Total Ozone Residual (m atm-cm)		6.3

tical data for solutions by Twomey's method, with $\gamma = 0.5$, $W_\Omega = 0.2$ (0.1 was too low), and other equations scaled with unity, are given in Table 13. The bracketed numbers in the table are for the case where $W_\Omega = 1.0$. We note the improvement in the total ozone "fit" when the conservation equation dominates the solution with no real change in the mean solution. A positive total ozone residual means that the observed value exceeds the solution value. Thus the difference between the two solutions, in the mean, is that the ozone solution deficit of 2.2 m atm-cm when $W_\Omega = 0.2$ has been put into the lower atmosphere when $W_\Omega = 1.0$.

Another obvious way of scaling the problem is to divide the elements of the ith row of D (and the ith residual) by the quantity $(\sum_j d_{ij}^2)^{1/2}$ to get matrix D'. Next, we may scale the jth column of D' by dividing by the quantity $(\sum_i d_{ij}'^2)^{1/2}$ to get the matrix Δ. Then the matrix $(\Delta^*\Delta)$ is like a correlation matrix in the sense that the diagonal elements are all unity and the off-diagonal elements are less than unity in absolute value. The averages obtained in this manner are given in Table 14. The solutions are unrealistic in that tropospheric ozone concentrations are frequently negative and the concentration in layer 7 is sometimes less than that in layer 8, something not anticipated from photochemical theory. In addition, the residuals are somewhat larger than we would care to accept. Otherwise the solutions seem not unreasonable. The individual solutions show a strong increase in lower stratospheric ozone when the total amount is large. These solutions have been carried out with the truncated eigenvector expansion (hereinafter TEVE) method using

TABLE 13

AVERAGE SOLUTION FOR AROSA DATA SAMPLE BY TWOMEY'S METHOD WITH COLUMN SCALING EQUIVALENT TO STANDARD DISTRIBUTION LAYER PARTIAL PRESSURES, W_Ω = 0.2 (1.0), AND γ = 0.5

Layer	Layer-Mean Partial Pressures (μmb)	Standard Deviations of Layer-Mean Partial Pressures (μmb)
1	29 (30)	9.1 (10.9)
2	48 (49)	8.6 (9.7)
3	100 (100)	25.2 (26.8)
4	144 (144)	39.2 (39.5)
5	108 (107)	19.1 (19.0)
6	63 (64)	11.9 (11.9)
7	47 (47)	7.1 (7.4)
8	26 (27)	3.7 (3.7)
9	9 (10)	1.1 (1.2)
Mean Residual Variance $(\text{N-units})^2$		3.8 (3.4)
RMS Residual (N-units)		0.56 (0.53)
Mean Total Ozone Residual (m atm-cm)		2.2 (0.1)
RMS Total Ozone Residual (m atm-cm)		4.1 (0.2)

TABLE 14

SOLUTION STATISTICS FOR AROSA DATA SAMPLE FOR SOLUTIONS BY TRUNCATED EIGENVECTOR EXPANSION METHOD WITH COLUMN AND EQUATION SCALING VECTORS DETERMINED FROM DERIVATIVE MATRIX

Layer or Equation	Equation Weights $\frac{1}{(\sum_i d_{ij}^2)^{1/2}}$	Column Weights $\frac{1}{(\sum_i d_{ij}'^2)^{1/2}}$	Layer-Mean Partial Pressures (μmb)	Standard Deviations of Layer-Mean Partial Pressures (μmb)
1	0.52 ($=W_\Omega$)	1.91	30	21.1
2	0.69	2.39	63	40.0
3	0.88	1.81	93	33.9
4	1.09	1.52	130	24.6
5	1.41	1.32	120	15.3
6	1.78	1.15	73	10.1
7	2.29	0.95	37	8.5
8	3.08	0.72	23	3.0
9	4.14	0.39	13	3.4
10	5.73			
11	9.38			
12	22.44			

Mean Residual Variance $(\text{N-units})^2$	13.8
RMS Residual (N-units)	1.08
Mean Total Ozone Residual (m atm-cm)	-0.8
RMS Total Ozone Residual (m atm-cm)	3.8

the first four eigenvectors.

Still another method of scaling would be to introduce an arbitrary value for W_Ω, but otherwise to scale only the columns of D by the method of the previous paragraph. Solution statistics for this procedure are given in Table 15. Both TEVE and Twomey methods have been used with $W_\Omega = 0.1$, and $\gamma = 0.1$ for Twomey's method. The solutions by the TEVE method are fairly reasonable, there being a few small negative ozone values in the troposphere and occasional low values in layer 6. The solution residuals are quite reasonable. The average solution by Twomey's method is not greatly different from the previous one, but the differences are characteristic and persist through all solutions carried out by the two methods. TEVE method always gives less tropospheric ozone, more in the stratosphere (layers 2 and 3), less in layers 6 and 7, and more in layer 8 than Twomey's method. Thus the tendency toward solution instability in the TEVE method (because of the introduction of the fourth eigenvector with full weight) is eliminated by using Twomey's method, with a sufficiently large γ, at some expense in increased residual variance.

Looking back over Tables 12-15, inclusive, we note evidence of a correspondence between the column weighting vector and the variability of the solution amounts in each layer. This suggests an additional constraint which we may impose on the solution, viz., we may choose a column weighting vector such that the variability of our solution layer-mean partial pressures approximates most closely that found in the atmosphere in

TABLE 15

SOLUTION STATISTICS FOR AROSA DATA SAMPLE FOR SOLUTIONS BY TEVE AND TWOMEY METHODS WITH COLUMN SCALING VECTOR DETERMINED FROM DERIVATIVE MATRIX, $W_\Omega = 0.1$, AND $\gamma = 0.1$

Layer	Column Weights	Layer-Mean Partial Pressures (μmb)		Standard Deviations of Layer-Mean Partial Pressures (μmb)	
		TEVE	Twomey	TEVE	Twomey
1	7.52	29	33	16.4	13.6
2	8.90	62	57	26.3	25.9
3	7.34	96	90	27.2	24.6
4	6.05	130	126	21.4	18.6
5	5.19	117	116	15.9	14.3
6	4.32	65	70	11.7	11.2
7	2.60	44	46	5.7	5.8
8	1.10	26	25	3.2	2.7
9	0.48	10	10	1.7	1.3
Mean Residual Variance $(\text{N-units})^2$				2.3	4.7
RMS Residual (N-units)				0.44	0.63
Mean Total Ozone Residual (m atm-cm)				-0.7	1.9
RMS Total Ozone Residual (m atm-cm)				1.7	3.4

actual balloon soundings. The statistical parameters for the balloon sounding data available to the writer are given in Table 16. The method of processing the data is described in Appendix D along with a listing of the sources of the data. We find that two distinct patterns of variability are in evidence in the lower layers of the atmosphere. The first pattern, applicable to moderate and large ozone amounts, indicates a maximum of variability in layers 2 or 3, while the second pattern, based, however, on relatively few soundings for low ozone, shows a maximum variability in layer 4.

Column weighting vectors actually selected for use in the solution procedures used for further work are given in Table 17. The solutions described in Chapter 4 were all calculated from Dütsch's Standard Distribution I (hereinafter SI) using column weighting vector CI with $W_\Omega = 0.1$.

Statistics for solutions with column weighting vector CI, with $W_\Omega = 0.1$, for both TEVE and Twomey methods are listed in Table 18. Solutions by the Twomey method have been carried out using $\gamma = 0.25$, 0.5, and 1.0. The differences between the two methods, as described earlier, are readily apparent. In addition, as we decrease γ, we note the two solutions approach each other. When we increase γ, the persistent differences increase in magnitude, the solution variability decreases, and the unexplained variance increases.

In Table 19, solution statistics are listed to demonstrate the effect of changing the weight W_Ω of the ozone conservation equation in the

TABLE 16

AVERAGES AND STANDARD DEVIATIONS OF LAYER-MEAN PARTIAL PRESSURES FOR BALLOON SOUNDINGS AND UMKEHR DATA

Layer	Standard Deviations of Layer-Mean Partial Pressures (μmb)					Layer-Mean Partial Pressures (μmb)				
	I	II	III	IV	V	I	II	III	IV	V
1	14	12	6	18	15	23	22	13	32	23
2	35	26	13	26	36	57	49	22	97	46
3	31	22	19	30	14	104	102	68	130	91
4	28	22	27	23	17	149	143	128	174	141
5	(17)	(17)	(12)	(20)	(14)	(116)	(114)	(111)	(122)	(116)
6	(11)	(12)	(8)	(10)	(10)	(78)	(79)	(74)	(80)	(82)
7	(6)	(6)	(5)	(6)	(7)	(48)	(47)	(45)	(51)	(51)
8	(2.3)	(2.2)	(2.3)	(2.2)	(3.2)	(22)	(22)	(22)	(22)	(23)
9	(1.7)	(1.8)	(1.7)	(1.3)	(2.3)	(11)	(11)	(10)	(11)	(11)
Average Total Ozone (m atm-cm)						345	334	279	408	333

I: 121 soundings — II + III + IV
II: 71 soundings — $300 \leq \Omega \leq 375$ m atm-cm
III: 18 soundings — $\Omega < 300$
IV: 32 soundings — $\Omega > 375$
V: 29 soundings simultaneous with Umkehr observations

TABLE 17

COLUMN WEIGHTING VECTORS
USED WITH DERIVATIVE MATRICES IN SOLUTIONS

Column (Layer)	Weighting Vectors		
	CI	CII	CIII
1	12	10	5
2	30	20	10
3	24	24	15
4	18	18	20
5	14	14	15
6	9	9	9
7	6	6	6
8	3	3	3
9	1.5	1.5	1.5

two methods. Except for an increase in the variability of the solution in the troposphere, a decrease in the variability of the total ozone residual, and in its average, the results are virtually the same, on the average, as W_Ω is increased. In the case of the TEVE solutions, the stronger forcing on ozone conservation gives ozone partial pressures in the troposphere which are just negative in two cases.

Next, we shall illustrate two effects. First, we have used column vectors CII and CIII, with $W_\Omega = 0.1$ and $\gamma = 0.5$, to obtain solutions by Twomey's method. Second, we have computed solutions with the combined method referred to in the last chapter, where only the first four eigenvectors are used but the fourth one is weighted by using $\gamma = 0.5$. Column weighting vector CI has been used in this case. These results are presented in Table 20. The solutions statistics for CII and CIII illustrate rather clearly the effect of the column weighting vector on solution vari-

TABLE 18

STATISTICS FOR AROSA DATA SAMPLE SOLUTIONS CARRIED OUT BY TEVE AND TWOMEY METHODS USING COLUMN WEIGHTING VECTOR CI, W_Ω = 0.1, AND SI

Layer	Layer-Mean Partial Pressures (μmb)				Standard Derivations of Layer-Mean Partial Pressures (μmb)			
	TEVE	Twomey			TEVE	Twomey		
		γ=.25	γ=.5	γ=1.0		γ=.25	γ=.5	γ=1.0
1	26	27	28	29	11.8	11.0	8.9	7.1
2	73	73	70	66	33.3	36.0	33.3	30.7
3	96	94	92	88	29.3	30.5	28.7	26.9
4	124	123	122	121	20.8	19.2	19.0	18.5
5	112	110	111	112	15.5	14.6	14.5	14.3
6	73	75	76	77	9.7	9.4	9.1	8.7
7	43	44	45	46	6.6	6.7	6.1	5.6
8	24	24	24	23	2.8	2.8	2.6	2.4
9	11	11	10	10	1.9	1.6	1.5	1.4
Mean Residual Variance $(\text{N-units})^2$					2.1	2.2	3.4	6.4
RMS Residual (N-units)					0.42	0.43	0.53	0.73
Mean Total Ozone Residual (m atm-cm)					-0.5	0.1	0.9	3.0
RMS Total Ozone Residual (m atm-cm)					2.4	2.5	3.8	6.3

TABLE 19

STATISTICS FOR AROSA DATA SAMPLE SOLUTIONS TO ILLUSTRATE THE EFFECT OF VARIATIONS IN THE WEIGHT ON THE OZONE CONSERVATION EQUATION, WITH $\gamma = 0.5$

Layer	Layer-Mean Partial Pressures (μmb)				Standard Deviation of Layer-Mean Partial Pressures (μmb)			
	TEVE		Twomey		TEVE		Twomey	
	$W_\Omega = 0.2$	$W_\Omega = 1.0$	$W_\Omega = 0.2$	$W_\Omega = 1.0$	$W_\Omega = 0.2$	$W_\Omega = 1.0$	$W_\Omega = 0.2$	$W_\Omega = 1.0$
1	26	25	28	29	12.4	12.6	10.7	11.4
2	72	72	71	71	32.3	32.1	33.9	34.2
3	97	97	92	92	29.4	29.4	28.7	28.7
4	125	125	122	122	21.0	21.1	19.0	19.0
5	112	112	111	111	15.7	15.7	14.4	14.4
6	73	73	76	76	9.7	9.7	9.1	9.2
7	43	43	45	45	6.4	6.4	6.2	6.2
8	24	24	24	24	2.7	2.7	2.6	2.6
9	11	11	10	10	1.9	1.9	1.5	1.5
Mean Residual Variance $(\text{N-units})^2$					2.2	2.2	3.4	3.4
RMS Residual (N-units)					0.43	0.43	0.53	0.53
Mean Total Ozone Residual (m atm-cm)					-0.1	0.0	0.3	0.01
RMS Total Ozone Residual (m atm-cm)					0.5	0.02	0.5	0.05

TABLE 20

STATISTICS FOR AROSA DATA SAMPLE SOLUTIONS USING CII AND CIII WITH TWOMEY'S METHOD AND USING CI WITH THE "COMBINED" TEVE-TWOMEY METHOD

(γ = 0.5 and W_Ω = 0.1)

Layer	Layer-Mean Partial Pressures (μmb)			Standard Deviations of Layer-Mean Partial Pressures (μmb)		
	Combined	Twomey		Combined	Twomey	
		CII	CIII		CII	CIII
1	30	29	27	8.8	8.7	5.0
2	76	60	51	33.2	20.9	11.3
3	94	97	98	28.4	34.5	23.2
4	122	123	131	19.8	20.6	34.3
5	110	111	110	15.3	14.4	16.3
6	74	75	74	9.4	8.9	8.2
7	44	45	44	6.0	6.0	5.6
8	24	24	24	2.8	2.6	2.6
9	11	10	10	1.8	1.5	1.6
Mean Residual Variance $(\text{N-units})^2$				2.7	3.7	5.4
RMS Residual (N-units)				0.47	0.55	0.67
Mean Total Ozone Residual (m atm-cm)				-3.7	2.1	6.2
RMS Total Ozone Residual (m atm-cm)				5.7	5.1	11.6

ability. We note also some tendency, with CIII, which has a large weight in the fourth column, to produce a more pronounced maximum in layer 4 in the mean solution. It is also evident that a larger value of W_Ω needs to be used with CIII and possibly also with CII to improve the fit with total ozone. The "combined" method results are not much different from those with CI and TEVE or Twomey's methods. The explained variance is somewhere between the other two. The main difference is that ozone has been added in the troposphere and lower stratosphere in the mean and the resulting fit with total ozone is not as good.

Statistics for solutions with respect to Dütsch's Standard Distribution SII, for 42 Arosa curves when total ozone was less than 300 m atm-cm, are listed in Table 21. In view of the persistent secondary maximum obtained when CI was used, this column weighting vector was considered unsuitable for use with SII. Although there is not much to choose between CII and CIII, it was decided to use CII for future solutions with SII, largely because of the somewhat better fit obtained.

The CI column weighting vector has been used for solutions with Standard Distribution III with $\gamma = 0.5$ and $W_\Omega = 0.1$ and the solution statistics are listed in Table 22. These quantities have been used in future solutions with Standard Distribution III. However, in view of the moderately large mean residual for total ozone, it is evident that a larger value of W_Ω should have been used. Since these residuals are negative, we know from the earlier results that the effect of increasing W_Ω would be to decrease the solution values in the lowest layers of the atmosphere.

TABLE 21

STATISTICS FOR AROSA DATA SAMPLE SOLUTIONS WITH RESPECT TO STANDARD DISTRIBUTION II WHEN TOTAL OZONE IS LESS THAN 300 M ATM-CM, WITH $W_\Omega = 0.5$

Layer	Layer-Mean Partial Pressures (μmb)				Standard Deviations of Layer-Mean Partial Pressures (μmb)			
	TEVE	Twomey (γ=.5)			TEVE	Twomey (γ=.5)		
	CII	CI	CII	CIII	CII	CI	CII	CIII
1	24	25	27	25	9.7	9.6	9.0	6.0
2	47	54	43	37	6.7	7.8	5.8	5.8
3	63	49	56	60	8.5	7.9	8.1	4.9
4	88	85	86	96	8.0	6.8	7.0	9.1
5	114	117	116	113	7.3	6.5	6.5	7.9
6	71	75	74	72	6.5	5.6	5.6	5.4
7	40	41	41	41	4.0	3.5	3.5	3.5
8	24	24	24	24	1.2	1.1	1.1	1.1
9	10	10	10	10	1.1	0.8	0.8	0.8
Mean Residual Variance $(\text{N-units})^2$					1.8	2.4	2.5	3.4
RMS Residual (N-units)					0.39	0.45	0.46	0.53
Mean Total Ozone Residual (m atm-cm)					0.04	0.2	0.2	1.1
RMS Total Ozone Residual (m atm-cm)					0.07	0.2	0.2	0.5

TABLE 22

STATISTICS FOR AROSA DATA SAMPLE SOLUTIONS WITH RESPECT TO STANDARD DISTRIBUTION III WHEN TOTAL OZONE EXCEEDS 375 M ATM-CM

(CI, $\gamma = 0.5$ and $W_\Omega = 0.1$)

Layer	Layer-Mean Partial Pressures (μmb)		Standard Deviations of Layer-Mean Partial Pressures (μmb)	
	TEVE	Twomey	TEVE	Twomey
1	34	39	11.7	9.3
2	82	91	21.1	19.5
3	152	146	17.0	16.2
4	158	149	13.5	10.0
5	132	127	8.5	6.6
6	81	84	5.2	4.6
7	46	51	5.3	4.3
8	28	27	2.2	2.1
9	13	12	1.5	1.3
Mean Residual Variance $(\text{N-units})^2$			3.0	4.8
RMS Residual (N-units)			0.50	0.63
Mean Total Ozone Residual (m atm-cm)			-2.3	-4.0
RMS Total Ozone Residual (m atm-cm)			3.3	5.7

5.2 THE EFFECT OF ADDING RANDOM NOISE TO THE OBSERVATIONS

In order to be sure that our solution procedure is a computationally stable one, noise has been added to the observations using a random number generation subroutine directly available as a system subroutine at the Computing Center, The University of Michigan. The random numbers generated had a normal distribution with zero mean and a standard deviation of 0.5 N-units. Solutions have been obtained for these curves by the TEVE and Twomey methods, with respect to SI, using CI, $W_\Omega = 0.1$, and $\gamma = 0.5$. The solution statistics are given in Table 23. We find that the average solutions are virtually identical to their counterparts in Table 18. The solutions are, however, slightly more variable. The total ozone fit is about the same. The slight increase in tropospheric solution variability has given rise to a few very small negative ozone concentrations in the troposphere in the solutions by the TEVE method. The fact that the solution variability has increased by only a small amount indicates that the above procedures are essentially stable ones for evaluation of Umkehr observations.

5.3 THE NEED FOR MORE THAN ONE STANDARD DISTRIBUTION

5.3.1 Convergence of the Iterative Procedure Using the Second Derivatives

One way of examining the need for more than one standard distribution is to look at the number of iterations required to achieve convergence when the second order partial derivatives are used as indicated in Eqs. (21), (22), and (23). To carry out such a test, the Arosa data sample

TABLE 23

STATISTICS FOR AROSA DATA SAMPLE SOLUTIONS WHEN RANDOM NOISE HAS BEEN ADDED TO THE UMKEHR CURVES

(Solutions are relative to SI, with CI, $W_\Omega = 0.1$, and $\gamma = 0.5$)

Layer	Layer-Mean Partial Pressures (μmb)		Standard Deviations of Layer-Mean Partial Pressures (μmb)	
	TEVE	Twomey	TEVE	Twomey
1	25	27	12.2	9.1
2	72	71	33.1	33.1
3	97	92	29.8	29.0
4	125	122	21.4	19.5
5	112	111	15.9	14.9
6	73	76	9.8	9.3
7	43	45	6.7	6.3
8	24	24	2.8	2.2
9	11	10	1.9	1.6
Mean Residual Variance $(\text{N-units})^2$			4.5	5.8
RMS Residual (N-units)			0.61	0.69
Mean Total Ozone Residual (m atm-cm)			-0.8	0.6
RMS Total Ozone Residual (m atm-cm)			2.7	3.8

was divided up into the following subsamples, according to the total amount of ozone: BI($\Omega < 275$); BII($275 \leq \Omega < 300$); BIII($300 \leq \Omega \leq 375$); BIV($375 < \Omega < 410$), BV($\Omega \geq 410$). Subsamples BI and BII were evaluated with respect to SI and SII; BIII with respect to SI; and BIV and BV with respect to SI and SIII. The evaluation was carried out using both the TEVE and Twomey methods and the final solution was that obtained on the mth iteration, such that, in the notation of (23),

$$\sum_{k=1}^{12} \left| S_k^{(m)} - S_k^{(m-1)} \right| \leq 1.0 \text{ N-units} \quad . \tag{70}$$

The frequency distribution of the number of iterations required is given in Table 24. Looking at the frequency distributions, we note an increase in the number of iterations required as the total ozone deviation from the standard distribution value becomes greater (336 m atm-cm for SI). There is a marked improvement when three standard distributions are used, with 90 out of 100 cases converging in two iterations, whereas only 56 cases converge in two iterations when SI is used alone. The above is for Twomey's method; for the TEVE method the corresponding numbers are 84 and 39. Thus we note that the additional smoothing imposed by Twomey's solution method appears to be benificial in terms of reducing the number of iterations required.

5.3.2 Average Solutions

First, we shall consider those cases where total ozone is less than

TABLE 24

FREQUENCY DISTRIBUTIONS OF THE NUMBER OF ITERATIONS REQUIRED FOR CONVERGENCE WHEN THE SECOND ORDER PARTIAL DERIVATIVES ARE USED

Sample	Standard Distribution	Frequency Distributions Number of Iterations						
		1	2	3	4	5	6	7
		Twomey's Method						
BI	SI	0	0	10	10	1	0	0
BII		0	12	7	2	0	0	0
BIII		2	22	4	0	1	0	0
BIV		0	14	2	0	0	0	0
BV		0	6	7	0	0	0	0
BI	SII	0	19	2	0	0	0	0
BII		0	21	0	0	0	0	0
BIV	SIII	0	16	0	0	0	0	0
BV		0	10	3	0	0	0	0
		TEVE Method						
BI	SI	0	0	2	10	9	0	0
BII		0	9	10	3	1	0	0
BIII		1	20	5	2	0	0	1
BIV		0	9	7	0	0	0	0
BV		0	0	13	0	0	0	0
BI	SII	0	19	2	0	0	0	0
BII		1	20	0	0	0	0	0
BIV	SIII	0	13	3	0	0	0	0
BV		0	10	3	0	0	0	0

300 m atm-cm, for which average solutions are listed in Table 25. The usual characteristic differences between the TEVE and Twomey methods are apparent. However, the main difference is between solutions carried out with respect to SI and SII. In every case, the ozone maximum is shifted from layer 4 with SI to layer 5 with SII. The difference cannot be attributed to the choice of the column weighting vector (CI with SI and CII with SII) since the same pattern is evident when we use CI with SII (Table 21). The reason for the difference lies in the fact that we are obtaining a solution which represents a minimum deviation from a trial solution (Twomey), the trial solution being the standard distribution. Examining the standard vertical distributions in Table B-1, we find that SII does have a maximum in layer 5, whereas SI has a rather broad maximum with layers 4 and 5 having approximately equal concentrations. We must conclude that, if indeed there is a significant difference between the mean vertical distributions at low and moderate ozone values, then a separate standard distribution should be used. The evidence of Table 16 is that the solutions with respect to SI are more nearly correct. However, the sample, on which the low-ozone means of Table 16 are based, is much too small and, in addition, contains more soundings for Liverpool (11) than for Arosa (5). Moreover, the concentration in layer 5 is based in part on average Umkehr results. Although Twomey's method as presented here, can be modified to obtain a solution which is a minimum deviation from a trial distribution other than the standard, we are in favor, in view of the iteration results, of using an additional standard distribu-

TABLE 25

AVERAGE SOLUTIONS FOR AROSA DATA SAMPLE WITH SECOND DERIVATIVE CORRECTIONS INCLUDED WHEN TOTAL OZONE IS LESS THAN 300 M ATM-CM .

Solution Method:	Layer-Mean Partial Pressures							
	TEVE				Twomey			
Standard Distribution:	SI	SII	SI	SII	SI	SII	SI	SII
Sub-Sample:	BI	BI	BII	BII	BI	BI	BII	BII
Layer								
1	22	21	26	27	24	24	28	29
2	38	45	43	49	36	42	37	46
3	64	60	67	65	61	54	64	60
4	101	84	107	91	100	82	107	90
5	95	109	104	117	95	111	106	120
6	65	66	74	75	68	70	77	78
7	40	38	45	42	41	40	45	43
8	24	25	23	24	23	24	23	24
9	11	11	10	10	10	11	10	10
Solution Total Ozone	264	264	287	288	264	263	286	288

tion for low total ozone.

Next, we shall consider cases where total ozone exceeds 375 m atm-cm, for which average results are listed in Table 26. In this case, statistics were computed for subsample BIV and for BIV + BV combined. Comparing the differences between the SI and SIII solutions, we find them less pronounced. The major difference, in all cases, is that ozone is removed from the lower stratosphere (layer 2) and added to the troposphere (layer 1) and to layer 3 in large amounts and to layers 4, 5, 6, and 7 in small amounts when solutions are with respect to SIII instead of SI. This difference is probably due to the nature of the CI column weighting vector used with both standard distributions. When much ozone has to be added to the standard distribution, as is the case when SI is used with high total ozone, there is a tendency to add it in layer 2 because of its larger weight in the solution procedure. Comparing these results with those of the balloon soundings as given in Table 16, we find that we should probably have a more pronounced peak in layer 4 in our standard distribution SIII.

5.4 THE NEED FOR SECOND DERIVATIVE CORRECTIONS

What is the effect of applying the corrections for the second order derivatives in the Taylor expansion? Since we are already well aware of the differences between the two solution methods, TEVE and Twomey, average solutions with and without these corrections are given in Table 27 for the Twomey method only. Moreover, since the differences will be

TABLE 26

AVERAGE SOLUTIONS FOR AROSA DATA SAMPLE WITH SECOND DERIVATIVE CORRECTIONS INCLUDED WHEN TOTAL OZONE EXCEEDS 375 M ATM-CM

	Layer-Mean Partial Pressures							
Solution Method:	TEVE				Twomey			
Standard Distribution:	SI	SIII	SI	SIII	SI	SIII	SI	SIII
Sub-Sample:	BIV	BIV	BIV+V	BIV+V	BIV	BIV	BIV+V	BIV+V
Layer								
1	24	33	27	36	25	37	27	39
2	99	70	113	83	100	79	116	92
3	131	142	140	151	126	138	136	147
4	150	152	153	156	145	145	148	149
5	129	129	129	130	136	125	125	125
6	80	82	78	81	82	84	80	83
7	47	48	47	47	51	52	51	52
8	28	28	29	29	27	27	28	28
9	14	13	14	14	12	12	13	13
Solution Total Ozone	398	398	415	414	395	400	411	415

TABLE 27

AVERAGE SOLUTIONS FOR AROSA DATA SAMPLE TO ILLUSTRATE DIFFERENCES BETWEEN LINEAR (L) AND NONLINEAR (NL) SOLUTIONS

Layer	Layer-Mean Partial Pressures					
	$\Omega < 300$		All Ω		$\Omega > 375$	
	L	NL	L	NL	L	NL
1	26	26	28	27	31	27
2	44	37	70	67	115	116
3	66	62	92	91	131	136
4	104	104	122	122	145	148
5	98	101	111	112	125	125
6	69	72	76	77	82	80
7	40	43	45	47	50	51
8	22	23	24	24	27	28
9	10	10	10	11	12	13

greatest when we use SI for low and high ozone, only solutions with respect to SI are given. For low ozone, the effect of the second order derivatives is to transfer ozone from layers 2 and 3 to layers 5, 6, and 7. A similar comment applies, but to a lesser extent, when all values of total ozone are lumped together. The effect for high total ozone is less clear-cut. The influence of the corrections is to remove ozone from layers 1 and 6 and to add it in layers 3 and 4.

It is somewhat more instructive to look at individual solutions since, on the average, we might expect the effect of the second derivative corrections to cancel out. Solution instability first manifests itself, in the linear solution system, in the form of low ozone values in layers 6 and/or 7 and in the troposphere. Since these effects show up in a more pronounced manner in the TEVE solutions, examples of each

are shown in Table 28. The solution which required 7 iterations, which also suffers from low ozone in layers 6 and 7, is one of those listed. We see that the effect of introducing the second order corrections is to improve the smoothness of the solutions. Thus, although we might be inclined to discard the second order corrections as unnecessary in viewing only the average solutions, they do serve a useful purpose in smoothing out unrealistic irregularities in some solutions.

TABLE 28

INDIVIDUAL SOLUTIONS CHOSEN TO ILLUSTRATE THE DIFFERENCES BETWEEN LINEAR (L) AND NONLINEAR (NL) SOLUTIONS

Layer	Layer-Mean Partial Pressures					
	4/4/61		10/20/61		10/31/61	
	L	NL	L	NL	L	NL
1	0	4	22	32	15	18
2	61	62	100	99	43	34
3	122	118	115	102	72	64
4	150	146	126	116	104	101
5	128	125	97	94	91	93
6	71	72	52	57	57	63
7	36	38	27	34	32	38
8	24	25	24	25	23	24
9	12	12	12	12	11	11
Observed Ω	334	334	327	327	254	254
Solution Ω	335	335	327	329	255	255
No. of iterations		3		7		5

5.5 COMPARISON WITH DÜTSCH'S SOLUTIONS

Dr. Dütsch has kindly provided the writer with a duplicate card deck of solutions for the cases given in his 1963 report. However, the card

deck solutions had undergone a further processing to achieve a closer fit between observed total ozone and that implied by the solution. In selecting those cards which corresponded to the sample used in this study, it was found that our sample contained five duplicates, all for clear sky Umkehrs, where Umkehr curves had been included for the cases with and without luxmeter corrections. In addition there were two curves in our sample for which no solution card was available in Dütsch's solution deck. Thus the sample for which an exact correspondence existed was reduced to 93 cases. In setting up duplicate decks, the appropriate solution from SI, SII or SIII was chosen from the present work. Average solutions and solution variabilities are listed in Table 29 for this sample, for the three methods: Dütsch, TEVE, and Twomey. The individual solutions are listed in Appendix E, which also includes the duplicates and the two missing solutions. The data are listed in order of increasing total ozone and, in the case of the duplicates, the first solution listed corresponds to Dütsch's. Also listed in Table 29 are the fractional eigenvalues of the correlation matrix of the solution partial pressures. On the whole, we find only rather small differences between the solution statistics, indicating that Dütsch's technique of averaging solutions from several systems of overlapping layers has been successful in eliminating the instabilities from the system. The correlation matrix eigenvalues are an indication of the number of independent linear combinations that are present in the normalized solutions. As it should, from its basic formulation, the TEVE solution method explains more of the normalized

TABLE 29

SOLUTION STATISTICS FOR AROSA DATA SAMPLE TO COMPARE THE DÜTSCH, TEVE, AND TWOMEY METHODS OF SOLUTION WITH SECOND DERIVATIVE CORRECTIONS APPLIED

Layer	Layer-Mean Partial Pressures (μmb)			Standard Deviation of Layer-Mean Partial Pressures (μmb)			Fractional Eigenvalues of Partial Pressure Correlation Matrix		
	Dütsch	TEVE	Twomey	Dütsch	TEVE	Twomey	Dütsch	TEVE	Twomey
1	32	28	30	11.9	11.8	10.6	.424	.536	.578
2	57	63	63	25.4	23.2	26.6	.339	.230	.176
3	97	96	92	41.1	38.6	39.2	.121	.144	.135
4	122	120	117	28.6	28.9	26.3	.081	.064	.061
5	113	117	116	11.4	11.4	8.8	.032	.016	.035
6	78	75	78	7.7	7.2	6.5	.002	.009	.012
7	47	44	46	5.9	5.1	5.4	-	-	.003
8	23	25	25	2.4	3.0	2.8	-	-	.001
9	11	11	11	1.8	2.2	1.7	-	-	-

solution variance with the first four eigenvectors, but the differences do not appear to be significant.

5.6 ANOTHER ORTHOGONAL VECTOR EXPANSION FOR SOLUTIONS

Another possibility is to expand the vertical distribution in terms of its own characteristic patterns, or empirical orthogonal functions, truncating the expansion after the first three or four pattern vectors have been used. One of the problems here is to secure empirical data giving the vertical distribution in all of the nine layers of the atmosphere that are used in the current study. The data available for ozonesonde intercomparisons carried out at Arosa in July-August, 1958 (Brewer et al., 1960), in the summer of 1961, and again during the spring of 1962, with simultaneous Umkehr data on most occasions, provide the closest approach to the required information. A total of 29 such vertical distributions were synthesized by matching up the balloon results for the lower atmosphere and the Umkehr results for higher levels. The correlation matrix, and its eigenvalues and vectors were calculated for this small sample. Solutions have been carried out using the first four eigenvectors of the correlation matrix. In this case, we set

$$\underset{\sim}{\pi} = \Sigma^{-1}(\underset{\sim}{p}-\bar{\underset{\sim}{p}})$$

or

$$\underset{\sim}{p} = \Sigma\underset{\sim}{\pi} + \bar{\underset{\sim}{p}} \qquad (71)$$

where Σ and $\bar{p}$ are the standard deviations and means, respectively, of the ozone partial pressures in the various layers for the sample of 29. These are given in the columns designated V in Table 16.

The linear equation system (42) now becomes

$$D\Sigma\underset{\sim}{\pi} = \underset{\sim}{u} - D\bar{p} \quad . \tag{72}$$

Setting

$$\underset{\sim}{\pi} = W^{*}\underset{\sim}{b} \tag{73}$$

we have

$$D\Sigma W^{*}\underset{\sim}{b} = \Delta W^{*}\underset{\sim}{b} = \underset{\sim}{u} - D\bar{p} \tag{74}$$

with the least squares solution

$$\underset{\sim}{b} = (W\Delta^{*}\Delta W^{*})^{-1}W\Delta^{*}(\underset{\sim}{u}-D\bar{p}) \quad . \tag{75}$$

In this case, the coefficients b_j do not explain independent segments of Umkehr curve variance, nor can they be computed independently, since $(W\Delta^{*}\Delta W^{*})$ is no longer a completely diagonal matrix. It should be noted that the matrix W, as used in this context, comprises only the first four eigenvectors of the correlation matrix. Solutions have been carried out according to this scheme using the Arosa data sample for low ozone ($\Omega < 300$) re SII, for all ozone re SI, and for high ozone ($\Omega > 375$) re SIII. In each case, $W_{\Omega} = 0.1$ was used.

In this section and the next one, average solution results are presented in the form of smooth curves on ozonagrams. In drawing these smooth curves through the block distributions implied by the actual solutions, the smoothest curve which keeps the same amount of ozone in each layer is drawn subjectively. This is illustrated in Fig. 24 which shows the block distribution and the smooth curve for the case SI (TEVE) of Fig. 25. In drawing this curve, use has been made of our a priori knowledge from balloon soundings that the tropospheric distribution tends to follow a constant mixing ratio line. The usual sharp increase in partial pressure at the tropopause has been smoothed out since we are dealing with mean solutions. A discussion of objective criteria for drawing these curves has been given by Godson (1962).

It has to be emphasized that all of the smoothed curves presented here are for average solutions and that the subtle changes in curvature of the curves from one layer to the next are properties of the solution system used. Inferences about differences in mean solutions (i.e., in solution systems) and about differences between individual solutions computed from the same system should be made only for rather broad atmospheric layers.

Average solutions for 42 low ozone cases are shown in Fig. 25, where $\overline{p}$ has been taken as zero (reference CP, 0 in the figure). In addition, curves for average linear solutions from the previous work are shown.

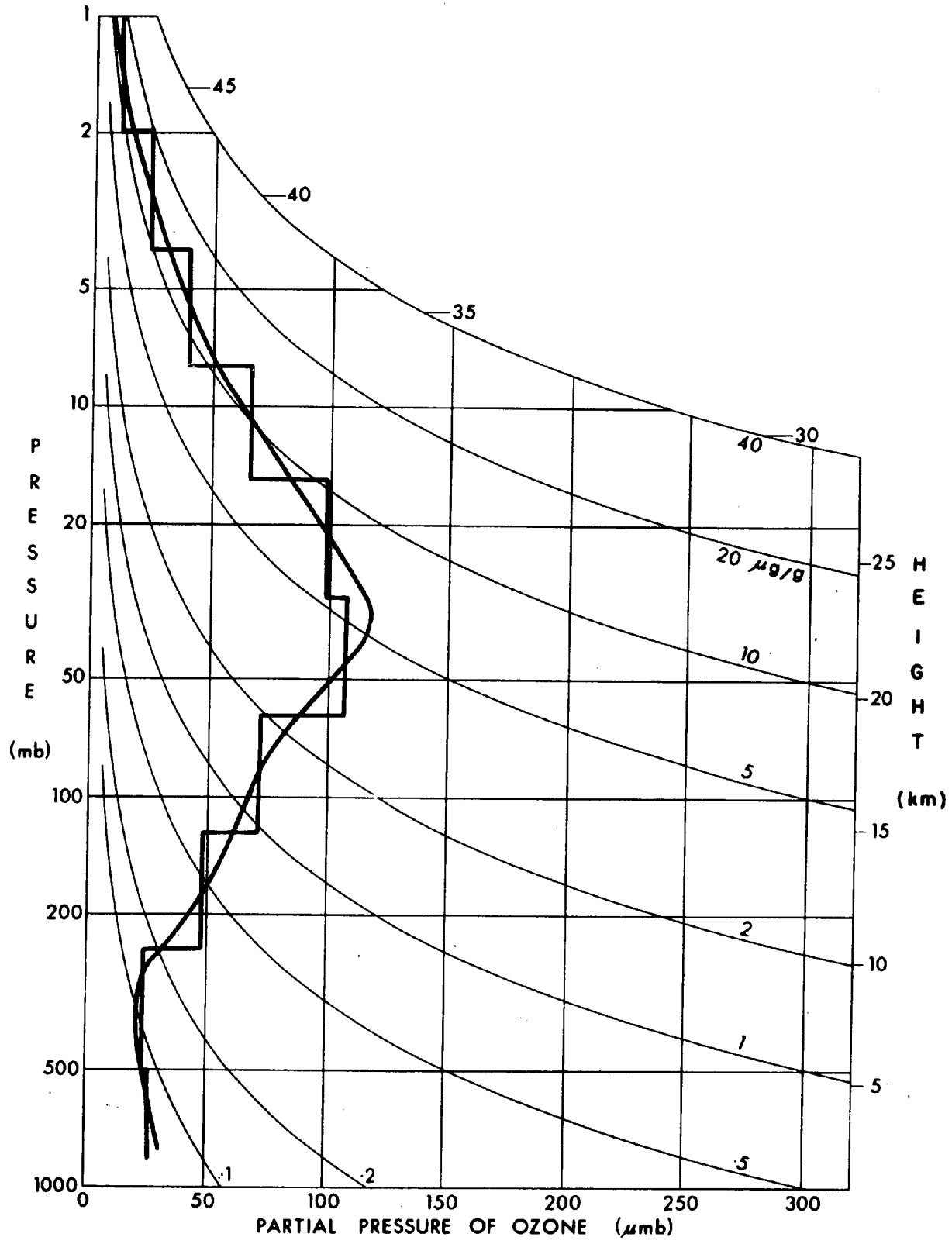


Fig. 24. Illustrating the smooth curve obtained from the original block distribution.

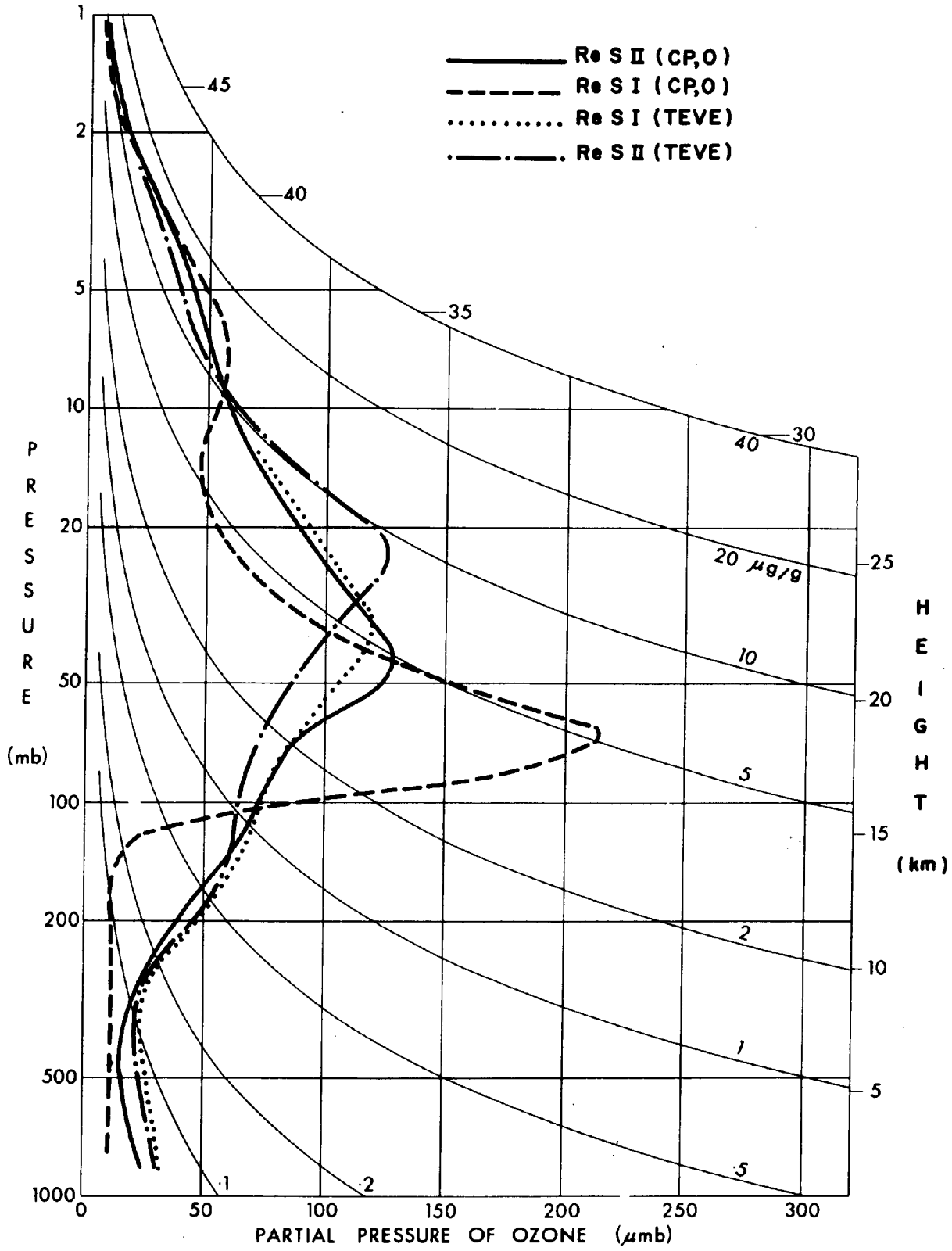


Fig. 25. Average solutions for 42 low-ozone cases at Arosa using the Characteristic Pattern method, with TEVE solutions for comparison.

The result using the characteristic patterns with respect to SI is quite ridiculous and indicates that the linear combinations implied by the characteristic patterns are not necessarily ones whose coefficients can be inferred from the Umkehr observations, at least when the C. P.'s are determined from such a small sample.

Average solutions for 29 high ozone cases are shown in Fig. 26. In one case (designated CP,V) $\bar{p}$ has been set equal to the appropriate vector in Table 16. The characteristic pattern solutions, except perhaps for case CP, O re SIII, are considerably less smooth than those obtained by the linear TEVE method. The interesting feature of these solutions is the ozone maximum in the lower stratosphere in cases CP, O re SI and CP, V re SIII. There is, of course, also a suggestion of such a maximum in the TEVE solution. The reasons for a high ozone content in layer 2 in this case have already been discussed. The reason for the high ozone content in layer 2 in the other two cases is that the $\bar{p}$ vector corresponds to about the same amount of ozone as is present in SI. Moreover, the column weighting vector used here assigns a high weight to layers 2 and 4, but a low weight to layer 3. Thus, there is a tendency to add ozone in layers 2 and 4 in preference to layer 3. Since much ozone has to be added for these high ozone cases, we end up with the double maximum structure. Thus we do not get the lower stratospheric maximum from the Umkehr curve, but rather because we said in advance that it would be there whenever total ozone is high.

In Fig. 27, average linear solutions, all with respect to SI, for

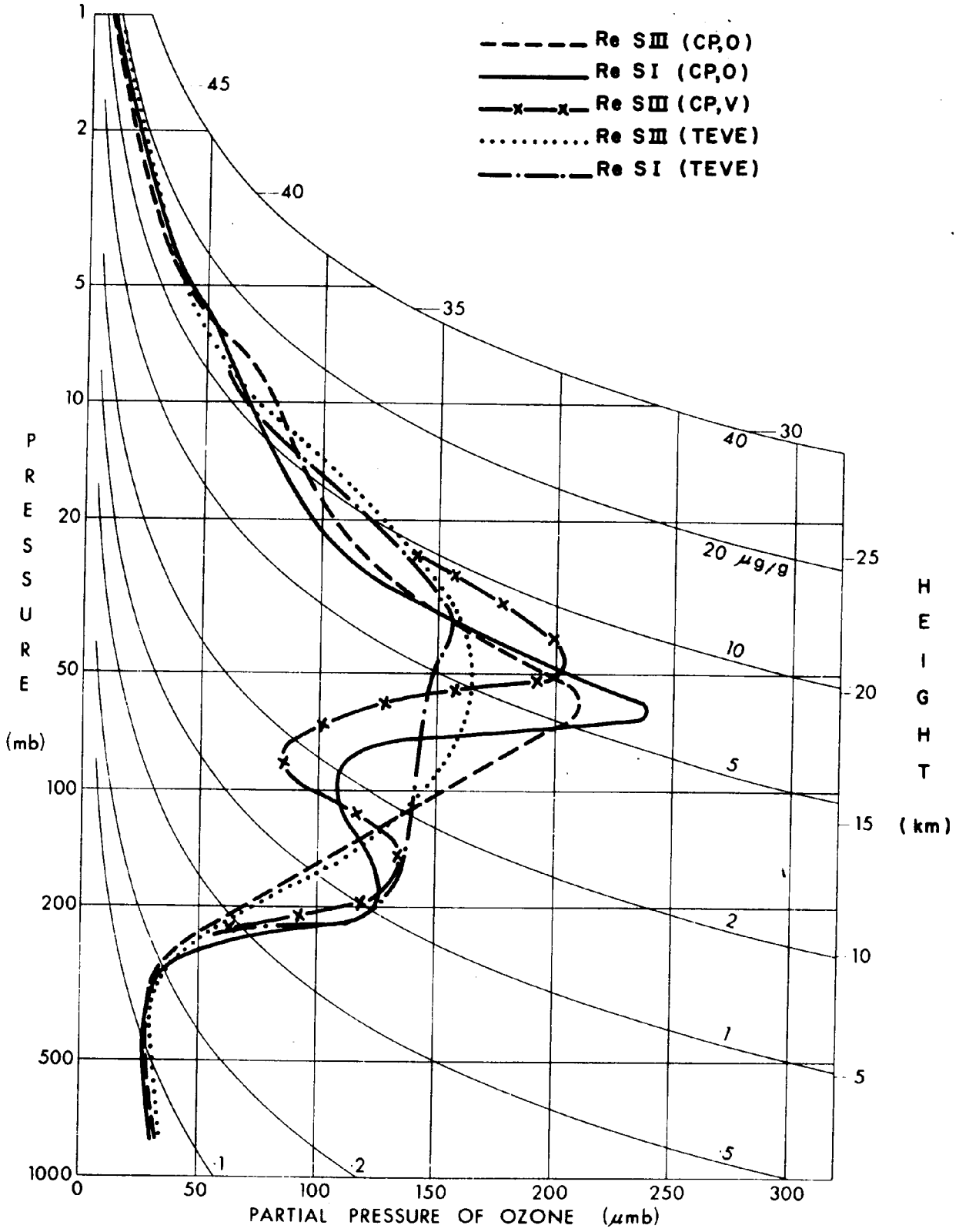


Fig. 26. Average solutions for 29 high-ozone cases at Arosa using the Characteristic Pattern method, with TEVE solutions for comparison.

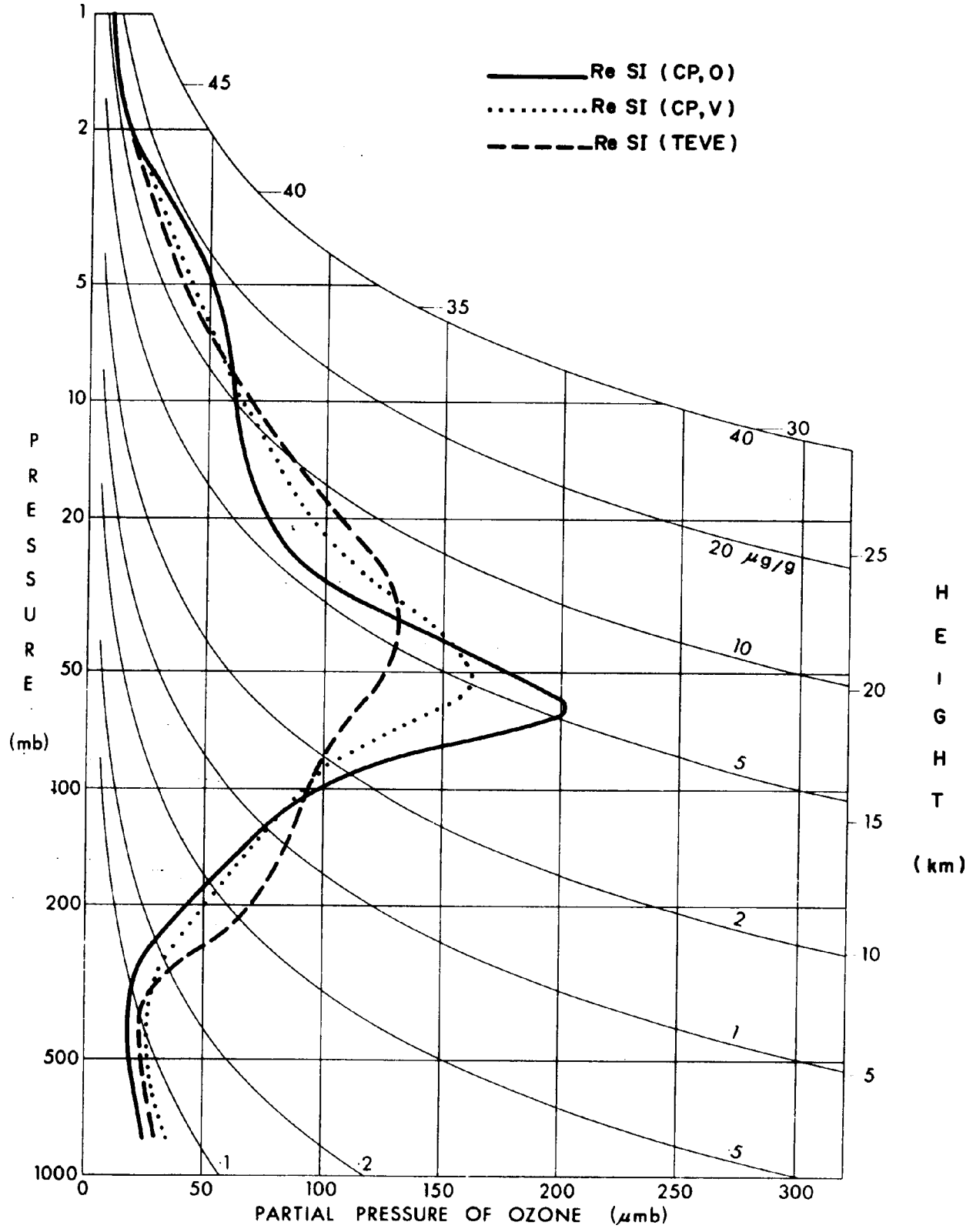


Fig. 27. Average solutions for 100 Arosa Umkehr curves using the Characteristic Pattern method, with TEVE solutions for comparison.

the entire Arosa data sample are plotted. The tendency toward a small hump in the lower stratosphere on the TEVE curve largely disappears when the curves for high ozone values entered in the average are replaced by those taken with respect to SIII.

Although the use of the empirical orthogonal functions or characteristic patterns of the vertical distribution is an attractive way of imposing a priori knowledge on the solution system, it clearly requires a reasonably sized sample of complete vertical distributions for calculation of the Characteristic Patterns. In addition, the $\underset{\sim}{\bar{p}}$ vector should be used in the selection of the standard vertical distribution. Thus, with the column weighting vector also smoothed out by a larger sample, we should tend to have smooth solutions similar to those obtained by the previously discussed methods. The advantage of the previous methods is that the solution is expanded in terms of those linear combinations of the unknowns on which the measurements can provide information, within the restrictions of the physical-mathematical model used.

5.7 VERTICAL DISTRIBUTIONS USING OTHER WAVELENGTH PAIRS

Heretofore, only Umkehr observations on the C wavelength pair have been much used to estimate the vertical distribution of ozone. It is well known that discrepancies exist between observations of total ozone amounts on the different wavelength pairs, when the ozone absorption coefficients determined in the laboratory are used with the spectrophotometer (see Appendix A for a brief discussion of this point).

To gain some insight into this problem, solutions have been carried out, using the Twomey technique (with $\gamma = 0.5$) on wavelength pairs A, C, D, AD, AC, and CD, and on the combined pairs A-C-D, AC-CD, and AD-AC. The sample of 98 Umkehr curves from the North American network and Dütsch's first derivative matrices for Arosa have been used. Although this procedure is not strictly correct because Arosa has a mean surface pressure of 814 mb, the differences are not large (see Dütsch, 1957, and Mateer, 1960), and the results will serve to indicate the general nature of the problem. Unfortunately, Dütsch's second derivatives were not computed for the full range of zenith angle used here, so that only linear solutions are possible and these are all with respect to SI.

Column weighting vector CIII was used for these solutions since it was found that CI gave negative partial pressures in layer 2 for low total ozone due to the large weight assigned to that layer by CI. In addition, a value of $W_\Omega = 1.0$ was used throughout. Total ozone amounts in the North American network are based on the double-pair AD measurements. Corrections, indicated in Table 30 (after Dobson, 1963) were applied to the total ozone amounts to render them "compatible" with the ozone absorption coefficients actually used in the construction of the derivative matrices. The solution amounts were then "recorrected" back to the AD ozone scale. When multiple pairs were used, viz., A-C-D, AC-CD, and AD-AC, no corrections were applied. The average solutions are shown in Figs. 28, 29, and 30. In addition, solutions have been carried without corrections for total ozone, and the result for the C wavelengths is given

TABLE 30

CORRECTION FACTORS FOR AD TOTAL OZONE MEASUREMENTS USED IN UMKEHR EVALUATIONS

Wavelength Pair	Correction Factor for AD Total Ozone	Re-Correction Factor for Solution Ozone
AD	1.00	1.000
A	0.99	1.011
C	0.93	1.076
D	0.95	1.056
AC	1.05	0.956
CD	0.92	1.091

in Fig. 31, for comparison with the corrected solution. For the C wavelengths, solutions were also carried out with the CI column weighting vector, using SI, $W_\Omega = 0.1$, $\gamma = 0.5$, Twomey's method, and applying the second derivative corrections. The average of these latter solutions is also shown in Fig. 31, as Case III, and the solutions are listed in full detail in Appendix E.

Looking first at the individual wavelength solutions in Fig. 28, we note a progressive decrease in the amount of ozone at high levels as we go from A to C to D. The reverse is true at low levels. The main maximum on the A and C curves is at about the same level, but that for the D curve is a little lower. Referring to Fig. 31, where Case I is the curve of Fig. 28 and Case II is the mean curve when total ozone is uncorrected, we note a downward shift of the C curve maximum in the latter case, and an increase in the low-level concentration. Similar remarks apply to the uncorrected D curve (not shown). We note, however, that the application

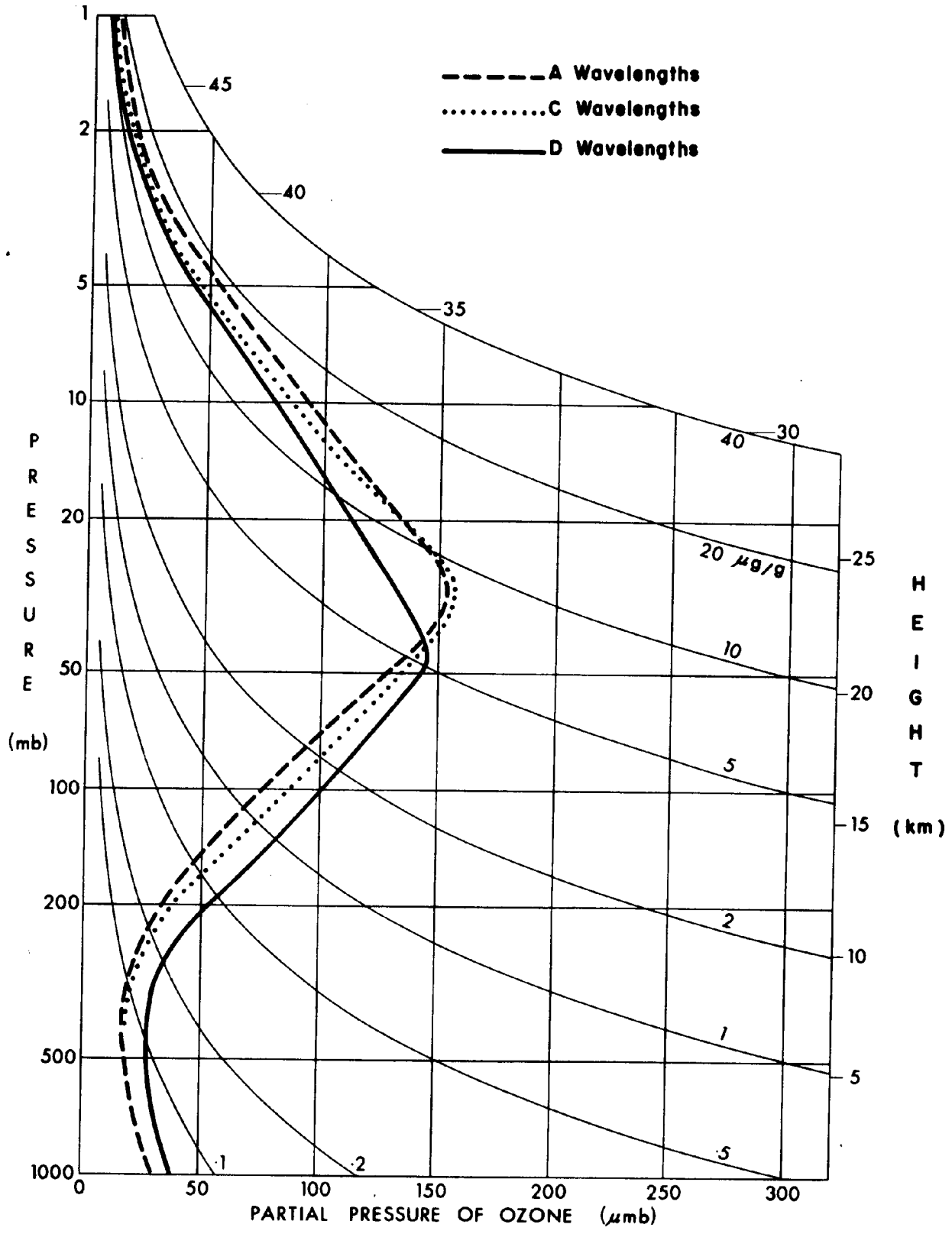


Fig. 28. Average solutions for 98 North American Umkehr curves for the individual wavelength pairs.

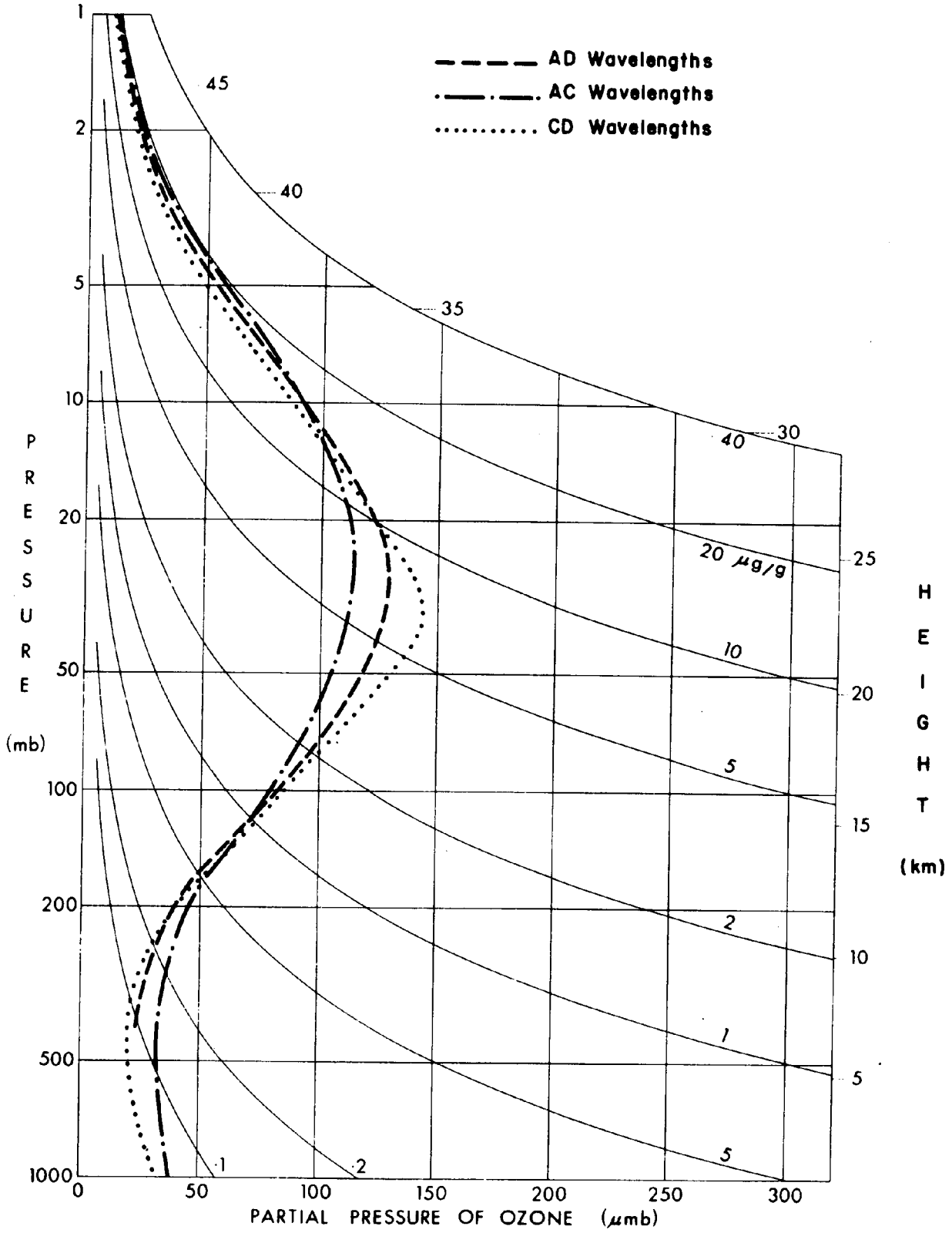


Fig. 29. Average solutions for 98 North American Umkehr curves for the double wavelength pairs.

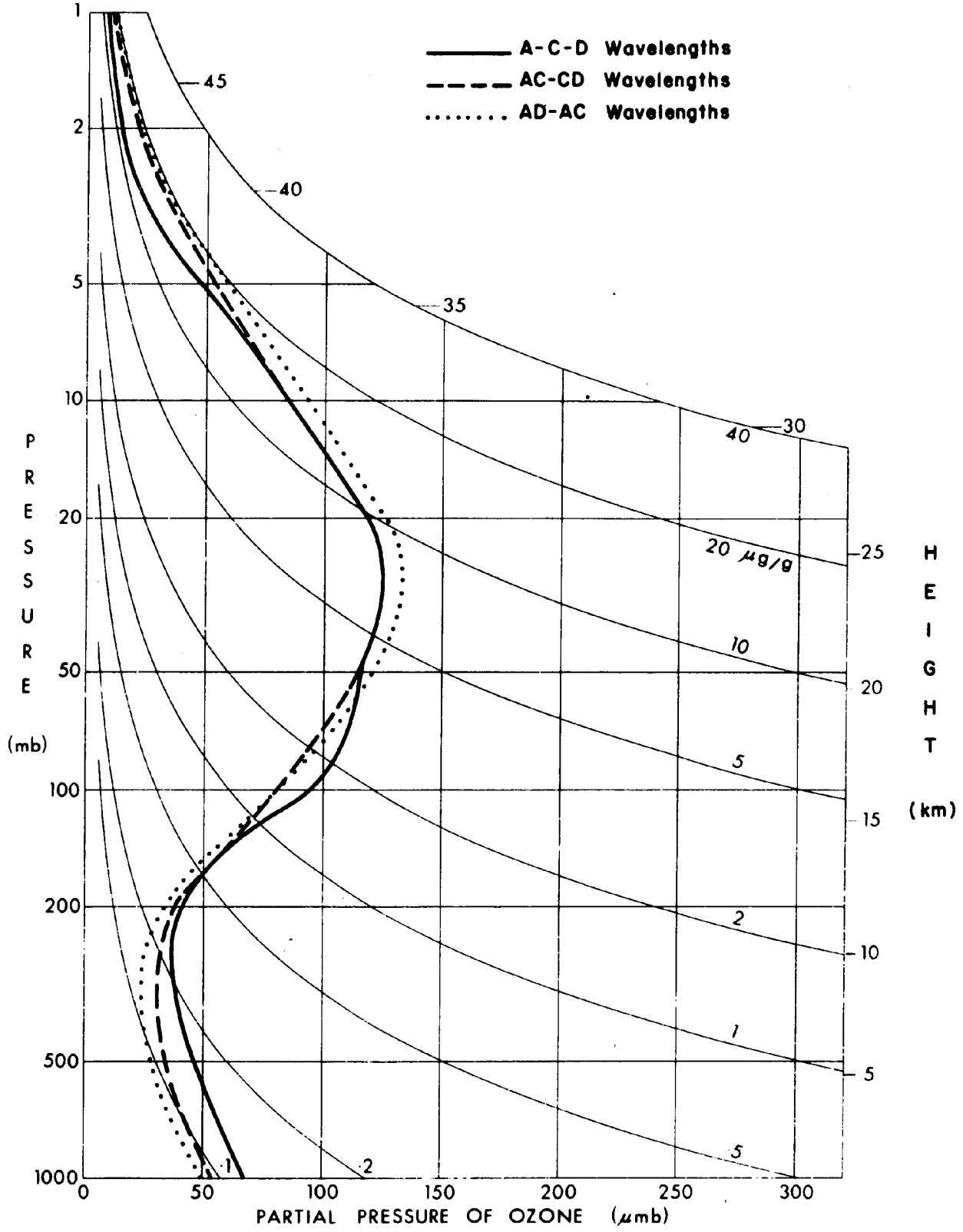


Fig. 30. Average solutions for 98 North American Umkehr curves for combined wavelength pairs and double pairs.

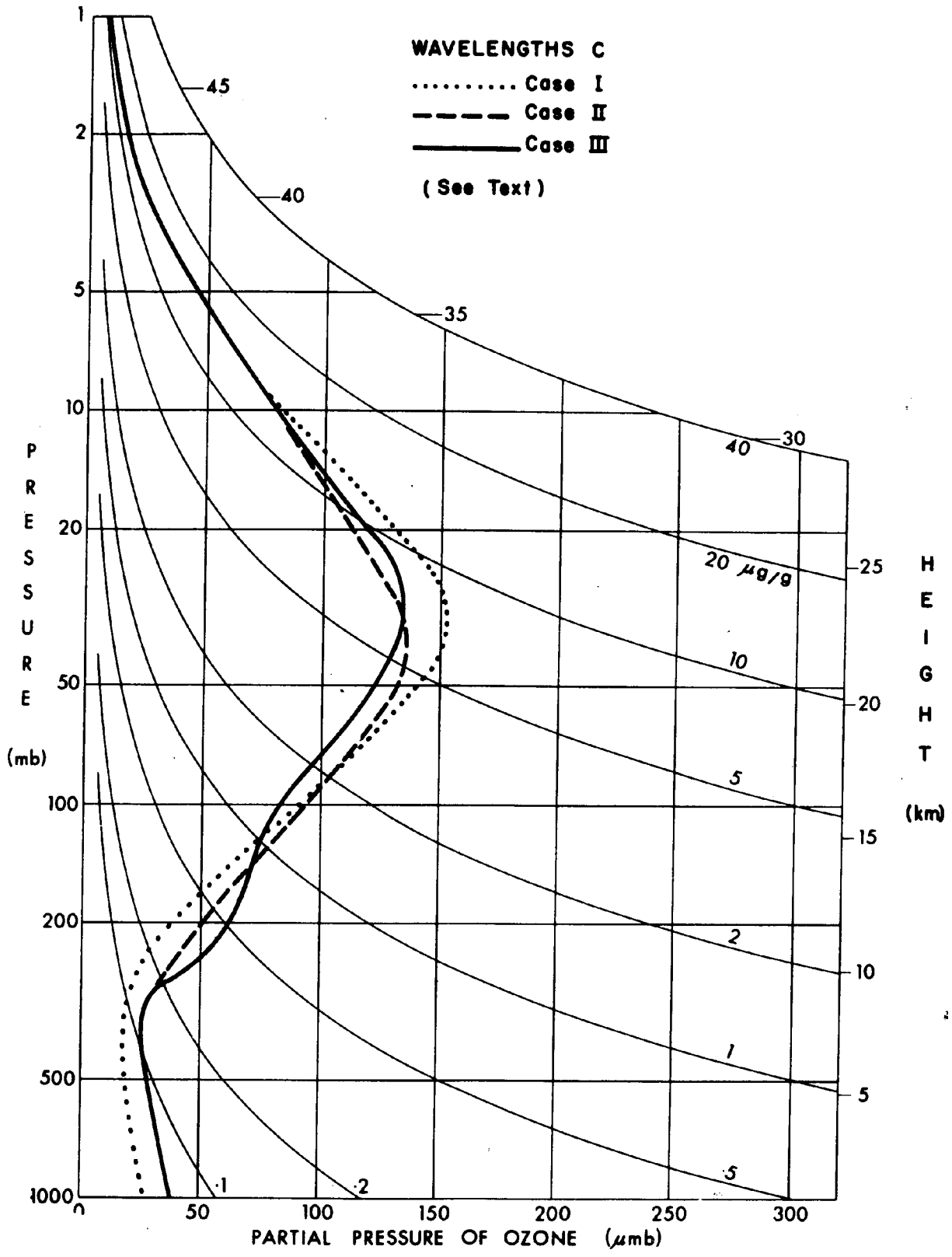


Fig. 31. Average solutions for 98 North American Umkehr curves for the C wavelength pair by different methods.

of the total ozone correction does not appear to change high level ozone. Actually there is a slight increase in high level ozone when the correction is applied, but it is too small to show up on the scale of the ozonogram. We may conclude that the application of the total ozone correction in the solution acts to decrease the discrepancies that would otherwise be observed when we compare solutions for the individual wavelength pairs.

Referring next to Fig. 29, we again find differences in solutions with the double pairs. Comparing the AD and AC curves, we find a somewhat more flattened maximum and more ozone at high and low levels with the latter. Comparing AD and CD curves, we find that the latter curve has a sharper maximum at a slightly lower level, and slightly less ozone at high and low levels. The curves shown all embody the total ozone corrections. If we do not include these corrections, the uncorrected CD curve (not shown), has a somewhat more flattened maximum at a lower level, with less ozone at high levels and more at low levels, than the corrected curve. In the case of the uncorrected AC curve (not shown), the maximum is somewhat more intense and there is a little less ozone at low levels. The effect of not applying the correction is to transfer ozone from levels below about 16 km to the 16-33 km layer. From Fig. 29 and the above description, we may conclude that the agreement is somewhat better perhaps when the corrections are not applied. However, it is quite clear that neither of the methods used is the "correct" one.

In Fig. 30, we again find differences between the various solutions. The AD-AC combination suggests more ozone above about 20 km and less be-

low than either of the other two combinations and also has the sharpest maximum. The A-C-D solutions provide the other extreme with more ozone below 20 km and less above this level. All three curves show maxima at about the same level.

In Fig. 31, comparing the solutions with total ozone uncorrected but with the second derivative corrections applied and using CI as a column weighting vector, we find a tendency toward a maximum in the low stratosphere, characteristic of solutions using CI which also cover a wide range of total ozone. These characteristic differences should be borne in mind in examining the individual solutions of Appendix E.

We may inquire into the information that may be detected by the systems of linear equations with which the above solutions have been carried out and into the goodness of fit of the solutions. The first four eigenvalues of $\Delta^*\Delta$ for each of the systems, together with the mean and rms residuals for the linear solutions, are given in Table 31. Statistics on the solution residuals were not computed by the program used for the combined pairs, which also computes the solutions when the second order corrections are applied. We note that the first eigenvalue dominates the trace of Λ when we choose $W_\Omega = 1.0$. However, the third and fourth eigenvalues are about the same as those given for the C wavelength pairs in Table 7. Thus, although there is strong forcing on total ozone to be the same in the solution as observed, the predictability of the third and fourth eigenvector coefficients is not impaired. We note also that there is somewhat less information in the D measurements than in the

TABLE 31

FIRST FOUR EIGENVALUES OF Δ*Δ WITH MEAN AND RMS RESIDUALS FOR THE VARIOUS WAVELENGTH COMBINATIONS

Wavelengths	Eigenvalues				Mean Residual (N-units)	RMS Residual (N-units)
	1	2	3	4		
A	423.0	42.7	8.7	1.5	0.19	0.64
C	365.3	24.2	4.9	0.8	0.07	0.60
D	360.6	11.1	1.8	0.2	-0.06	0.65
AD	475.0	32.4	10.0	2.1	0.46	0.88
AC	399.3	13.4	4.1	1.2	0.82	1.19
CD	368.5	8.5	3.1	0.7	0.28	0.60
A-C-D	427.2	42.2	14.9	1.8	-	-
AD-AC	366.4	57.3	6.4	0.8	-	-
AC-CD	379.2	22.9	7.9	0.9	-	-

C, and less in C than in A, as evidenced by the magnitude of the fourth eigenvalue.

Insofar as the goodness of fit is concerned, we have about the same rms residual in each case for the single wavelength pairs, but the mean residual is considerably larger for the A pair, largely because of persistent positive residuals for zenith angles of 65°, 70°, and 74°. All of the double pair solutions show fairly large mean residuals and also rms residuals. We may attribute this, at least in part, to the use of incorrect tables for the standard distributions. As one might expect, the fit becomes quite poor in the case of the multiple pairs and double pairs, a visual examination suggesting that rms residuals will be of the order of 2 N-units. This may be attributed in part to the use of the Arosa tables, but is more likely due to absorption coefficient uncertainties and modeling errors.

Since we would expect the effects of multiple scattering and aerosol scattering to be somewhat less for the double wavelength pairs, the above difficulties should be further explored. The use of multiple pairs is particularly attractive for Arctic and Antarctic regions, where the range of solar elevation is small, because the A wavelength measurements are always sampling the atmosphere at a higher level, and the D at a lower level, than those of the C wavelength pair.

6. CONCLUSIONS AND SUGGESTIONS FOR FUTURE WORK

We have shown from a statistical examination of the Umkehr curves themselves, from a mathematical examination of the linearized solution system, and from studies of the curves plus the system, that there are at most four pieces of information about the vertical distribution of ozone to be obtained from Umkehr observations. Moreover, even when we solve for four pieces of information about the vertical distribution, the solution depends on the way in which the problem is set up, viz., on the standard distribution from which the solution is computed, and on the scaling of the equations and the variables. The main information contained in the Umkehr curve concerns the total amount of ozone in the atmosphere and the fact that there is much more ozone between the tropopause and 30 km than there is above and below this layer. Any intercomparisons between day-to-day changes in the vertical distribution and inferences therefrom on atmospheric motions, as computed from Umkehr observations, are meaningful only when the solutions are computed by the same objective technique.

In addition, it appears that little or no additional information is obtained by observations on more than a single wavelength pair, except in the rather special circumstances of Arctic or Antarctic observations where the range of solar zenith angle is somewhat restricted. Even here, the additional information that may be gained is jeopardized by uncer-

tainties in the ozone absorption coefficients that are used with the ozone spectrophotometer.

In setting up an objective solution technique, we should use more than one standard distribution. These standard distributions should be based upon information about the mean vertical distribution obtained from balloon soundings. If the vertical distributions of ozone obtained from Umkehr observations are to be compared with each other, then the same set of standard vertical distributions should be used for data from all stations. However (see below), if vertical distributions are to be compared with those obtained from balloon soundings, different criteria will have to be established.

We may well inquire into the present-day usefulness of Umkehr observations, now that the gross features of the vertical distribution have been known for some time and information on the finer structure must await the more wide-spread use of ozone sondes. First, the Umkehr evaluations do give fairly consistent results in the uppermost layers of the atmosphere and the relative seasonal variation in these layers may be inferred with some degree of confidence. These are also the layers which are most nearly in photochemical equilibrium so that comparisons may be made with photochemical calculations for the purpose of checking the latter.

Second, the absolute calibrations of the various ozone sondes still leave something to be desired. Thus, when Umkehr observations are combined with sonde measurements, it should be possible to have the ozone

sonde measurements specify the fine structure and to use the Umkehr observations to infer an adjustment factor for this fine structure plus the distribution picture at higher levels. Third, since ozone sondes are still expensive and are not used every day, Umkehr observations should provide a useful means of interpolating between soundings so that some continuity may be maintained.

Finally, within the context of an objective evaluation system, the vast number of Umkehr observations now available may be used to determine the main features of the differences in the vertical distributions in different geographical areas. All of these are worthy of further work and investigation at the present time. Inevitably, in the future, as ozone sondes improve in reliability and become less expensive, as balloon performance improves, and as rocket techniques are developed, the Umkehr technique will gradually be replaced completely by these direct methods.

APPENDIX A

TERMINOLOGY AND UNITS USED IN OZONE-METEOROLOGICAL RESEARCH

The instrument commonly used for the measurements discussed in this report is the Dobson (1931) ozone spectrophotometer, manufactured commercially by R & J Beck, London. This is a double monochromator which compares the intensities of two wavelengths in the solar ultraviolet. The shorter and less intense of these wavelengths is strongly absorbed by ozone, the longer and more intense weakly absorbed. The instrument, which employs a photo-multiplier as detector, is very sensitive and observations may be taken on the light scattered downwards from the zenith sky as well as on the direct solar beam. The use of the instrument and its adjustment and calibration have been described by Dobson (1957 a, b).

The measurements of the instrument, when taken on direct sunlight, are adjusted to read directly in units of

$$100 \left\{ \log \frac{I'}{I} - \log \frac{I_o'}{I_o} \right\}$$

where the logarithm is to the base 10, I_o', I_o, are the extra-terrestrial intensities of the long and short wavelengths, respectively, and I', I, are the intensities at the point of measurement. The measured values are commonly referred to as N-values and the units as N-units and this procedure is followed throughout this report. Since $I' > I$ and $I'/I > I_o'/I_o$, because of the greater absorption of the shorter wavelength, the N-values are always positive. Measurements on direct sunlight are used for determination of the total amount of ozone in the atmosphere. When the measurements are taken on zenith skylight, an additional unknown

constant enters into the picture and we may consider the measured quantity, quite simply, to be

$$100 \log \frac{I'}{I} + C$$

where C is the unknown constant, now including the extra-terrestrial log-intensity ratio. These measured values are also referred to as N-values.

Four pairs of wavelengths are used with the spectrophotometer, and these have been designated A (3055/3254 Å), B (3088/3291), C (3114/3324), and D (3176/3398). Most observations of the Umkehr effect have been taken (on zenith skylight) with the C wavelength pair, although a large body of data including the A and D pairs is being built up, particularly in North America. The B wavelength pairs are used rather infrequently. In most measurements of total ozone, the difference between two pairs of wavelengths is used (AD is standard) because the effects of scattering by air molecules, aerosols, and dust are largely eliminated. Unfortunately, the laboratory measurements of the ozone absorption coefficients (Vigroux, 1953), when used with the Dobson spectrophotometer, do not lead to consistent results. These inconsistencies have been summarized recently by Dobson (1963). In the case of total ozone measurements, the problem of correcting the measurements to a uniform or standard scale is a relatively simple one, since one is concerned only with differences (α-α') in the absorption coefficients for the short and long wavelengths. However, in the case of Umkehr evaluations, the two coefficients α,α' enter individually into the calculations and, since the

corrections for the individual coefficients are almost certainly not the same, these corrections will also differ from that for the difference. This problem is still unresolved and is one of the reasons why the additional wavelength pairs are not much used in Umkehr evaluations.

The unit used to express ozone amount is the reduced thickness. This is the thickness of the layer of pure ozone, at standard temperature (0°C) and pressure (1013.250 mb), which would result if all the ozone in a vertical column (encompassing that layer of the atmosphere in which we are interested) were collected into such a layer. The reduced thickness is expressed in atmosphere-centimeters, abbreviated atm-cm, or milli atmosphere-centimeters, abbreviated m atm-cm. If all the ozone in the entire atmosphere were collected into a layer of pure gas, it would occupy a layer between 2 and 6 mm thick. Consequently, total ozone amounts are between 200 and 600 m atm-cm. These units are occasionally referred to in the literature as Dobsons or Dobson units, as 10^{-3} cm STP, or just as 10^{-3} cm.

Ozone concentrations are referred to in terms of ozone density (micrograms per cubic meter or $\mu g/m^3$), ozone partial pressure (micromillibars or μmb), or ozone mixing ratio (by mass: micrograms per gram or $\mu g/g$; by volume: parts per million or per hundred million). The only quantities used in this report are the partial pressure (p in μmb), the reduced thickness for a layer (x in m atm-cm), or total amount (Ω in m atm-cm), and the mixing ratio (r_3).

In order that vertical distributions of ozone might be displayed in

a common format by all workers in the field, the International Ozone Commission asked Godson to prepare a suitable diagram for this purpose. This diagram, known as the ozonogram, was described by Godson (1962) and is gradually being adopted by most workers in published papers and in routine work. The ozonogram, or at least that portion of it used to plot the vertical distribution of ozone, is used exclusively in the present report. It first appears in Fig. 2. The abscissa is ozone partial pressure in μmb. The ordinate is the logarithm of atmospheric pressure in millibars (mb). Along the right-hand side of the diagram is a height scale (km) corresponding to the pressure-height relationship in the standard atmosphere. The curved lines which slope down from upper left to lower right are lines of constant ozone mixing ratio, r_3, in μg/g. The relationship between partial pressure, p, atmospheric pressure, P, and ozone mixing ratio is

$$r_3(\mu g/g) = \frac{1.657\ p(\mu mb)}{P(mb)} \quad .$$

APPENDIX B

FURTHER DETAILS OF DÜTSCH'S EVALUATION METHOD

The material presented here is intended to supplement the description of the method as presented in Section 2.4 of the study. First of all, the standard distributions used are listed in Table B-1. The original layers used were chosen such that the pressure at the bottom of each layer was $\sqrt{2}$ times that at the top, with 500 mb as a reference. In actual practice, these smaller layers have been combined into broader layers with bottom pressure twice that at the top.

The standard distribution Umkehr curves, which include the effects of secondary scattering, are listed in Table B-2. The first order partial derivatives for the various standard distributions and wavelength pairs are listed in Tables B-3 through B-7, inclusive. As noted in the text, the derivatives have units: (N-units)/(unit fractional change in layer ozone content), and also have the effects of secondary scattering incorporated in them. It has to be emphasized that these tables contain data appropriate to stations at a mean surface pressure of 814 mb.

The formulation used by Dütsch to evaluate secondary scattering is summarized in the following equation:

$$S = I_o \beta k \sum_{i=1}^{n} (0.025)\beta \frac{\Delta p_i}{p_o} \sum_{j=1}^{n} \sum_{k=1}^{4} \sum_{\ell=1}^{10} \frac{\Delta p_j}{p_o} G_{i,j,\ell} F_{k,\ell,\theta}$$

$$\times \exp\left\{-\beta \left[1 - \frac{p_i}{p_o} + (b_{i,j,\ell}) \frac{|p_j - p_i|}{p_o} + e_{j,\ell,\theta} \frac{p_i}{p_o}\right]\right\}$$

$$\times \exp\left\{-\alpha \left[\sum_{m=1}^{i} x_m + \sum_{m=i+1}^{j} c_m x_m + \sum_{m=j+1}^{n} a_{j,m,k,\ell,\theta} x_m\right]\right\}$$

where quantities not previously defined are:

S = intensity of secondary scattered light at the instrument

n = number of layers in scattering atmosphere. The scattering atmosphere extends well above the ozone absorbing atmosphere.

i = index referring to zenith layer in which secondary scattering occurs

j = index referring to layer in which primary scattering occurs

k = index referring to azimuth angle. Four azimuth angles: 0°, 90°, 180°, and 270° were used.

ℓ = index referring to angle of incidence of primary scattered beam arriving at secondary scattering layer. Ten angles were chosen such that each was at the midpoint of equal solid angles.

$G_{i,j,\ell}$ = scattering volume determined by geometry

$F_{k,\ell,\Theta}$ = scattering function (cf., $1+\cos^2\Theta$ for primary scattering in the zenith)

$b_{i,j,\ell}$ = Bemporad's function for the path between primary and secondary scattering layers

$e_{j,\ell,\Theta}$ = Bemporad's function for the path from outer space to primary scattering layer

c_m = relative ozone absorption slant path through mth layer between primary and secondary scattering layers.

$a_{j,m,k,\ell,\theta}$ = relative ozone absorption slant path through the mth layer between the primary scattering layer and outer space

x_m = ozone content of mth layer.

The numerical constant 0.025 (= 1/40) takes account of the fact that the contributions from 40 equal solid angles are being summed. This constant could equally well be incorporated in the quantity $G_{i,j,\ell}$. Ground reflection is not considered in this model for secondary scattering.

Also of interest is the elaborate system of overlapping layers which Dütsch has used to suppress the instabilities and obtain a smooth solution. One such system is shown in Table B-8. This system is used whenever all zenith angles are available. Each subset is solved as an even-determined system using the zenith angles shown in the individual columns. The final solution for the fractional change in layer 1, for example, is obtained by averaging the solutions over each set and combining these into a final average. Thus

$$f_1 = \frac{1}{4}\left\{\frac{1}{2}\left[f_1(1.1)+f_1(1.2)\right] + \frac{1}{2}\left[f_1(2.1)+f_1(2.2)\right] + \frac{1}{2}\left[f_1(3.1)+f_1(3.2)\right] + \frac{1}{3}\left[f_1(4.1)+f_1(4.2)+f_1(4.3)\right]\right\} .$$

According to Dütsch, these smoothed solutions generally converge on the second iteration.

TABLE B-1

STANDARD VERTICAL DISTRIBUTIONS OF OZONE USED BY DÜTSCH

Layer	Pressure Range (mb)	Standard Distribution					
		SI		SII		SIII	
		x (m atm-cm)	p (μmb)	x (m atm-cm)	p (μmb)	x (m atm-cm)	p (μmb)
-	814 - 500	9.65	25.1	4.92	12.8	18.60	48.3
1	500 - 250	12.86	23.5	6.38	11.7	28.60	52.3
2	250 - 125	23.06	42.1	9.60	17.5	47.90	87.5
3	125 - 62.5	46.14	84.3	20.65	37.7	68.50	125.1
4	62.5 - 31.2	72.60	132.6	49.20	89.9	78.40	143.2
5	31.2 - 15.6	73.30	133.9	70.40	128.6	73.30	133.9
6	15.6 - 7.8	52.10	95.2	47.90	87.5	52.10	95.2
7	7.8 - 3.9	29.22	53.4	25.30	46.2	29.22	53.4
8	3.9 - 1.95	11.00	20.1	11.23	20.5	11.00	20.1
9	1.95 - .98	3.82	7.0	3.82	7.0	3.82	7.0
-	.98 - .03	3.06	-	3.06	-	3.06	-
Total ozone (m atm-cm)		335.8		251.5		413.5	

TABLE B-2

UMKEHR CURVE POINTS FOR THE VARIOUS STANDARD DISTRIBUTIONS AND WAVELENGTH PAIRS, WITH SECONDARY SCATTERING EFFECTS INCLUDED

Zenith Angle (degrees)	Distributions: Wavelengths:	N-Values for the Various Curve Points				
		I A	I C	I D	II C	III C
90		151.9	124.8	94.9	118.4	131.4
89		161.8	132.8	97.7	125.7	139.1
88		169.5	137.3	96.7	129.4	143.5
86.5		179.4	141.6	91.3	131.6	147.6
85		186.8	141.8	83.8	128.7	148.9
83		192.5	136.8	73.3	119.2	145.9
80		193.3	121.8	59.6	100.7	134.2
77		185.0	105.7	49.0	84.7	119.7
74		170.8	91.7	41.1	72.2	106.1
70		150.4	77.1	33.5	59.5	90.9
65		128.7	64.1	26.8	48.7	76.5
60		111.9	54.6	22.1	41.0	66.3

TABLE B-3

FIRST ORDER PARTIAL DERIVATIVES FOR STANDARD DISTRIBUTION I,
A WAVELENGTH PAIR, WITH SECONDARY SCATTERING EFFECTS INCLUDED

Zenith Angle (degrees)	Layers:	Derivatives*								
		1	2	3	4	5	6	7	8	9
90		405	415	748	916	526	61	1	811	1849
89		403	402	666	768	470	156	313	1080	1497
88		400	388	634	738	534	326	673	1156	1241
86.5		400	369	613	773	565	633	1126	1120	981
85		394	360	621	869	878	1005	1414	1058	808
83		391	360	679	1051	1240	1488	1614	960	652
80		400	425	908	1584	2024	2100	1701	821	505
77		436	559	1270	2290	2750	2470	1688	717	414
74		486	680	1547	2740	3133	2530	1570	630	349
70		534	750	1690	2850	3090	2350	1379	533	288
65		553	746	1600	2641	2779	2044	1171	445	239
60		553	704	1450	2360	2445	1771	1003	380	203

*Derivatives above have to be multiplied by 10^{-2} to get units specified in text.

TABLE B-4

FIRST ORDER PARTIAL DERIVATIVES FOR STANDARD DISTRIBUTION I,
C WAVELENGTH PAIR, WITH SECONDARY SCATTERING EFFECTS INCLUDED

Zenith Angle (degrees)	Derivatives*								
Layers:	1	2	3	4	5	6	7	8	9
90	201	214	361	374	192	128	602	1158	1047
89	201	204	332	352	287	387	1018	1082	822
88	201	197	326	412	435	735	1265	961	670
86.5	200	194	364	578	809	1230	1405	814	524
85	201	218	477	900	1322	1596	1417	701	422
83	212	290	718	1431	1921	1870	1344	587	334
80	246	405	1021	1922	2290	1882	1175	468	255
77	276	462	1106	1963	2190	1682	993	383	206
74	292	467	1070	1833	1972	1469	849	323	173
70	300	446	975	1619	1701	1240	707	268	143
65	297	404	856	1386	1428	1031	586	220	118
60	289	372	758	1205	1230	882	498	187	101

*Derivatives above have to be multiplied by 10^{-2} to get units specified in text.

TABLE B-5

FIRST ORDER PARTIAL DERIVATIVES FOR STANDARD DISTRIBUTION I, D WAVELENGTH PAIR, WITH SECONDARY SCATTERING EFFECTS INCLUDED

Zenith Angle (degrees)	Layers:	Derivatives* 1	2	3	4	5	6	7	8	9
90		89	98	180	241	339	766	1205	800	441
89		90	100	212	402	717	1157	1232	642	345
88		90	111	291	658	1105	1370	1150	525	281
86.5		93	147	451	1034	1475	1438	997	417	219
85		101	194	587	1249	1600	1370	863	340	179
83		114	236	663	1300	1520	1200	712	273	143
80		130	255	647	1170	1284	960	553	209	110
77		138	248	587	1010	1073	789	448	169	90
74		141	232	522	875	915	663	375	141	75
70		139	209	452	737	760	545	308	116	61
65		135	186	387	617	630	449	253	95	51
60		130	168	338	532	540	384	215	81	43

*Derivatives above have to be multiplied by 10^{-2} to get units specified in text.

TABLE B-6

FIRST ORDER PARTIAL DERIVATIVES FOR STANDARD DISTRIBUTION II, C WAVELENGTH PAIR, WITH SECONDARY SCATTERING EFFECTS INCLUDED

Zenith Angle (degrees)	Layers:	Derivatives*								
		1	2	3	4	5	6	7	8	9
90		102	90	160	244	199	167	717	1195	1042
89		101	87	152	257	291	469	1072	1134	819
88		101	86	161	331	517	842	1257	1013	669
86.5		102	95	220	578	1082	1380	1352	852	520
85		106	121	331	960	1761	1776	1351	730	419
83		117	168	483	1391	2370	1990	1250	612	335
80		138	212	576	1573	2490	1864	1054	485	255
77		150	220	563	1465	2240	1604	876	395	206
74		152	213	519	1315	1964	1383	743	333	173
70		152	196	458	1130	1652	1150	614	274	143
65		151	178	395	956	1381	952	506	225	117
60		148	160	346	827	1187	811	430	191	100

*Derivatives above have to be multiplied by 10^{-2} to get units specified in text.

TABLE B-7

FIRST ORDER PARTIAL DERIVATIVES FOR STANDARD DISTRIBUTION III, C WAVELENGTH PAIR, WITH SECONDARY SCATTERING EFFECTS INCLUDED

Zenith Angle (degrees)	Derivatives*								
Layers:	1	2	3	4	5	6	7	8	9
90	420	435	544	408	187	119	595	1160	1048
89	421	419	494	391	274	378	1014	1082	821
88	419	410	480	435	423	715	1256	963	669
86.5	416	395	504	576	770	1193	1391	805	520
85	413	409	597	836	1211	1542	1400	697	421
83	420	490	845	1295	1734	1780	1320	584	335
80	473	682	1254	1818	2110	1810	1151	468	256
77	532	817	1451	1963	2090	1643	982	382	206
74	575	871	1474	1884	1929	1456	846	324	173
70	602	862	1386	1704	1680	1235	705	267	144
65	604	803	1254	1476	1421	1031	582	220	117
60	596	738	1095	1288	1222	880	496	187	100

*Derivatives above have to be multiplied by 10^{-2} to get units specified in text.

TABLE B-8

THE OVERLAPPING-LAYER ZENITH-ANGLE SYSTEM USED BY DÜTSCH TO OBTAIN SMOOTH SOLUTIONS

	Zenith Angles Used								
Set	1		2		3		4		
Sub-Set	1.1	1.2	2.1	2.2	3.1	3.2	4.1	4.2	4.3
Layer									
1	70	60	65	74	77	70	65	60	74
2		77						77	
3	80		80			80	80		
4		83		83					83
5	85		85		85			85	
6		86.5		86.5		86.5	86.5		
7	88		88		88				88
8		89		89		89		89	
9	90		90		90		90		

APPENDIX C

THE COMPUTATION OF THE GENERATING FUNCTION CURVES FOR PRIMARY SCATTERING

The basic equations used in this computation are (6) and (7) of Section 2.1. Pressure and density data were taken from U.S. Standard Atmosphere, 1962, for 1 km intervals from the surface to 80 km. Ozone mixing ratio values were used for the same height interval (Fig. 18). Values of the total atmospheric refraction were inferred from Table 137, Smithsonian Meteorological Tables (List, 1958), for each of the 12 zenith angles used by Dütsch. It was assumed that atmospheric refractive index could be represented by the simple formula:

$$\eta(z) = 1 + C_1\rho(z) \tag{76}$$

where the value $C_1 = 2.357\text{x}10^{-4}$ m^3/kg was taken from work by Komhyr (1956) on refraction of air in the ultraviolet. In a spherical atmosphere, we use the modified index of refraction M(z),

$$M(z) = N(z)(1+z/R) \tag{77}$$

where R is the radius of the earth. Snell's law now takes the form

$$(\sin \zeta_{z,h})M(h) = C_z, \text{ a constant} \tag{78}$$

where $\zeta_{z,h}$ is the angle of incidence, at height h, of the direct solar beam which is incident in the zenith direction at height z. The ray constant C_z was calculated from (78), based on the assumed value of atmospheric refraction for the appropriate zenith angle. It was further assumed that the amount of refraction at level z was given by

$$\delta(z) = \delta(o) \cdot \frac{p(z)}{p(o)} \quad . \tag{79}$$

The angle $\zeta_{z,h}$ could then be computed from Eq. (78). Although the above model for atmospheric refraction is somewhat crude, it will suffice for the present purposes since the sphericity of the atmosphere is the dominating influence.

The integral of Eq. (7) was evaluated for z = 0 (2) 80 km. Above 80 km, only scattering is important and atmospheric attenuation of the incoming solar beam was assumed to be negligibly small. The integration was carried out using 4-point Gaussian quadrature in each 2 km interval above the scattering point z. Quadratic interpolation was used, within each 2 km interval, to obtain values of $\rho(h)$, $r_3(h)$ at the appropriate abscissas. Finally, $\chi(\Theta,z)$ was calculated and the integration of Eq. (6)

$$Q(\Theta) = \int_0^\infty \chi(\Theta,z)dz \tag{80}$$

was performed using the 2-point Newton-Coates quadrature formula in each 2 km interval (i.e., the trapezoidal rule). As $z \to 80$ km, it was found that $\chi(\Theta,z) \to \rho(z)$. Hence, based on the densities at 70 and 80 km, an exponential density decrease with height was assumed to obtain a small correction for the downward scattering from the layer above 80 km.

APPENDIX D

THE PROCEDURE USED WITH OZONE SONDE DATA

The ozone sounding data used here were mostly for the ozone sondes developed at Oxford by Brewer and Milford (1960) and by Griggs (unpublished Ph.D. thesis). Most of the flights were made at Liverpool. In addition, data for 13 flights were kindly provided by Hering (personal communication) for Fort Collins during the winter 1962-63. Data for an additional 29 flights at Arosa during ozone-sonde intercomparisons were provided by Dütsch.

The Arosa data were matched up subjectively with the corresponding results of the evaluation of simultaneous Umkehr observations.

The remaining data were treated as follows. No sounding was used unless it extended above the middle of layer 4, i.e., about 45 mb. An estimate of the ozone content for the layer in which the ascent terminated was made whenever the ascent went above the middle of the layer. The ozone content, or mean concentration, for each of the layers was read off and converted to layer-mean partial pressures, if not already in these units. When a total ozone measurement was not available, as was the case for seven soundings, an estimate was made based on the sum of the partial pressures in layers 1 through 4, inclusive. This estimate was based on the following equation which was derived from those cases where total ozone was available

$$\hat{\Omega} = \overline{\Omega} + b(\Sigma p_i - \overline{\Sigma p_i}) + N_d(0,\sigma) \qquad (81)$$

where

$\hat{\Omega}$ = is the estimate

$\overline{\Omega}$ = average total ozone for the sample = 347 m atm-cm

b = 0.307 (m atm-cm/μmb)

Σp_i = sum of the partial pressures in layers 1 to 4 (μmb)

$\overline{\Sigma p_i}$ = mean sum for the sample (μmb)

$N_d(0,\sigma)$ = normally distributed random variable with zero mean and standard deviation σ generated by random number generator subroutine

σ = standard error of estimate of the regression equation = 31.4 m atm-cm.

The partial pressures in the layers above the top of the balloon sounding were estimated from a regression based on the Arosa solutions given by Dütsch (1963), using only those cases where cloudiness (on his scale) was 0 or 1. The regression equation used was based on the total amount of ozone and is

$$\hat{p}_j = \overline{p}_j + b_j(\Omega-\overline{\Omega}) + N_d(0,\sigma_j) \qquad (82)$$

where

$\hat{p}_j$ = the estimate of layer-mean partial pressure in layer j (μmb)

$\overline{p}_j$ = the average layer-mean partial pressure in layer j for the sample (μmb), tabulated in the second column of Table D-1

b_j = the regression coefficients, tabulated in the third column of Table D-1.

Ω = total ozone for the case being estimate (m atm-cm)

$\overline{\Omega}$ = mean total ozone for the sample = 314 (m atm-cm)

σ_j = standard error of estimate of the regression equation (μmb), listed in the fourth column of Table D-1.

TABLE D-1

STATISTICAL PARAMETERS USED IN ESTIMATING LAYER-MEAN PARTIAL PRESSURES FROM TOTAL OZONE

Layer	Average Layer-Mean Partial Pressure (μmb)	Regression Coefficient (μmb/m atm-cm)	Standard Error of Estimate (μmb)
5	110.1	.0926	9.1
6	76.4	.0678	8.3
7	45.9	.0567	4.3
8	21.7	.0057	1.8
9	10.5	.0031	1.5

The unusual procedure of adding random noise to the regression estimates was used so that the estimates would have the same variability as in the original sample. It was originally intended to derive characteristic patterns of the vertical distribution from these data and to use these patterns in the solution procedure outlined in Section 5.6. However, these solutions proved rather unstable and the method was discarded. In the present context, it is simply an elaborate way of ensuring that the "processed" balloon sounding data will have the same variability in the upper layers as the Umkehr solutions.

Finally, the synthesized vertical distribution was summed to obtain

a total amount of ozone and an adjustment factor for the balloon sounding portion was calculated to ensure agreement between observed total ozone and that in the synthetic distribution.

APPENDIX E

TABULATIONS OF INDIVIDUAL SOLUTIONS

TABLE E-1

INDIVIDUAL SOLUTIONS FOR AROSA DATA SAMPLE, BY TWOMEY'S METHOD, WITH RESPECT TO SI, AND WITH SECOND DERIVATIVE CORRECTIONS APPLIED

Station	Date	Vertical Distribution of Ozone — Mean Ozone Partial Pressures for the Various Layers									Total Ozone		Cloudiness
		1	2	3	4	5	6	7	8	9	Observed	Solution	
ARCSA	2 11 61 P	21	23	52	95	92	66	40	24	11	243	244	0
ARCSA	1 11 61 A	23	25	51	94	92	66	41	24	11	247	247	0
ARCSA	31 10 61 P	20	34	61	99	92	64	41	24	11	254	256	0
ARCSA	9 10 61 A	12	30	68	106	98	69	43	24	11	256	261	0
ARCSA	31 10 61 A	27	41	58	95	89	62	38	23	10	257	257	0
ARCSA	15 10 61 P	19	36	65	102	95	66	41	24	11	259	262	0
ARCSA	11 10 61 A	19	37	65	101	94	66	43	24	11	260	263	0
ARCSA	15 10 61 A	18	36	67	104	97	66	41	24	11	262	265	0
ARCSA	10 2 62 A	20	35	67	110	105	69	37	20	8	266	269	0
ARCSA	13 10 61 P	20	36	65	103	98	69	41	24	11	266	268	0
ARCSA	13 10 61 A	23	36	62	101	96	68	43	24	11	266	266	0
ARCSA	23 9 61 A	32	40	53	93	91	68	43	23	10	267	264	0
ARCSA	23 9 61 A	33	46	55	92	88	66	41	23	10	267	265	0
ARCSA	24 9 61 A	26	38	61	100	95	68	42	24	11	269	268	0
ARCSA	25 9 61 P	33	35	51	94	95	70	42	23	10	269	265	0
ARCSA	25 9 61 A	26	35	59	100	99	71	43	23	10	270	269	0
ARCSA	10 2 62 P	17	43	73	108	99	68	40	23	10	270	274	0
ARCSA	22 9 61 A	30	48	60	95	90	67	42	24	11	273	271	0
ARCSA	21 9 61 A	29	39	59	100	96	69	42	23	10	273	271	1
ARCSA	21 9 61 A	24	34	62	104	100	72	44	24	10	273	272	1
ARCSA	20 9 61 A	23	29	63	107	105	74	43	24	11	274	274	0
ARCSA	22 9 61 P	38	54	56	91	87	64	41	22	10	276	272	0
ARCSA	22 9 61 P	36	44	54	94	93	68	41	23	10	276	271	0
ARCSA	19 9 61 A	25	35	62	105	103	74	45	23	10	278	277	0
ARCSA	16 9 61 P	34	29	54	103	105	74	41	21	9	279	274	0

A refers to AM observations
P refers to PM observations

TABLE E-1 (Continued)

Station	Date	Vertical Distribution of Ozone: Mean Ozone Partial Pressures for the Various Layers									Total Ozone		Cloudiness
		1	2	3	4	5	6	7	8	9	Observed	Solution	
ARCSA	16 9 61 A	24	31	63	106	105	75	46	24	10	279	278	0
ARCSA	19 2 62 P	13	26	73	119	116	82	46	22	9	281	286	0
ARCSA	26 7 62 A	29	28	55	104	108	83	48	22	9	283	281	0
ARCSA	1 9 61 A	30	39	60	102	103	77	46	22	10	285	283	1
ARCSA	27 8 61 P	32	31	57	105	108	79	46	22	10	288	284	0
ARCSA	29 8 61 P	30	34	61	106	107	79	45	22	10	289	286	0
ARCSA	4 9 61 A	33	52	67	103	97	69	41	23	10	290	287	3
ARCSA	25 7 62 P	35	43	61	104	105	75	41	21	9	292	288	3
ARCSA	11 9 61 A	19	33	73	116	113	79	48	25	11	293	294	0
ARCSA	20 7 62 P	29	41	64	107	107	81	49	22	9	294	292	0
ARCSA	20 2 62 A	13	27	79	125	121	83	47	24	11	295	298	0
ARCSA	10 9 61 A	20	42	76	114	109	78	49	25	11	296	298	0
ARCSA	30 8 61 P	32	44	64	105	104	78	48	23	9	296	293	0
ARCSA	15 9 61 P	32	35	66	112	111	74	38	23	11	296	291	2
ARCSA	21 7 62 A	43	38	51	102	107	81	43	18	7	297	289	1
ARCSA	20 7 62 A	22	29	69	118	119	86	49	21	8	297	297	2
ARCSA	13 9 61 P	23	47	76	110	103	75	48	26	12	298	298	2
ARCSA	20 2 62 P	20	36	75	118	116	81	48	24	10	300	301	1
ARCSA	14 7 62 A	32	43	68	111	110	78	46	21	9	302	299	2
ARCSA	26 8 61 A	20	38	77	119	116	83	49	23	10	303	304	0
ARCSA	14 7 61 A	6	37	91	131	122	85	50	24	11	304	311	0
ARCSA	24 6 62 P	33	49	69	109	107	76	47	23	10	306	302	3
ARCSA	9 7 62 A	40	57	65	105	105	80	45	19	7	309	304	2
ARCSA	5 5 61 P	26	58	81	114	106	77	51	23	9	312	312	2
ARCSA	5 5 61 A	17	50	89	124	116	80	49	24	10	313	316	2

A refers to AM observations
P refers to PM observations

TABLE E-1 (Continued)

Station	Date	Vertical Distribution of Ozone: Mean Ozone Partial Pressures for the Various Layers									Total Ozone		Cloudiness
		1	2	3	4	5	6	7	8	9	Observed	Solution	
ARCSA	26 7 61 P	35	57	76	115	112	78	38	19	8	314	311	3
ARCSA	31 5 62 A	19	51	89	128	121	84	49	24	11	325	326	3
ARCSA	20 10 61 A	26	91	101	118	97	64	41	25	12	327	329	1
ARCSA	20 10 61 P	31	97	101	116	93	58	38	24	11	327	327	2
ARCSA	24 4 62 P	23	68	96	128	117	77	43	21	9	329	331	1
ARCSA	23 7 61 P	32	54	80	122	120	84	46	22	9	331	328	1
ARCSA	21 2 62 A	20	47	90	131	126	86	51	25	11	331	332	0
ARCSA	4 4 61 A	13	65	109	139	123	77	42	24	11	334	339	2
ARCSA	24 7 61 A	22	61	94	129	122	84	49	24	10	337	338	0
ARCSA	28 6 62 A	31	65	87	122	117	83	49	22	8	337	335	0
ARCSA	22 4 62 P	32	61	86	125	120	80	44	23	10	338	335	2
ARCSA	19 10 61 A	31	101	104	118	98	65	42	25	12	343	342	0
ARCSA	30 5 61 A	25	56	90	130	127	91	51	23	10	344	343	0
ARCSA	9 6 62 A	25	67	98	133	124	84	48	21	8	346	346	0
ARCSA	17 5 62 A	29	66	94	131	126	90	53	22	8	355	353	2
ARCSA	2 5 61 A	33	84	101	127	115	76	44	24	11	356	353	3
ARCSA	6 6 62 A	55	71	70	112	115	86	52	21	8	361	348	2
ARCSA	26 4 62 P	40	77	87	120	118	88	53	24	10	365	358	3
ARCSA	28 2 62 P	19	61	108	141	130	85	54	32	15	367	365	3
ARCSA	28 3 61 P	41	74	93	131	125	82	44	22	9	367	360	3
ARCSA	7 3 62 P	30	91	110	134	120	79	46	24	11	370	368	0
ARCSA	25 5 61 A	23	85	115	141	128	88	53	24	10	377	378	0
ARCSA	20 3 62 A	16	93	129	148	125	79	49	27	12	379	382	0
ARCSA	27 2 62 P	29	112	124	138	116	75	46	25	11	386	386	0
ARCSA	12 4 62 A	31	100	116	135	118	80	52	27	12	386	383	1

A refers to AM observations
P refers to PM observations

TABLE E-1 (Concluded)

Station	Date	Vertical Distribution of Ozone: Mean Ozone Partial Pressures for the Various Layers									Total Ozone		Cloudiness
		1	2	3	4	5	6	7	8	9	Observed	Solution	
ARCSA	12 4 62 A	38	84	102	133	125	86	53	26	11	386	379	1
ARCSA	21 3 62 A	23	101	128	146	126	80	50	28	13	394	394	0
ARCSA	12 4 62 P	34	99	118	137	119	77	50	29	14	394	368	3
ARCSA	19 3 62 A	17	109	143	153	126	76	46	29	14	398	401	0
ARCSA	19 3 62 P	31	113	128	143	122	78	45	26	13	400	398	0
ARCSA	24 3 62 A	20	89	125	148	133	91	62	30	13	401	401	0
ARCSA	24 3 62 A	13	84	133	156	139	90	57	32	15	401	403	0
ARCSA	21 3 62 P	22	98	132	152	130	83	52	29	13	403	403	1
ARCSA	21 3 62 P	17	92	133	154	133	85	57	31	15	403	404	1
ARCSA	2 4 62 P	39	122	122	135	116	77	49	25	11	404	400	1
ARCSA	25 3 62 A	28	101	125	145	129	87	55	27	12	405	403	3
ARCSA	20 3 61 P	20	125	148	156	127	78	44	24	11	408	413	0
ARCSA	25 2 62 A	9	125	159	161	128	79	50	28	13	410	418	0
ARCSA	1 4 62 P	25	127	142	148	122	79	51	27	12	413	415	2
ARCSA	11 4 62 A	42	120	123	137	119	83	52	26	11	417	410	2
ARCSA	11 4 62 P	48	101	109	137	128	86	51	27	12	418	406	4
ARCSA	18 3 62 P	22	123	148	155	127	78	50	30	14	422	423	3
ARCSA	24 2 62 A	21	155	162	154	117	71	48	27	12	427	432	0
ARCSA	24 2 62 P	27	152	155	151	117	73	47	26	12	428	430	0
ARCSA	22 3 61 P	27	142	155	157	127	79	47	25	11	434	436	1
ARCSA	17 3 62 A	20	135	160	161	128	77	51	32	15	438	440	3
ARCSA	18 3 62 A	28	134	150	153	125	78	53	33	16	441	438	3
ARCSA	26 3 62 A	26	148	160	159	128	82	54	30	14	452	453	3
ARCSA	16 4 62 A	49	164	142	138	111	76	53	26	11	453	446	1
ARCSA	26 3 62 P	27	132	156	163	134	83	55	32	15	455	452	3

A refers to AM observations
P refers to PM observations

TABLE E-2

INDIVIDUAL SOLUTIONS FOR 42 LOW-OZONE AROSA UMKEHRS, BY TWOMEY'S METHOD, WITH RESPECT TO SII, AND WITH SECOND DERIVATIVE CORRECTIONS APPLIED

Station	Date	Vertical Distribution of Ozone: Mean Ozone Partial Pressures for the Various Layers									Total Ozone		Cloudiness
		1	2	3	4	5	6	7	8	9	Observed	Solution	
ARCSA	2 11 61 P	20	31	42	78	109	69	39	25	11	243	243	0
ARCSA	1 11 61 A	23	32	41	77	109	69	40	25	11	247	247	0
ARCSA	31 10 61 P	19	40	54	81	107	67	40	25	11	254	254	0
ARCSA	9 10 61 A	10	37	59	87	113	71	41	25	11	256	256	0
ARCSA	31 10 61 A	28	46	52	77	104	64	36	24	11	257	257	0
ARCSA	15 10 61 P	18	42	58	84	110	68	39	25	11	259	259	0
ARCSA	11 10 61 A	19	42	56	82	109	69	41	25	11	260	260	0
ARCSA	15 10 61 A	17	42	61	86	111	68	39	25	11	262	262	0
ARCSA	10 2 62 A	19	43	65	93	117	68	34	21	9	266	266	0
ARCSA	13 10 61 P	20	42	57	85	113	71	40	25	11	266	266	0
ARCSA	13 10 61 A	23	43	54	83	110	71	42	25	11	266	266	0
ARCSA	23 9 61 A	33	45	46	76	108	71	41	25	11	267	267	0
ARCSA	23 9 61 A	35	50	48	74	105	69	39	24	11	267	266	0
ARCSA	24 9 61 A	27	44	53	81	110	71	41	25	11	269	269	0
ARCSA	25 9 61 P	35	42	43	77	111	74	42	24	10	269	268	0
ARCSA	25 9 61 A	27	42	51	82	114	74	41	24	11	270	270	0
ARCSA	10 2 62 P	16	48	69	90	112	68	38	24	10	270	270	0
ARCSA	22 9 61 A	32	52	54	77	106	69	41	25	11	273	273	0
ARCSA	21 9 61 A	31	46	53	81	111	72	41	24	10	273	273	1
ARCSA	21 9 61 A	25	42	55	86	114	74	43	25	10	273	273	1
ARCSA	20 9 61 A	22	38	56	89	119	76	42	25	11	274	274	0
ARCSA	22 9 61 P	41	58	51	73	102	67	39	24	10	276	275	0
ARCSA	22 9 61 P	39	50	49	77	108	70	39	24	11	276	275	0
ARCSA	19 9 61 A	26	43	56	87	117	76	43	24	10	278	278	0
ARCSA	16 9 61 P	36	41	48	85	118	76	40	23	9	279	278	0

A refers to AM observations
P refers to PM observations

TABLE E-2 (Concluded)

Station	Date	Vertical Distribution of Ozone — Mean Ozone Partial Pressures for the Various Layers									Total Ozone		Cloudiness
		1	2	3	4	5	6	7	8	9	Observed	Solution	
ARCSA	16 9 61 A	24	40	57	89	119	76	43	25	11	279	279	0
ARCSA	19 2 62 P	10	37	69	101	128	81	43	23	9	281	281	0
ARCSA	26 7 62 A	29	38	49	87	124	84	46	23	9	283	283	0
ARCSA	1 9 61 A	32	45	54	85	118	79	44	24	10	285	285	1
ARCSA	27 8 61 P	33	42	53	88	122	80	44	24	10	288	287	0
ARCSA	29 8 61 P	31	44	57	89	121	79	43	24	10	289	289	0
ARCSA	4 9 61 A	36	58	63	84	110	70	40	24	11	290	289	3
ARCSA	25 7 62 P	38	51	57	87	118	75	39	23	10	292	291	3
ARCSA	11 9 61 A	18	43	70	98	124	79	46	26	11	293	293	0
ARCSA	20 7 62 P	30	49	60	89	120	82	47	23	9	294	294	0
ARCSA	20 2 62 A	11	39	77	107	132	81	44	25	11	295	295	0
ARCSA	10 9 61 A	19	49	73	96	121	79	46	25	11	296	296	0
ARCSA	30 8 61 P	34	51	60	87	118	80	45	24	10	296	296	0
ARCSA	15 9 61 P	34	47	65	95	122	72	37	25	11	296	295	2
ARCSA	21 7 62 A	48	49	47	85	122	82	41	20	8	297	296	1
ARCSA	20 7 62 A	21	40	66	101	131	86	46	22	8	297	297	2
ARCSA	13 9 61 P	25	54	72	91	116	76	46	27	12	298	298	2

A refers to AM observations
P refers to PM observations

TABLE E-3

INDIVIDUAL SOLUTIONS FOR 29 HIGH-OZONE AROSA UMKEHRS, BY TWOMEY'S METHOD, WITH RESPECT TO SIII, AND WITH SECOND DERIVATIVE CORRECTIONS APPLIED

Station	Date	Vertical Distribution of Ozone: Mean Ozone Partial Pressures for the Various Layers									Total Ozone		Cloudiness
		1	2	3	4	5	6	7	8	9	Observed	Solution	
ARCSA	25 5 61 A	34	66	127	140	126	90	54	24	10	377	383	0
ARCSA	20 3 62 A	29	67	141	150	125	81	49	27	12	379	387	0
ARCSA	27 2 62 P	40	91	138	138	115	77	46	25	11	386	391	0
ARCSA	12 4 62 A	43	81	128	135	116	81	53	27	12	386	389	1
ARCSA	12 4 62 A	49	71	114	131	122	88	54	26	11	386	385	1
ARCSA	21 3 62 A	35	77	140	147	125	82	51	28	13	394	399	0
ARCSA	12 4 62 P	46	80	129	138	117	78	51	29	14	394	393	3
ARCSA	19 3 62 A	29	80	154	155	127	79	47	29	14	398	406	0
ARCSA	19 3 62 P	42	92	141	142	121	80	46	26	13	400	404	0
ARCSA	24 3 62 A	32	69	136	147	131	93	63	30	13	401	406	0
ARCSA	24 3 62 A	25	60	145	156	138	93	58	31	15	401	408	0
ARCSA	21 3 62 P	35	75	143	152	130	85	53	29	13	403	407	1
ARCSA	21 3 62 P	30	68	143	153	133	88	58	31	14	403	408	1
ARCSA	2 4 62 P	49	104	135	135	114	79	50	25	11	404	405	1
ARCSA	25 3 62 A	40	81	137	145	127	89	56	27	12	405	408	3
ARCSA	20 3 61 P	32	96	161	157	129	81	44	24	11	408	417	0
ARCSA	25 2 62 A	22	92	170	163	130	82	50	28	13	410	422	0
ARCSA	1 4 62 P	36	101	155	149	122	81	52	27	12	413	419	2
ARCSA	11 4 62 A	53	102	134	137	118	85	53	26	11	417	416	2
ARCSA	11 4 62 P	60	87	120	135	125	88	53	27	12	418	412	4
ARCSA	18 3 62 P	35	95	158	157	129	81	51	30	14	422	427	3
ARCSA	24 2 62 A	33	123	175	156	119	75	49	27	12	427	436	0
ARCSA	24 2 62 P	39	122	167	154	119	76	47	26	12	428	434	0
ARCSA	22 3 61 P	40	112	165	160	130	83	48	25	11	434	440	1
ARCSA	17 3 62 A	34	104	170	162	130	81	51	32	15	438	443	3

A refers to AM observations
P refers to PM observations

TABLE E-3 (Concluded)

Station	Date	Vertical Distribution of Ozone: Mean Ozone Partial Pressures for the Various Layers									Total Ozone		Cloudiness
		1	2	3	4	5	6	7	8	9	Observed	Solution	
ARCSA	18 3 62 A	41	108	161	154	125	81	54	33	16	441	442	3
ARCSA	26 3 62 A	39	119	171	160	130	85	55	29	13	452	456	3
ARCSA	16 4 62 A	61	144	153	138	111	79	54	26	11	453	450	1
ARCSA	26 3 62 P	42	103	163	164	136	86	55	32	15	455	455	3

A refers to AM observations
P refers to PM observations

TABLE E-4

INDIVIDUAL SOLUTIONS FOR AROSA DATA SAMPLE, BY TEVE METHOD, WITH RESPECT TO SI, AND WITH SECOND DERIVATIVE CORRECTIONS APPLIED

Station	Date	Vertical Distribution of Ozone: Mean Ozone Partial Pressures for the Various Layers									Total Ozone		Cloudiness
		1	2	3	4	5	6	7	8	9	Observed	Solution	
ARCSA	2 11 61 P	21	23	52	95	92	66	40	24	11	243	244	0
ARCSA	1 11 61 A	23	25	51	94	92	66	41	24	11	247	247	0
ARCSA	31 10 61 P	20	34	61	99	92	64	41	24	11	254	256	0
ARCSA	9 10 61 A	12	30	68	106	98	69	43	24	11	256	261	0
ARCSA	31 10 61 A	27	41	58	95	89	62	38	23	10	257	257	0
ARCSA	15 10 61 P	19	36	65	102	95	66	41	24	11	259	262	0
ARCSA	11 10 61 A	19	37	65	101	94	66	43	24	11	260	263	0
ARCSA	15 10 61 A	18	36	67	104	97	66	41	24	11	262	265	0
ARCSA	10 2 62 A	20	35	67	110	105	69	37	20	8	266	269	0
ARCSA	13 10 61 P	20	36	65	103	98	69	41	24	11	266	268	0
ARCSA	13 10 61 A	23	36	62	101	96	68	43	24	11	266	266	0
ARCSA	23 9 61 A	32	40	53	93	91	68	43	23	10	267	264	0
ARCSA	23 9 61 A	33	46	55	92	88	66	41	23	10	267	265	0
ARCSA	24 9 61 A	26	38	61	100	95	68	42	24	11	269	268	0
ARCSA	25 9 61 P	33	35	51	94	95	70	42	23	10	269	265	0
ARCSA	25 9 61 A	26	35	59	100	99	71	43	23	10	270	269	0
ARCSA	10 2 62 P	17	43	73	108	99	68	40	23	10	270	274	0
ARCSA	22 9 61 A	30	48	60	95	90	67	42	24	11	273	271	0
ARCSA	21 9 61 A	29	39	59	100	96	69	42	23	10	273	271	1
ARCSA	21 9 61 A	24	34	62	104	100	72	44	24	10	273	272	1
ARCSA	20 9 61 A	23	29	63	107	105	74	43	24	11	274	274	0
ARCSA	22 9 61 P	38	54	56	91	87	64	41	22	10	276	272	0
ARCSA	22 9 61 P	36	44	54	94	93	68	41	23	10	276	271	0
ARCSA	19 9 61 A	25	35	62	105	103	74	45	23	10	278	277	0
ARCSA	16 9 61 P	34	29	54	103	105	74	41	21	9	279	274	0

A refers to AM observations
P refers to PM observations

TABLE E-4 (Continued)

Station	Date	Vertical Distribution of Ozone: Mean Ozone Partial Pressures for the Various Layers									Total Ozone		Cloudiness
		1	2	3	4	5	6	7	8	9	Observed	Solution	
ARCSA	16 9 61 A	20	36	68	108	103	72	44	24	11	279	278	0
ARCSA	19 2 62 P	9	23	77	123	118	79	44	23	10	281	282	0
ARCSA	26 7 62 A	29	33	57	103	106	80	49	22	9	283	282	0
ARCSA	1 9 61 A	30	43	62	102	101	74	46	23	10	285	285	1
ARCSA	27 8 61 P	29	40	63	104	104	76	46	23	10	288	285	0
ARCSA	29 8 61 P	27	42	67	107	104	75	45	23	10	289	287	0
ARCSA	4 9 61 A	33	59	69	100	94	67	42	24	11	290	289	3
ARCSA	25 7 62 P	31	53	67	104	99	71	42	22	9	292	289	3
ARCSA	11 9 61 A	16	35	77	118	112	77	46	25	11	293	293	0
ARCSA	20 7 62 P	32	43	62	105	107	80	49	22	9	294	295	0
ARCSA	20 2 62 A	6	26	85	129	121	79	45	24	11	295	294	0
ARCSA	10 9 61 A	20	41	77	116	111	76	46	25	11	296	298	0
ARCSA	30 8 61 P	34	49	64	103	103	77	48	23	10	296	296	0
ARCSA	15 9 61 P	22	51	78	111	102	68	41	24	11	296	290	2
ARCSA	21 7 62 A	43	52	54	96	101	79	47	19	7	297	292	1
ARCSA	20 7 62 A	21	30	70	118	119	85	49	21	8	297	296	2
ARCSA	13 9 61 P	24	49	77	111	104	73	46	27	12	298	300	2
ARCSA	20 2 62 P	17	38	79	120	115	78	47	25	11	300	300	1
ARCSA	14 7 62 A	31	50	70	109	107	77	46	22	9	302	300	2
ARCSA	26 8 61 A	18	38	79	121	117	81	47	24	10	303	304	0
ARCSA	14 7 61 A	3	28	94	137	128	82	46	25	11	304	307	0
ARCSA	24 6 62 P	33	56	71	107	104	75	47	23	10	306	305	3
ARCSA	9 7 62 A	44	64	64	102	103	78	46	19	7	309	308	2
ARCSA	5 5 61 P	31	57	77	113	109	78	48	24	10	312	315	2
ARCSA	5 5 61 A	16	47	90	127	119	78	45	24	11	313	315	2

A refers to AM observations
P refers to PM observations

TABLE E-4 (Continued)

Station	Date	Vertical Distribution of Ozone: Mean Ozone Partial Pressures for the Various Layers									Total Ozone		Cloudiness
		1	2	3	4	5	6	7	8	9	Observed	Solution	
ARCSA	26 7 61 P	30	65	83	116	108	73	40	20	8	314	311	3
ARCSA	31 5 62 A	16	5C	94	131	122	81	47	25	11	325	326	3
ARCSA	20 10 61 A	29	8S	101	119	100	62	38	26	13	327	331	1
ARCSA	20 1C 61 P	32	9S	102	116	94	57	34	25	12	327	329	2
ARCSA	24 4 62 P	20	67	100	132	118	75	40	22	9	329	330	1
ARCSA	23 7 61 P	28	61	86	122	116	81	47	23	9	331	329	1
ARCSA	21 2 62 A	15	48	95	134	126	84	49	26	11	331	331	0
ARCSA	4 4 61 A	4	62	118	146	125	72	38	25	12	334	335	2
ARCSA	24 7 61 A	21	5S	97	132	123	82	48	24	10	337	338	0
ARCSA	28 6 62 A	33	67	86	122	117	83	48	22	9	337	336	0
ARCSA	22 4 62 P	27	7C	95	126	115	76	44	23	1C	338	335	2
ARCSA	19 1C 61 A	35	101	105	12C	100	63	39	27	13	343	347	0
ARCSA	30 5 61 A	24	57	94	132	127	87	51	24	10	344	345	0
ARCSA	9 6 62 A	24	67	99	134	125	83	46	22	9	346	347	0
ARCSA	17 5 62 A	32	67	92	131	127	90	53	22	8	355	356	2
ARCSA	2 5 61 A	31	9C	106	129	113	73	43	25	11	356	356	3
ARCSA	6 6 62 A	61	8S	7C	104	108	88	56	21	7	361	357	2
ARCSA	26 4 62 P	45	84	88	119	116	86	55	25	10	365	365	3
ARCSA	28 2 62 P	10	66	12C	147	128	80	51	33	16	367	366	3
ARCSA	28 3 61 P	35	8S	103	129	118	79	46	23	9	367	362	3
ARCSA	7 3 62 P	29	94	114	136	120	76	44	25	11	37C	371	0
ARCSA	25 5 61 A	25	81	115	145	132	87	50	25	11	377	380	0
ARCSA	2C 3 62 A	13	88	133	154	131	77	43	28	14	379	382	0
ARCSA	27 2 62 P	3C	111	127	142	119	73	42	26	12	386	390	0
ARCSA	12 4 62 A	34	101	118	137	121	79	48	28	13	386	388	1

A refers to AM observations
P refers to PM observations

TABLE E-4 (Concluded)

Station	Date	Vertical Distribution of Ozone: Mean Ozone Partial Pressures for the Various Layers									Total Ozone		Cloudiness
		1	2	3	4	5	6	7	8	9	Observed	Solution	
ARCSA	12 4 62 A	37	93	109	133	122	84	53	27	12	386	385	1
ARCSA	21 3 62 A	20	100	135	152	128	77	46	29	14	394	396	0
ARCSA	12 4 62 P	31	108	126	139	118	74	47	30	15	394	394	3
ARCSA	19 3 62 A	11	104	150	161	130	72	41	30	16	398	401	0
ARCSA	19 3 62 P	28	115	136	148	122	73	42	28	13	400	402	0
ARCSA	24 3 62 A	24	83	124	152	139	92	57	30	14	401	405	0
ARCSA	24 3 62 A	7	78	141	166	144	87	53	33	16	401	404	0
ARCSA	21 3 62 P	18	98	139	157	133	80	48	30	15	403	405	1
ARCSA	21 3 62 P	14	89	139	160	137	84	52	32	16	403	406	1
ARCSA	2 4 62 P	43	124	124	137	118	76	46	26	12	404	407	1
ARCSA	25 3 62 A	29	100	127	149	132	85	52	28	13	405	408	3
ARCSA	20 3 61 P	19	117	151	163	133	75	39	25	12	408	413	0
ARCSA	25 2 62 A	9	108	159	171	139	76	42	30	15	410	418	0
ARCSA	1 4 62 P	28	119	143	154	129	77	45	28	14	413	419	2
ARCSA	11 4 62 A	46	125	123	138	121	81	51	27	12	417	419	2
ARCSA	11 4 62 P	45	118	120	136	121	83	53	28	13	418	414	4
ARCSA	18 3 62 P	19	119	155	163	132	75	45	31	16	422	426	3
ARCSA	24 2 62 A	28	140	159	161	128	71	40	28	14	427	437	0
ARCSA	24 2 62 P	33	142	154	157	126	72	41	27	13	428	435	0
ARCSA	22 3 61 P	29	134	155	163	135	78	42	26	12	434	439	1
ARCSA	17 3 62 A	17	129	167	170	135	74	45	33	17	438	443	3
ARCSA	18 3 62 A	27	133	158	161	129	75	48	35	18	441	445	3
ARCSA	26 3 62 A	30	139	161	166	136	80	48	31	15	452	459	3
ARCSA	16 4 62 A	62	165	138	138	116	77	50	27	12	453	459	1
ARCSA	26 3 62 P	23	131	165	170	139	80	50	34	17	455	457	3

A refers to AM observations
P refers to PM observations

TABLE E-5

INDIVIDUAL SOLUTIONS FOR 42 LOW-OZONE AROSA UMKEHRS, BY TEVE METHOD, WITH RESPECT TO SII, AND WITH SECOND DERIVATIVE CORRECTIONS APPLIED

Station	Date	Vertical Distribution of Ozone: Mean Ozone Partial Pressures for the Various Layers									Total Ozone		Cloudiness
		1	2	3	4	5	6	7	8	9	Observed	Solution	
ARCSA	2 11 61 P	16	36	50	79	106	65	38	25	12	243	243	0
ARCSA	1 11 61 A	18	38	50	78	105	65	39	26	12	247	247	0
ARCSA	31 10 61 P	17	42	58	83	107	64	37	25	12	254	254	0
ARCSA	9 10 61 A	7	35	64	91	114	67	38	26	12	256	256	0
ARCSA	31 10 61 A	25	51	59	78	101	60	34	25	11	257	257	0
ARCSA	15 10 61 P	15	43	65	87	109	63	36	26	12	259	259	0
ARCSA	11 10 61 A	17	42	60	85	110	66	38	26	12	260	260	0
ARCSA	15 10 61 A	14	44	68	89	110	63	36	26	12	262	262	0
ARCSA	10 2 62 A	15	47	72	95	115	65	32	21	9	266	266	0
ARCSA	13 10 61 P	17	44	65	88	111	66	38	26	12	266	266	0
ARCSA	13 10 61 A	21	45	60	84	109	67	39	26	12	266	266	0
ARCSA	23 9 61 A	32	49	51	76	105	68	41	25	11	267	267	0
ARCSA	23 9 61 A	33	53	54	75	102	65	38	25	11	267	267	0
ARCSA	24 9 61 A	25	48	59	83	108	67	40	25	11	269	269	0
ARCSA	25 9 61 P	33	49	49	76	106	70	42	25	10	269	269	0
ARCSA	25 9 61 A	24	46	58	84	111	70	41	25	11	270	270	0
ARCSA	10 2 62 P	15	47	73	93	113	64	35	25	11	270	270	0
ARCSA	22 9 61 A	31	54	59	79	104	65	39	25	11	273	273	0
ARCSA	21 9 61 A	29	50	58	82	109	69	40	25	11	273	273	1
ARCSA	21 9 61 A	23	45	60	87	113	71	41	25	11	273	273	1
ARCSA	20 9 61 A	18	43	65	91	116	71	41	25	11	274	274	0
ARCSA	22 9 61 P	41	61	55	73	100	64	38	24	11	276	276	0
ARCSA	22 9 61 P	36	57	57	77	103	66	39	25	11	276	276	0
ARCSA	19 9 61 A	24	45	61	88	116	74	42	25	10	278	278	0
ARCSA	16 9 61 P	32	50	56	83	112	73	41	23	9	279	279	0

A refers to AM observations
P refers to PM observations

TABLE E-5 (Concluded)

Station	Date	Vertical Distribution of Ozone: Mean Ozone Partial Pressures for the Various Layers									Total Ozone		Cloudiness
		1	2	3	4	5	6	7	8	9	Observed	Solution	
ARCSA	16 9 61 A	21	44	64	91	117	73	42	25	11	279	279	0
ARCSA	19 2 62 P	7	35	74	106	129	77	40	24	10	281	281	0
ARCSA	26 7 62 A	29	41	51	87	121	82	47	23	9	283	283	0
ARCSA	1 9 61 A	30	48	58	86	116	76	44	24	10	285	285	1
ARCSA	27 8 61 P	30	48	59	88	117	77	44	24	10	288	288	0
ARCSA	29 8 61 P	28	49	64	90	118	76	43	24	10	289	289	0
ARCSA	4 9 61 A	34	61	69	85	108	66	39	25	11	290	290	3
ARCSA	25 7 62 P	35	58	66	87	113	71	40	23	10	292	292	3
ARCSA	11 9 61 A	15	44	76	101	124	76	43	26	12	293	293	0
ARCSA	20 7 62 P	32	48	59	90	121	81	46	23	9	294	294	0
ARCSA	20 2 62 A	6	40	85	111	131	77	41	25	11	295	295	0
ARCSA	10 9 61 A	18	47	76	100	123	75	43	26	12	296	296	0
ARCSA	30 8 61 P	34	53	62	88	117	78	45	24	10	296	296	0
ARCSA	15 9 61 P	26	59	81	95	113	66	37	25	12	296	296	2
ARCSA	21 7 62 A	46	57	51	81	115	81	44	20	7	297	297	1
ARCSA	20 7 62 A	21	40	67	102	132	85	46	22	8	297	297	2
ARCSA	13 9 61 P	23	52	76	95	117	72	43	28	13	298	298	2

A refers to AM observations
P refers to PM observations

INDIVIDUAL SOLUTIONS FOR 29 HIGH-OZONE AROSA UMKEHRS, BY TEVE METHOD, WITH RESPECT TO SIII, AND WITH SECOND DERIVATIVE CORRECTIONS APPLIED

Station	Date	Vertical Distribution of Ozone — Mean Ozone Partial Pressures for the Various Layers									Total Ozone		Cloudiness
		1	2	3	4	5	6	7	8	9	Observed	Solution	
ARCSA	25 5 61 A	34	55	126	147	132	88	50	25	11	377	381	0
ARCSA	20 3 62 A	23	55	145	158	132	79	43	28	14	379	382	0
ARCSA	27 2 62 P	38	83	140	144	119	74	43	26	12	386	389	C
ARCSA	12 4 62 A	42	77	130	139	120	80	49	27	13	386	388	1
ARCSA	12 4 62 A	46	72	119	134	121	86	53	27	12	386	386	1
ARCSA	21 3 62 A	30	68	146	155	129	79	46	29	14	394	396	0
ARCSA	12 4 62 P	40	81	137	141	118	76	48	30	15	394	393	3
ARCSA	19 3 62 A	21	67	161	166	133	75	41	30	16	398	401	0
ARCSA	19 3 62 P	36	85	149	151	123	75	43	28	13	400	401	0
ARCSA	24 3 62 A	33	57	134	154	139	94	57	30	14	401	406	0
ARCSA	24 3 62 A	18	44	151	169	146	89	53	33	16	401	404	0
ARCSA	21 3 62 P	28	66	150	160	135	83	48	30	15	403	404	1
ARCSA	21 3 62 P	24	56	149	163	139	86	52	32	16	403	406	1
ARCSA	2 4 62 P	50	101	136	138	117	78	47	26	12	404	407	1
ARCSA	25 3 62 A	38	74	138	151	133	87	52	28	13	405	408	3
ARCSA	20 3 61 P	26	81	164	169	136	77	39	25	12	408	412	0
ARCSA	25 2 62 A	19	69	170	176	142	80	42	29	15	410	417	0
ARCSA	1 4 62 P	36	88	154	157	130	80	46	28	14	413	418	2
AROSA	11 4 62 A	54	103	135	139	120	83	51	26	12	417	418	2
ARCSA	11 4 62 P	53	97	130	136	120	85	54	28	12	418	414	4
ARCSA	18 3 62 P	29	84	165	166	134	78	45	31	16	422	425	3
ARCSA	24 2 62 A	36	106	170	165	130	74	41	28	14	427	435	0
ARCSA	24 2 62 P	41	110	165	160	127	75	42	27	13	428	434	0
ARCSA	22 3 61 P	37	102	166	167	136	81	43	25	12	434	438	1
ARCSA	17 3 62 A	27	91	178	174	137	77	45	33	17	438	441	3

A refers to AM observations
A refers to PM observations

TABLE E-6 (Concluded)

Station	Date	Vertical Distribution of Ozone: Mean Ozone Partial Pressures for the Various Layers									Total Ozone		Cloudiness
		1	2	3	4	5	6	7	8	9	Observed	Solution	
ARCSA	18 3 62 A	36	10C	169	164	130	77	49	34	18	441	443	3
ARCSA	26 3 62 A	39	107	172	169	138	83	49	30	15	452	457	3
ARCSA	16 4 62 A	68	145	149	138	115	79	51	27	12	453	457	1
ARCSA	26 3 62 P	33	97	174	173	140	84	5C	33	17	455	455	3

A refers to AM observations
P refers to PM observations

TABLE E-7

INDIVIDUAL SOLUTIONS FOR 93 AROSA UMKEHRS BY DUTSCH'S TECHNIQUE

Station	Date	Vertical Distribution of Ozone: Mean Ozone Partial Pressures for the Various Layers									Total Ozone		Cloudiness
		1	2	3	4	5	6	7	8	9	Observed	Solution	
ARCSA	2 11 61 P	20	31	42	78	109	69	39	25	11	243	243	0
ARCSA	1 11 61 A	23	32	41	77	109	69	40	25	11	247	247	0
ARCSA	31 10 61 P	19	40	54	81	107	67	40	25	11	254	254	0
ARCSA	9 10 61 A	10	37	59	87	113	71	41	25	11	256	256	0
ARCSA	31 10 61 A	28	46	52	77	104	64	36	24	11	257	257	0
ARCSA	15 10 61 P	18	42	58	84	110	68	39	25	11	259	259	0
ARCSA	11 10 61 A	19	42	56	82	109	69	41	25	11	260	260	0
ARCSA	15 10 61 A	17	42	61	86	111	68	39	25	11	262	262	0
ARCSA	10 2 62 A	19	43	65	93	117	68	34	21	9	266	266	0
ARCSA	13 10 61 P	20	42	57	85	113	71	40	25	11	266	266	0
ARCSA	13 10 61 A	23	43	54	83	110	71	42	25	11	266	266	0
ARCSA	23 9 61 A	33	45	46	76	108	71	41	25	11	267	267	0
ARCSA	23 9 61 A	35	50	48	74	105	69	39	24	11	267	266	0
ARCSA	24 9 61 A	27	44	53	81	110	71	41	25	11	269	269	0
ARCSA	25 9 61 P	35	42	43	77	111	74	42	24	10	269	268	0
ARCSA	25 9 61 A	27	42	51	82	114	74	41	24	11	270	270	0
ARCSA	10 2 62 P	16	48	69	90	112	68	38	24	10	270	270	0
ARCSA	22 9 61 A	32	52	54	77	106	69	41	25	11	273	273	0
ARCSA	21 9 61 A	31	46	53	81	111	72	41	24	10	273	273	1
ARCSA	21 9 61 A	25	42	55	86	114	74	43	25	10	273	273	1
ARCSA	20 9 61 A	22	38	56	89	119	76	42	25	11	274	274	0
ARCSA	22 9 61 P	41	58	51	73	102	67	39	24	10	276	275	0
ARCSA	22 9 61 P	39	50	49	77	108	70	39	24	11	276	275	0
ARCSA	19 9 61 A	26	43	56	87	117	76	43	24	10	278	278	0
ARCSA	16 9 61 P	36	41	48	85	118	76	40	23	9	279	278	0

A refers to AM observations
P refers to PM observations

TABLE E-7 (Continued)

Station	Date	Vertical Distribution of Ozone: Mean Ozone Partial Pressures for the Various Layers									Total Ozone		Cloudiness
		1	2	3	4	5	6	7	8	9	Observed	Solution	
AROSA	26 7 62 A	30	41	54	85	114	91	49	20	10	283	283	0
AROSA	1 9 61 A	36	52	65	77	103	85	47	22	10	285	285	1
AROSA	27 8 61 P	32	38	58	99	113	83	47	21	11	288	286	0
AROSA	29 8 61 P	28	40	68	97	109	84	47	20	11	289	288	0
AROSA	4 9 61 A	35	47	75	100	96	71	46	22	11	290	290	3
AROSA	25 7 62 P	40	49	57	90	117	82	39	19	12	292	292	3
AROSA	11 9 61 A	20	33	72	116	115	80	48	23	11	293	293	0
AROSA	20 7 62 P	29	42	76	102	100	82	54	22	8	294	294	0
AROSA	20 2 62 A	10	25	81	126	123	83	46	21	11	295	295	0
AROSA	10 9 61 A	20	45	85	104	104	84	50	22	11	296	296	0
AROSA	30 8 61 P	28	46	82	96	96	84	53	21	9	296	294	0
AROSA	15 9 61 P	33	34	58	115	127	75	36	21	14	296	296	2
AROSA	21 7 62 A	40	43	69	91	107	87	49	18	9	297	297	1
AROSA	20 7 62 A	17	32	81	115	115	88	52	21	8	297	297	2
AROSA	13 9 61 P	19	48	97	99	92	84	53	23	12	298	298	2
AROSA	20 2 62 P	23	36	71	116	122	82	46	22	11	300	300	1
AROSA	14 7 62 A	30	40	82	115	107	78	49	22	10	302	305	2
AROSA	26 8 61 A	20	37	83	115	115	85	49	21	10	303	303	0
AROSA	14 7 61 A	2	33	105	127	109	86	52	21	10	304	301	0
AROSA	24 6 62 P	34	41	78	118	106	74	50	23	10	306	306	3
AROSA	9 7 62 A	41	61	84	90	97	87	50	17	7	309	309	2
AROSA	5 5 61 P	23	45	107	125	86	73	59	25	8	312	312	2
AROSA	5 5 61 A	14	42	103	131	106	77	51	23	10	313	313	2
AROSA	26 7 61 P	40	62	77	95	123	86	35	15	11	314	314	3
AROSA	31 5 62 A	23	46	90	128	121	84	49	22	11	325	325	3

A refers to AM observations
P refers to PM observations

TABLE E-7 (Continued)

Station	Date	Vertical Distribution of Ozone: Mean Ozone Partial Pressures for the Various Layers									Total Ozone		Cloudiness
		1	2	3	4	5	6	7	8	9	Observed	Solution	
AROSA	20 10 61 A	36	66	112	123	90	65	45	23	12	327	327	1
AROSA	24 4 62 P	31	54	96	137	119	72	42	20	9	329	331	1
AROSA	23 7 61 P	38	52	80	124	124	84	47	21	10	331	333	1
AROSA	21 2 62 A	24	43	84	137	129	84	49	24	11	331	331	0
AROSA	4 4 61 A	15	48	113	152	121	73	41	21	12	334	334	2
AROSA	24 7 61 A	28	56	96	126	122	86	48	22	10	337	337	0
AROSA	28 6 62 A	32	60	104	122	107	86	53	21	9	337	337	0
AROSA	19 10 61 A	41	81	118	117	91	70	44	22	12	343	343	0
AROSA	30 5 61 A	32	61	89	115	130	97	50	20	10	344	344	0
AROSA	9 6 62 A	24	55	115	145	112	80	53	21	8	346	346	0
AROSA	17 5 62 A	31	60	111	135	113	89	58	22	8	355	355	2
AROSA	2 5 61 A	42	70	104	133	118	76	43	22	12	356	356	3
AROSA	6 6 62 A	61	65	84	125	110	83	59	24	8	361	361	2
AROSA	26 4 62 P	54	80	85	107	122	94	53	23	11	365	365	3
AROSA	28 2 62 P	27	44	102	159	137	82	51	29	16	367	367	3
AROSA	28 3 61 P	49	52	89	157	133	74	46	23	11	367	367	3
AROSA	7 3 62 P	41	72	116	144	118	77	46	22	11	370	371	0
AROSA	25 5 61 A	29	75	131	142	115	88	55	22	9	377	377	0
AROSA	20 3 62 A	18	61	148	178	112	70	52	26	12	379	379	0
AROSA	27 2 62 P	43	91	137	138	110	77	46	22	11	386	387	0
AROSA	12 4 62 A	39	82	136	141	108	79	55	26	11	386	386	1
AROSA	21 3 62 A	33	78	141	155	121	79	50	26	13	394	395	0
AROSA	12 4 62 P	38	73	143	153	112	76	54	28	14	394	394	3
AROSA	19 3 62 A	25	82	156	158	125	78	43	24	15	398	398	0
AROSA	19 3 62 P	52	93	124	141	128	80	41	22	13	400	400	0

A refers to AM observations
P refers to PM observations

TABLE E-7 (Concluded)

Station	Date	Vertical Distribution of Ozone: Mean Ozone Partial Pressures for the Various Layers									Total Ozone		Cloudiness
		1	2	3	4	5	6	7	8	9	Observed	Solution	
AROSA	24 3 62 A	25	77	134	149	141	95	50	26	15	401	401	0
AROSA	21 3 62 P	30	62	151	174	123	76	54	28	13	403	403	1
AROSA	2 4 62 P	56	99	132	138	114	76	50	24	11	404	404	1
AROSA	25 3 62 A	38	87	143	144	118	89	56	25	11	405	405	3
AROSA	20 3 61 P	33	95	164	157	120	80	42	19	11	408	409	0
AROSA	25 2 62 A	19	98	179	160	114	80	46	23	12	410	411	0
AROSA	1 4 62 P	37	104	160	145	114	81	50	24	12	413	413	2
AROSA	11 4 62 A	49	104	155	134	102	89	59	24	11	417	417	2
AROSA	11 4 62 P	62	85	113	143	134	89	52	26	14	418	418	4
AROSA	18 2 62 P	58	83	156	174	127	74	48	27	14	422	422	3
AROSA	24 2 62 A	41	111	180	166	104	67	49	24	10	427	428	0
AROSA	24 2 62 P	41	111	163	162	102	71	50	23	10	426	429	0
AROSA	22 3 61 P	38	104	179	168	117	79	49	22	10	434	434	1
AROSA	17 3 62 A	37	91	172	179	126	75	49	28	15	438	438	3
AROSA	18 3 62 A	48	106	153	158	129	82	49	28	16	441	441	3
AROSA	26 3 62 A	47	114	172	167	120	80	53	26	12	452	453	3
AROSA	16 4 62 A	70	130	169	143	95	78	59	26	10	453	454	1
AROSA	26 3 62 P	37	88	176	186	133	82	54	30	16	455	455	3

A refers to AM observations
P refers to PM observations

TABLE E-8

INDIVIDUAL SOLUTIONS FOR 98 NORTH AMERICAN UMKEHRS ON C WAVELENGTHS, BY TWOMEY'S METHOD, WITH RESPECT TO SI, AND WITH SECOND DERIVATIVE CORRECTIONS APPLIED

Station	Date	Vertical Distribution of Ozone — Mean Ozone Partial Pressures for the Various Layers									Total Ozone		Cloudiness
		1	2	3	4	5	6	7	8	9	Observed	Solution	
EDMONTON	9 3 59 A	22	106	149	166	143	89	55	31	15	440	438	0
EDMONTON	22 3 59 P	42	126	138	156	137	86	44	23	10	443	437	0
EDMONTON	24 3 59 A	15	132	164	168	136	87	57	30	12	445	450	0
EDMONTON	11 4 59 P	21	96	125	144	128	87	52	25	11	385	384	0
EDMONTON	14 5 59 A	32	55	89	133	130	88	49	22	9	352	348	0
EDMONTON	5 7 60 A	18	64	96	126	115	80	51	24	10	325	329	0
EDMONTON	9 8 60 A	34	49	70	111	109	77	45	23	10	309	305	0
EDMONTON	10 8 60 A	29	37	66	111	112	81	45	22	9	297	295	0
EDMONTON	18 5 61 P	19	77	120	149	133	87	52	26	11	378	379	0
EDMONTON	19 5 61 P	40	76	92	126	122	85	49	24	10	368	361	0
EDMONTON	22 5 61 P	39	68	84	122	121	87	50	22	9	354	348	0
EDMONTON	14 6 61 P	35	56	74	114	111	78	43	20	8	315	311	0
EDMONTON	16 6 61 P	42	45	54	101	103	75	40	18	7	291	285	0
EDMONTON	7 8 61 A	29	56	74	112	106	74	38	17	6	294	295	0
EDMONTON	14 9 61 A	29	35	59	102	99	68	39	22	10	270	268	0
EDMONTON	3 4 62 A	26	73	111	141	126	81	48	27	12	370	367	0
EDMONTON	27 6 62 A	35	90	99	123	112	79	49	23	10	360	357	0
EDMONTON	1 8 62 A	36	52	66	106	104	75	41	21	9	301	297	0
MOOSONEE	19 4 60 P	44	162	146	144	118	78	48	23	10	448	444	0
MOOSONEE	11 5 60 P	31	98	114	136	122	83	51	25	11	385	383	0
MOOSONEE	12 5 60 P	20	102	121	137	115	74	43	21	8	356	362	0
MOOSONEE	13 5 60 P	41	111	116	128	114	78	46	23	10	387	382	0
MOOSONEE	26 5 60 P	27	60	93	131	124	84	50	24	11	347	345	0
MOOSONEE	14 6 60 P	32	71	92	127	122	88	50	22	9	354	351	0
MOOSONEE	21 6 60 A	25	76	110	143	132	89	51	23	10	375	374	0

A refers to AM observations
P refers to PM observations

TABLE E-8 (Continued)

Station	Date	Vertical Distribution of Ozone: Mean Ozone Partial Pressures for the Various Layers									Total Ozone		Cloudiness
		1	2	3	4	5	6	7	8	9	Observed	Solution	
MOOSONEE	20 7 60 P	35	67	92	130	128	91	52	23	10	367	362	0
MOOSONEE	23 7 60 P	41	65	78	117	116	85	47	20	8	342	336	0
MOOSONEE	4 8 60 P	35	80	97	129	123	88	52	24	10	371	367	0
MOOSONEE	23 8 60 P	35	59	75	113	111	81	47	22	9	325	321	0
MOOSONEE	24 8 60 A	24	42	73	114	112	81	48	24	10	302	301	0
MOOSONEE	27 8 60 A	30	57	77	113	109	80	48	23	10	316	314	0
MOOSONEE	21 3 61 P	29	73	107	143	137	96	56	26	11	390	386	0
MOOSONEE	3 5 61 P	48	123	116	133	119	80	46	21	9	409	402	0
MOOSONEE	4 5 61 P	35	114	126	144	127	86	50	22	9	410	408	0
STERLING	28 3 62 P	32	62	92	131	128	92	55	26	11	365	360	0
STERLING	25 4 62 A	35	49	78	124	127	94	55	23	9	349	343	0
STERLING	27 4 62 A	39	60	79	122	125	95	57	24	9	359	352	0
STERLING	7 11 62 P	28	25	60	110	115	86	52	25	11	299	295	0
STERLING	8 3 63 P	42	63	91	136	140	101	57	25	10	394	384	0
STERLING	24 6 63 P	35	67	94	134	133	97	56	23	9	377	372	0
STERLING	25 6 63 P	42	65	79	120	123	94	57	23	9	363	355	0
STERLING	26 6 63 P	39	58	78	121	125	94	56	23	9	355	348	0
STERLING	4 7 63 P	33	45	74	120	124	93	52	22	9	333	329	0
TORONTO	22 2 60 P	47	139	138	148	126	81	50	29	13	454	444	0
TORONTO	9 3 60 A	20	104	142	160	136	84	51	29	13	416	417	0
TORONTO	11 3 60 P	26	133	153	161	134	83	49	26	12	439	439	0
TORONTO	15 3 60 P	23	121	161	177	155	99	59	29	13	473	471	0
TORONTO	2 5 60 A	32	102	126	150	136	92	59	28	12	425	420	0
TORONTO	7 6 60 A	40	94	109	140	132	88	49	23	10	400	394	0
TORONTO	8 6 60 A	30	75	106	139	133	94	58	28	12	390	385	0

A refers to AM observations
P refers to PM observations

TABLE E-8 (Continued)

Station	Date	Vertical Distribution of Ozone: Mean Ozone Partial Pressures for the Various Layers									Total Ozone		Cloudiness
		1	2	3	4	5	6	7	8	9	Observed	Solution	
TORONTO	8 6 60 P	32	106	120	142	129	91	55	23	9	404	403	0
TORONTO	9 6 60 A	25	64	96	132	129	97	63	25	9	365	364	0
TORONTO	10 6 60 A	31	52	83	125	126	92	56	26	11	350	345	0
TORONTO	20 6 60 A	23	81	117	147	138	98	61	27	12	398	398	0
TORONTO	28 6 60 A	41	39	62	113	123	97	58	23	9	338	329	0
TORONTO	20 7 60 P	28	87	109	135	124	87	54	25	10	375	374	0
TORONTO	28 7 60 A	28	57	87	126	122	87	52	26	11	344	341	0
TORONTO	16 6 61 A	23	67	107	141	130	89	53	25	11	368	367	0
TORONTO	16 6 61 P	37	64	88	131	129	90	48	21	8	360	354	0
TORONTO	17 6 61 A	37	86	103	133	125	87	51	24	10	384	379	0
TORONTO	1 7 61 A	37	31	55	106	114	87	49	21	9	302	296	0
TORONTO	1 7 61 P	47	35	52	105	116	90	49	21	9	321	310	0
TORONTO	4 7 61 A	37	80	101	133	125	87	54	26	11	384	377	0
TORONTO	5 7 61 A	30	83	103	129	118	83	52	25	11	364	362	0
TORONTO	5 7 61 P	49	67	80	123	125	88	44	20	8	364	353	0
TORONTO	6 7 61 A	34	70	90	124	118	84	50	25	11	353	349	0
TORONTO	6 7 61 P	43	67	84	126	125	88	47	21	9	361	353	0
TORONTO	17 7 61 A	39	64	84	124	122	89	53	25	11	361	353	0
TORONTO	27 7 61 A	29	40	72	117	119	87	52	25	10	320	316	0
TORONTO	3 8 61 P	37	54	77	121	123	91	51	22	9	343	337	0
TORONTO	5 8 61 P	41	48	72	119	123	88	48	22	9	340	331	0
TORONTO	12 8 61 A	25	39	77	122	122	87	53	25	11	323	321	0
TORONTO	13 8 61 A	32	76	103	136	128	89	51	24	10	375	371	0
TORONTO	14 8 61 P	31	46	80	124	127	96	57	25	10	347	342	0
TORONTO	17 8 61 A	30	36	70	116	118	87	52	25	11	319	314	0

A refers to AM observations
P refers to PM observations

TABLE E-8 (Concluded)

Station	Date	Vertical Distribution of Ozone: Mean Ozone Partial Pressures for the Various Layers									Total Ozone		Cloudiness
		1	2	3	4	5	6	7	8	9	Observed	Solution	
TORONTO	17 8 61 P	38	41	66	115	119	87	47	21	9	323	316	0
TORONTO	18 8 61 A	23	35	74	118	117	85	55	27	12	314	312	0
TORONTO	18 8 61 P	33	39	67	114	119	91	54	23	10	322	317	0
TORONTO	19 8 61 A	46	33	50	103	116	93	57	25	10	326	314	0
TORONTO	31 8 61 P	47	26	43	101	114	87	49	21	8	305	293	0
TORONTO	27 8 61 A	45	48	58	103	108	84	51	24	10	321	312	0
TORONTO	3 9 61 P	40	28	49	101	108	82	48	22	9	[illegible]	286	0
TORONTO	7 9 61 P	30	35	58	104	104	77	48	22	9		281	0
TORONTO	9 9 61 A	23	32	59	103	103	77	49	25	11		279	0
TORONTO	9 9 61 P	33	29	53	102	107	82	51	24	10		285	0
TORONTO	16 9 61 A	33	39	68	114	116	85	50	24	10	317	311	0
TORONTO	16 9 61 P	32	33	66	115	119	88	53	25	11	319	313	0
TORONTO	17 9 61 A	25	33	73	122	125	93	57	27	11	328	325	0
TORONTO	17 9 61 P	29	34	71	120	125	93	55	26	11	327	323	0
TORONTO	18 9 61 A	26	25	68	118	123	92	57	26	11	317	313	0
TORONTO	18 9 61 P	35	17	55	115	126	98	57	24	10	319	311	0
TORONTO	8 6 62 A	34	61	91	133	135	96	52	23	10	370	365	0
TORONTO	27 6 62 A	24	59	94	131	126	91	57	27	11	354	353	0
TORONTO	28 6 62 A	23	56	95	133	127	88	53	26	12	350	349	0
TORONTO	29 6 62 A	47	66	79	121	124	92	54	23	9	370	359	0
TORONTO	10 7 62 A	17	40	87	130	128	92	54	26	12	330	331	0
TORONTO	19 7 62 A	41	39	66	119	126	92	52	24	10	340	330	0
TORONTO	24 7 62 A	30	63	96	134	129	90	53	25	11	364	360	0

A refers to AM observations
P refers to PM observations

BIBLIOGRAPHY

Brewer, A. W., H. U. Dütsch, J. R. Milford, M. Migeotte, H. K. Paetzold, F. Piscalar, and E. Vigroux, 1960: Distribution verticale de l'ozone atmosphérique. Comparison de diverses méthodes. Ann. Geophys., 16, 196-222.

Brewer, A. W., and J. R. Milford, 1960: The Oxford-Kew ozone sonde. Proc. Phys. Soc. London, A 256, 470-495.

Chapman, S., 1930: A theory of upper atmospheric ozone. Mem. Roy. Met. Soc., 3, 103.

Craig, R. A., 1948: The Observations and Photochemistry of Atmospheric Ozone and Their Meteorological Significance. D. Sc. Thesis, Mass. Inst. Tech.

_____, 1950: The observations and photochemistry of atmospheric ozone and their meteorological significance. Met. Monogr., 1 (2), 1-50.

Dave, J. V., and P. Furukawa, 1964: The effect of Lambert-type ground reflection on Umkehr measurements. J. Atmos. Sci., 21, in press.

Dobson, G.M.B., 1930: Observations of the amount of ozone in the earth's atmosphere and its relation to other geophysical conditions. Part IV. Proc. Roy. Soc., London, A 129, 411-433.

_____, 1931: A photoelectric spectrophotometer for measuring the amount of atmospheric ozone. Proc. Phys. Soc., London, 43, 324-339.

_____, 1957a: Observers' handbook for the ozone spectrophotometer. Ann I.G.Y., 5 (1), 46-89.

_____, 1957b: Adjustment and calibration of ozone spectrophotometer. Ann I.G.Y., 5 (1), 90-114.

_____, 1963: Note on the measurement of ozone in the atmosphere. Quart. J. Roy. Met. Soc., 89, 409-411.

_____, and D. N. Harrison, 1926: Measurements of the amount of ozone in the earth's atmosphere and its relation to other geophysical conditions. Part I. Proc. Roy. Soc. London, A 110, 660-693.

BIBLIOGRAPHY (Continued)

_____, D. N. Harrison, and J. Lawrence, 1927: Measurements of the amount of ozone in the earth's atmosphere and its relation to other geophysical conditions. Part II. Proc. Roy. Soc. London, A 114, 521-541.

_____, D. N. Harrison, and J. Lawrence, 1929: Measurements of the amount of ozone in the earth's atmosphere and its relation to other geophysical conditions. Part III. Proc. Roy. Soc. London, A 122, 456-486.

Dütsch, H. U., 1946: Photochemische Theorie des Atmosphärischen Ozons unter Berücksichtigung von Nichtgleichgewichtszüstanden und Luftbewegungen. Doctoral dissertation, University of Zürich.

_____, 1957: Evaluation of the Umkehr effect by means of a digital electronic computer. Scientific Report No. 1, "Ozone and General Circulation in the Stratosphere." Arosa, Lichtklimatisches Observatorium.

_____, 1959 a: Vertical ozone distribution over Arosa. Final Report, "Ozone and General Circulation in the Stratosphere." Arosa, Lichtklimatisches Observatorium.

_____, 1959 b: Vertical ozone distribution from Umkehr observations. Arch. Met. Geophys. Biokl. A 11, 240-251.

_____, 1963: Vertical ozone distributions over Arosa. Tech. Rep. No. 1, Vertical Ozone Distribution and Stratospheric Circulation. Boulder, National Center for Atmospheric Research.

Epstein, E. S., C. Osterberg, and A. Adel, 1956: A new method for the determination of the vertical distribution of ozone from a ground station. J. Met., 13, 319-334.

Godson, W. L., 1962: The representation and analysis of vertical distributions of ozone. Quart. J. Roy. Met. Soc., 88, 220-232.

Goody, R. M., and W. T. Roach, 1956: Determination of the vertical distribution of ozone from emission spectra. Quart. J. Roy. Met. Soc., 82, 217-221.

Götz, F.W.P., 1931: Zum Strahlungsklima des Spitzbergen Sommers. Gerlands Beiträge zur Geophys., 31, 119-154.

BIBLIOGRAPHY (Continued)

_____, 1951: Ozone in the atmosphere. Compendium of Meteorology, Amer. Met. Soc., Boston, 275-291.

_____, A. R. Meetham, and G.M.B. Dobson, 1934: The vertical distribution of ozone in the atmosphere. Proc. Roy. Soc. London, A 145, 416-446.

Grimmer, M., 1963: The space-filtering of monthly surface anomaly data in terms of pattern, using empirical orthogonal functions. Quart. J. Roy. Met. Soc., 89, 395-408.

Johnson, F. S., J. D. Purcell, R. Tousey, and K. Watanabe, 1952: Direct measurements of the vertical distribution of atmospheric ozone to 70 km altitude. J. Geophys. Res., 57, 157-176.

Karandikar, R. V., and K. R. Ramanathan, 1949: Vertical distribution of atmospheric ozone in low latitudes. Proc. Ind. Acad. Sci., A 29, 330-348.

Kay, R. H., A. W. Brewer, and G.M.B. Dobson, 1954: Some measurements of the vertical distribution of atmospheric ozone by a chemical method to heights of 15 km from aircraft. Sci. Proc. Int. Assoc. Met., Rome, 189-193.

Kendall, M. G., 1957: A Course in Multivariate Analysis. London, Charles Griffin and Co., Ltd., 185 pp.

Komhyr, W. D., 1956: Unpublished M. Sc. Thesis, University of Alberta.

Kulcke, W., and H. K. Paetzold, 1957: Über ein Radiosonde zur Bestimmung der vertikalen Ozonverteilung. Ann. d. Met., 8, 47-53.

Lanczos, C., 1956: Applied Analysis. Englewood Cliffs, Prentice-Hall, 539 pp.

Larsen, S.H.H., 1959: On the scattering of ultraviolet radiation in the atmosphere with the ozone absorption considered. Geofys. Publ., 21 (4), 1-44.

Lawley, D. N., and A. E. Maxwell, 1963: Factor Analysis as a Statistical Method. London, Butterworths, 117 pp.

List, R. J., 1958: Smithsonian Meteorological Tables. Washington, Smithsonian Institution Pub. No. 4014, 527 pp.

BIBLIOGRAPHY (Continued)

Lorenz, E. N., 1956: Empirical orthogonal functions and statistical weather prediction. Sci. Rep. No. 1, Statistical Forecasting Project, Dept. of Met., Mass. Inst. Tech.

_____, 1959: Prospects for statistical weather forecasting. Final Rep., Statistical Forecasting Project, Dept. of Met., Mass. Inst. Tech.

Mateer, C. L., 1960: A rapid technique for estimating the vertical distribution of ozone from Umkehr observations. Met. Branch, Toronto, Circ. No. 3291.

Mecke, R., 1931: Zur Deutung des Ozongehalts der Atmosphäre. Z. phys. Chem., Bodenstein Festband, 392-404.

Muramatsu, H., 1961: Vertical distributions of ozone estimated from Umkehr observations at Marcus Island, Tateno and Sapporo. J. Aerol. Obs. Tateno, 7, 1-8.

Paetzold, H. K., 1952: Erfassung der vertikalen Ozonverteilung in verschiedenen geographischen Breiten bei Mondfinsternissen. J. Atmos. Terr. Phys., 2, 183-188.

_____, 1954: New experimental and theoretical investigations on the atmospheric ozone layer. Proc. Int. Assoc. Met., Rome, 201-212.

Phillips, D. L., 1962: A technique for the numerical solution of certain integral equations of the first kind. J. Assoc. Comp. Mach., 9, 84-97.

Pittock, A. B., 1961: A twilight method of determining the vertical distribution of ozone. Nature, 190, 426-427.

_____, 1963: Determination of the vertical distribution of ozone by twilight balloon photometry. J. Geophys. Res., 68, 5143-5155.

Ramanathan, K. R., V. R. Moorthy, and R. N. Kulkarni, 1952: The effect of secondary scattering in the calculation of the vertical distribution of atmospheric ozone from the Götz inversion-effect. Quart. J. Roy. Met. Soc., 78, 625-626.

Ramanathan, K. R., and J. V. Dave, 1957: The calculation of the vertical distribution of ozone by the Götz Umkehr-effect (Method B). Ann. I.G.Y., 5 (1), 23-45.

BIBLIOGRAPHY (Continued)

Rawcliffe, R. D., G. E. Meloy, R. M. Friedman, and E. H. Rogers, 1963: Measurement of vertical distribution of ozone from a polar orbiting satellite. J. Geophys. Res., 68, 6425-6429.

Regener, E., and V. H. Regener, 1934: Aufnahme des ultravioletten Sonnenspektrums in der Stratosphäre und die verticale Ozonverteilung, Phys. Zeit., 35, 788-793.

Regener, V. H., 1960: On a sensitive method for the recording of atmospheric ozone. J. Geophys. Res., 65, 3975-3977.

Scherhag, R., 1952: Die explosionsartigen Stratosphärenerwärmungen des Spätwinters 1951-1952. Berichte des Deutschen Wetterdienstes in der U. S. Zone, 6, 51-63.

Schröer, E., 1949: Theorie der Entstehung, Zersetzung, und Verteilung des atmosphärischen Ozons. Berichte des Deutschen Wetterdienstes in der U. S. Zone, No. 11, 13-23.

Sekera, Z., and J. V. Dave, 1961: Diffuse transmission of solar ultraviolet radiation in the presence of ozone. Astrophys. J., 133, 210-227.

Singer, S. F., and R. C. Wentworth, 1957: A method for the determination of the vertical ozone distribution from a satellite, J. Geophys. Res., 62, 299-308.

Taba, H., 1961: Ozone observations and their meteorological applications. Geneva, World Met. Org., Tech. Note. No. 36.

Teweles, S., and F. G. Finger, 1958: An abrupt change in stratospheric circulation beginning in mid-January 1958. Mon. Wea. Rev., 86, 23-28.

Tønsberg, E., and K. Langlo, 1944: Investigations on atmospheric ozone at Nordlysobservatoriet Tromsö. Geofys. Publ., 13 (12), 1-39.

Twomey, S., 1961: On the deduction of the vertical distribution of ozone by ultraviolet spectral measurements from a satellite. J. Geophys. Res., 66, 2153-2162.

_____, 1963: On the numerical solution of Fredholm integral equations of the first kind by the inversion of the linear system produced by quadrature. J. Assoc. Comp. Mach., 10, 97-101.

BIBLIOGRAPHY (Continued)

_____, and H. B. Howell, 1963: A discussion of indirect sounding methods with special reference to the deduction of vertical ozone distribution from light scattering measurements. Mon. Wea. Rev., 91, 659-664.

U. S. Standard Atmosphere, 1962. Washington, U. S. Government Printing Office, 278 pp.

Vassy, A., 1958: Radio-sonde spéciale pour la mesure de la répartition verticale de l'ozone atmosphérique. J. Sci. Mét., 10, 63-75.

Venkateswaran, S. V., J. G. Moore, and A. J. Kreuger, 1961: Determination of the vertical distribution of ozone by satellite photometry. J. Geophys. Res., 66, 1751-1771.

Vigroux, E., 1953: Contribution a l'étude expérimentale de l'absorption de l'ozone. Ann. de Phys., 8, 709-762.

_____, 1959: Distribution verticale de l'ozone atmosphérique d'après les observations de la bande 9.6 μ. C. R. Acad. Sci. Paris, 18, 2622-2624.

Walton, G. F., 1953: The vertical distribution of ozone. Bruxelles, I. U. G. G. General Assembly, Procès-Verbaux I. A. M., 316-322.

_____, 1957: The calculation of the vertical distribution of ozone by the Götz Umkehr-effect (Method A). Ann. I.G.Y., 5 (1), 9-22.

_____, 1959: Calculation of the vertical distribution of atmospheric ozone. J. Atmos. Terr. Phys., 16, 1-9.

Wilkes, M. V., 1954: A table of Chapman's grazing incidence integral Ch(x,χ). Proc. Phys. Soc. London, B 67, 304-308.

Wulf, O. R., 1932: A theory of the ozone of the lower atmosphere and its relation to the general problem of atmospheric ozone. Phys. Rev., 41, 375-376.

_____, 1934: Steady states produced by radiation with application to the distribution of atmospheric ozone. Phil. Mag., 17, 251-263.

BIBLIOGRAPHY (Concluded)

_____, and L. S. Deming, 1936 a: The theoretical calculation of the distribution of photo-chemically formed ozone in the atmosphere. Terr. Magn. Atmos. Elect., 41, 299-310.

_____, and L. S. Deming, 1936 b: The effect of visible solar radiation on the calculated distribution of atmospheric ozone. Terr. Magn. Atmos. Elect., 41, 375-378.

_____, and L. S. Deming, 1937: The distribution of atmospheric ozone in equilibrium with solar radiation and the rate of maintenance of the distribution. Terr. Magn. Atmos. Elect., 42, 195-202.